

CHARLES UNIVERSITY
FACULTY OF MEDICINE IN HRADEC KRÁLOVÉ

DISSERTATION THESIS

**CHARLES UNIVERSITY
FACULTY OF MEDICINE IN HRADEC KRÁLOVÉ**

Doctoral Study Programme
Radiology

**Utilization of CTA and CTP in Middle Cerebral Artery
Stroke**

**Využití CTA s CTP u pacientů s uzávěrem střední
mozkové tepny**

MUDr. Petra Cimflová

Supervisor: Prof. MUDr. Antonín Krajina, CSc.
Consultant Supervisor: Assoc. Prof. MUDr. Kamil Zeleňák, PhD

Hradec Králové / Calgary / Brno, 2022

SUMMARY

Introduction: Diagnostic imaging has a crucial role in the diagnosis and therapeutic management of acute ischemic stroke (AIS). Within the framework of AIS, computed tomography (CT) is still the most widespread and used imaging modality. Despite the known applications of CTA (occlusion detection, collateral assessment) and wide use of CT perfusion (CTP) as a part of the standard stroke management protocol, the main aim of this thesis was to further evaluate the utilization of these imaging modalities in the diagnosis and treatment decision in patients with acute ischemic stroke caused by the occlusion of the middle cerebral artery.

Methods: Study in *Chapter 2* retrospectively evaluated the automatically derived CT perfusion lesion volumes (PLV) defined as $T_{max} > 10s, > 8s, > 6s, > 4s, CBF < 30\%$ and hypoperfusion intensity ratio (HIR) with collateral score using multiphase CTA (mCTA). PLV and hypoperfusion intensity ratio (HIR) were compared across collateral score categories using Kruskal-Wallis and Wilcoxon rank-sum test. Correlation coefficients were calculated using Spearman's rho. In study in *Chapter 3*, the assessment of ischemic changes by expert reading and available automated software for non-contrast CT (NCCT) and CTP on baseline multimodal imaging was compared (retrospective analysis, the sensitivity, specificity, positive predictive value, and negative predictive value were calculated). The accuracy for the final infarct prediction was evaluated using Bland-Altman plots. In *Chapter 4*, the performance of StrokeSENS, an automated tool utilizing a machine learning algorithm, in detection of anterior large vessel occlusions (LVO) on CTA was tested using receiver operator characteristics analysis, reporting area under the curve, sensitivity and specificity. Study in *Chapter 5* aimed to determine whether mCTA-based prediction of clinical outcome and final infarct volume can be improved by assessing collateral status on time-variant mCTA color maps (retrospective analysis, multivariable logistic regression was used). The aims in *Chapter 6* were to determine if mCTA-derived tissue maps can accurately detect medium vessel occlusions (MeVOs), and predict infarction on 24h follow-up imaging with comparable accuracy to CTP maps (retrospective analysis, sensitivity, specificity, and AUC for MeVO detection were calculated, concordance correlation coefficient and intraclass correlation coefficient for volumetric and spatial agreement between predicted infarcts on mCTA and CTP, Cohen's Kappa analysis).

Results: In *Chapter 2*, we demonstrated that mCTA collateral score corresponds well with automatically-derived perfusion lesion volumes with significant difference of PLV between good and poor collaterals. High accuracy for the assessment of ischemic changes by different CT modalities with the best accuracy for CBF<30% and Tmax>10s was demonstrated in *Chapter 3*. We showed in *Chapter 4* StrokeSENS LVO machine learning algorithm detected anterior LVO with high accuracy from a wide range of scans in a large dataset. *Chapter 5* demonstrated that collateral extent assessment on time-variant mCTA maps improved prediction of good outcome and was comparable to conventional mCTA in predicting follow-up infarct volume. Study in *Chapter 6* showed that mCTA tissue maps can be used to reliably detect MeVO stroke and predict tissue fate, with good interrater agreement for the MeVO presence.

Conclusion: The correlation of mCTA collateral status and CTP-derived PLV suggests that PLV can be estimated by collateral grade in AIS patients presenting during first 6 hours from the symptom onset. High accuracy of early ischemic changes assessment using automated software analysis encourages its use in clinical practice, especially by less experienced readers. The reliable performance of the software tool in anterior LVO detection further supports the use of machine learning based software tools in acute care to quickly and accurately identify patients presenting with suspected AIS who can benefit from timely treatment. Time-variant mCTA display format represents a suitable alternative to facilitate interpretation of the collateral status. mCTA-derived tissue maps can be used to detect MeVO and estimate the volume of potentially salvageable tissue, particularly in centers in which CTP is not available.

Key words: acute ischemic stroke, stroke imaging, multiphase CTA, CT perfusion, automatic software analysis, collateral score

SOUHRN

Úvod a cíle: Diagnostické zobrazování má zásadní roli v diagnostice a terapeutickém managementu akutní ischemické cévní mozkové příhody (AIS). V rámci AIS je stále nejrozšířenější a nejpoužívanější zobrazovací modalitou počítačová tomografie (CT). Navzdory běžnému využití CTA (k detekci uzávěru, posouzení stavu kolaterál) a rozšiřujícímu se užití CT perfúze (CTP) jako součásti standardního protokolu v managementu pacientů s AIS, bylo hlavním cílem této práce zhodnotit další možnosti využití těchto zobrazovacích modalit u pacientů s AIS způsobenou uzávěrem střední mozkové tepny.

Metodika: Studie v *Kapitole 2* retrospektivně hodnotila automaticky odvozené objemy CT perfúzních lézí (PLV) definované jako $T_{max} > 10s, > 8s, > 6s, > 4s, CBF < 30\%$ a hypoperfúzní koeficient (HIR) s kolaterálním skóre pomocí multifázické CTA (mCTA). PLV a HIR byly porovnány napříč kategoriemi kolaterálního skóre pomocí Kruskal-Wallisova a Wilcoxonova rank-sum testu. Korelační koeficienty byly vypočteny pomocí Spearmanova rho. Ve studii v *Kapitole 3* bylo porovnáno hodnocení ischemických změn na vstupním multimodálním zobrazení hodnoceného experty a pomocí dostupného automatizovaného software na nativním CT (NCCT) a CTP (retrospektivní analýza, stanovení senzitivity, specifity, pozitivní prediktivní hodnoty a negativní prediktivní hodnoty). Dále byla zhodnocena přesnost hodnocení pro predikci výsledného infarktu pomocí Bland-Altman analýzy. V *Kapitole 4* byl testován StrokeSENS, automatizovaný nástroj využívající machine learning algoritmus, v detekci uzávěru velkých cév (LVO) v přední mozkové cirkulaci na CTA s využitím receiver operating characteristics, [stanovení area under the curve (AUC), senzitivity a specifity]. Cílem studie v *Kapitole 5* bylo zjistit, zda lze zlepšit predikci klinického výsledku a konečného objemu infarktu na základě posouzení stavu kolaterál na barevně kódovaných time-variant mCTA (retrospektivní analýza, použita multivariabilní logistická regrese). Cílem v *Kapitole 6* bylo určit, zda tkáňové mapy generované z mCTA umožňují přesnou detekci uzávěrů středních cév (MeVO) a predikovat infarkt na kontrolním zobrazení za 24 hodin se srovnatelnou přesností jako CTP (retrospektivní analýza, stanovení senzitivity, specifity a AUC pro detekci MeVO, koeficientu konkordanční korelace a koeficientu vnitrotřídní korelace pro objemovou a prostorovou shodu predikovaných infarktů na mCTA a CTP, Cohenova Kappa).

Výsledky: V *Kapitole 2* jsme prokázali, že mCTA kolaterální skóre dobře koreluje s automaticky odvozenými objemy perfúzních lézí s významným rozdílem velikosti PLV u

dobrých a chudých kolaterál. Vysoká přesnost pro hodnocení ischemických změn různými CT modalitami byla prokázána v *Kapitole 3* s nejvyšší přesností pro $CBF < 30\%$ a $T_{max} > 10s$. V *Kapitole 4* jsme ukázali, že software StrokeSENS LVO detekoval LVO v přední cirkulaci s vysokou přesností na velkém souboru dat s širokou škálou skenů. *Kapitola 5* demonstrovala, že hodnocení rozsahu kolaterálu na time-variant mCTA mapách zlepšilo predikci dobrého výsledku a mělo obdobnou hodnotu pro predikci následného objemu infarktu ve srovnání s konvenčním hodnocením kolaterál na mCTA. Studie v *Kapitole 6* ukázala, že tkáňové mapy mCTA lze použít ke spolehlivé detekci MeVO a k predikci infarktu, s dobrou shodou mezi hodnotiteli v detekci MeVO.

Závěr: Korelace kvality kolaterál na mCTA a PLV odvozené z CTP značí, že velikost PLV může být odhadnuta podle stavu kolaterál u pacientů s AIS přicházejících během prvních 6 hodin od začátku symptomů. Vysoká přesnost hodnocení časných ischemických změn pomocí automatizované softwarové analýzy vybízí k jeho využití v klinické praxi, a to zejména méně zkušenými uživateli. Spolehlivý výkon automatického softwaru v detekci LVO dále podporuje využití softwarových nástrojů založených na machine learning v akutní péči pacientů s podezřením na AIS k rychlé a přesné identifikaci těch, kteří mohou mít prospěch z včasné léčby. Formát zobrazení time-variant mCTA představuje vhodnou alternativu k usnadnění interpretace stavu kolaterál. Tkáňové mapy odvozené z mCTA lze spolehlivě využít k detekci MeVO a k odhadu objemu potenciálně zachranitelné tkáně, zejména v centrech, kde není k dispozici CTP.

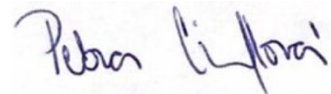
Klíčová slova: akutní ischemická cévní mozková příhoda, zobrazení u cévní mozkové příhody, multifázická CTA, CT perfúze, automatická softwarová analýza, kolaterální skóre

Author's Declaration

Declaration:

I declare hereby that this dissertation thesis is my own original work and that I indicated by references all used information sources. I also agree with depositing my dissertation in the Medical Library of the Charles University, Faculty of Medicine in Hradec Králové and with making use of it for study and educational purpose provided that anyone who will use it for his/her publication or lectures is obliged to refer to or cite my work properly.

I give my consent to availability of my dissertation's electronic version in the information system of the Charles University.



.....

Hradec Králové, 2022

Signature of the author

I would like to thank to professor Antonín Krajina for his guidance, enthusiasm, continuous support and encouragement to pursue my doctoral studies and complete this thesis.

My gratitude goes to my colleagues and friends both at the Saint Anne's University Hospital in Brno and at the University of Calgary for providing me with the priceless opportunity to learn from the best clinicians and researchers and to be constantly inspired by their enthusiasm and precise work. But more importantly, for becoming lifelong friends who has been here for me when needed and helping me on my way to grow both in my professional and personal life.

I want to thank you to my close friend and colleague, Ondřej Volný, for introducing me to the big world of stroke research, becoming my ultimate research buddy and being a fantastic role model I could look up to and follow.

I will always be infinitely grateful to my family for their love, support and understanding my desires to follow my heart and pursue adventures around the world.

TABLE OF CONTENTS

1. Introduction	19
1.1 Pathophysiology of Ischemic Stroke.....	19
1.1.1 Ischemic cascade.....	20
1.1.2 Ischemic core and penumbra.....	20
1.1.3 Role of leptomeningeal collaterals in acute ischemic stroke.....	21
1.2 CT imaging in acute ischemic stroke.....	21
1.2.1 Non-contrast CT.....	22
1.2.2 CT angiography.....	23
1.2.3 CT perfusion.....	26
1.2.3.1 CT perfusion acquisition and postprocessing.....	28
1.2.3.2 Technical pitfalls.....	28
1.2.3.1 Interpretation of CT perfusion.....	29
1.3 Current state of imaging in stroke diagnosis and treatment decision.....	31
1.4 Future directions in stroke imaging.....	32
1.5 Aims and outline of the thesis.....	33

Part I Utilization of CT Angiography and CT Perfusion in Acute Stroke Imaging

2. Chapter 2 - Correlation of the multiphase CTA collateral score and the automatically-derived CT perfusion volumes (submitted to Journal of Stroke and Cerebrovascular Diseases).....	41
2.1 Introduction.....	42
2.2 Materials & Methods.....	42
2.2.1 Patient selection.....	42
2.2.2 Imaging protocol.....	43
2.2.3 Image processing.....	43
2.2.4 Image review.....	44
2.2.5 Statistical analysis.....	44
2.3 Results.....	44
2.3.1 Baseline characteristics.....	44
2.3.2 Collateral score and hypoperfusion volumes.....	45
2.3.3 Optimal Cut-off values representing poor collaterals.....	47
2.3.4 Sensitivity analysis.....	47
2.4 Discussion.....	50

2.5 Conclusion.....	51
3. Chapter 3 - Detection of ischemic changes on baseline multimodal computed tomography: expert reading vs. Brainomix and RAPID software (Cimflova P., et al. Journal of Stroke and Cerebrovascular Diseases, 2020).....	55
3.1 Introduction.....	56
3.2 Materials & Methods.....	57
3.2.1 Patient selection.....	57
3.2.2 Imaging protocol.....	57
3.2.3 Image processing.....	58
3.2.4 Image review.....	58
3.2.5 Statistical analysis.....	60
3.3 Results.....	60
3.3.1 Sensitivity analysis.....	63
3.4 Discussion.....	69
3.5 Conclusion.....	71

Part II CT Angiography Advanced Postprocessing And Machine Learning

4. Chapter 4 - Validation of a machine learning software tool for automated large vessel occlusion detection in patients with suspected acute stroke (Cimflova P., et al. Neuroradiology, 2022).....	77
4.1 Introduction.....	78
4.2 Materials & Methods.....	78
4.2.1 Software development dataset.....	78
4.2.2 Image pre-processing and convolutional neural network.....	79
4.2.3 Software validation dataset.....	80
4.2.4 StrokeSENS LVO detection and notification.....	81
4.2.5 Statistical analysis.....	82
4.3 Results.....	83
4.4 Discussion.....	89
4.5 Conclusion.....	94
5. Chapter 5 - Utility of time-variant multiphase CTA color maps in outcome prediction for acute ischemic stroke due to anterior circulation large vessel occlusion (Ospel J., Cimflova P., et al. Clinical Neuroradiology, 2020).....	97
5.1 Introduction.....	99

5.2 Materials & Methods.....	100
5.2.1 Patient population.....	100
5.2.2 Image acquisition.....	100
5.2.3 Image interpretation.....	101
5.2.4 Interrater agreement.....	103
5.2.5 Statistical analysis.....	103
5.3 Results.....	103
5.3.1 Collateral grading and clinical outcome.....	104
5.3.2 Collateral grading and final infarct volume.....	104
5.3.3 Inter-rater agreement.....	104
5.4 Discussion.....	108
5.5 Conclusion.....	110
6. Chapter 6 - Multiphase CTA-derived tissue maps aid in detection of medium vessel occlusions (McDonough R., Qiu W., ... Petra Cimflova, et al. Neuroradiology, 2022).....	113
6.1 Introduction.....	114
6.2 Materials & Methods.....	115
6.2.1 Study participants.....	115
6.2.2 Imaging protocol.....	116
6.2.3 Image processing.....	117
6.2.4 Qualitative image analysis for MeVO detection.....	117
6.2.5 Volumetric and spatial analyses of mCTA-derived tissue maps.....	119
6.3 Results.....	120
6.3.1 Feasibility of mCTA-based MeVO detection.....	120
6.3.2 Agreement of mCTA and CTP predicted infarct volumes.....	120
6.3.3. Agreement of mCTA predicted infarct volume and measured final infarct volume...	121
6.3.3 Spatial agreement between mCTA and CTP predicted infarct volume and measured final infarct volume.....	123
6.4 Discussion.....	123
6.5 Conclusion.....	125
7. Chapter 7 – Results summary.....	129
8. List of Figures.....	131
9. List of Tables.....	132

List of abbreviations

ACA	Anterior Cerebral Artery
AIC	Akaike Information Criterion
AIS	Acute Ischemic Stroke
ASPECTS	Alberta Stroke Program Early CT Score
AUC	Area Under the Curve
BIC	Bayesian Information Criterion
CBF	Cerebral Blood Flow
CBV	Cerebral Blood Volume
CI	Confidence Interval
CNN	Convolutional Neural Network
CT	Computed Tomography
CTA	CT Angiography
CTP	CT Perfusion
dd-SVD	Delay- and Dispersion-corrected Singular Value Deconvolution
DSC	Dice similarity coefficient
EVT	Endovascular Thrombectomy
ICA	Internal Carotid Artery
ICH	Intracranial Hemorrhage
IQR	Interquartile Range
HIR	Hypoperfusion Intensity Ratio
HU	Hounsfield Units
LVO	Large Vessel Occlusion
MCA	Middle Cerebral Artery
MeVO	Medium Vessel Occlusion
MIP	Maximum Intensity Projection
mCTA	Multiphase CTA
MTT	Mean Transit Time
mTICI	modified Treatment in Cerebral Ischemia Score
NCCT	Non-contrast CT
NIHSS	National Institutes of Health Stroke Scale
NPV	Negative Predictive Value
OR	Odds Ratio

PCA	Posterior Cerebral Artery
PLV	Perfusion lesion Volume
PPV	Positive Predictive Value
ROC	Receiver Operator Characteristics
SVD	Singular Value Decomposition
TICI	Treatment in Cerebral Ischemia Score
Tmax	Time to Maximum of the Residual Function

1. Chapter 1 - Introduction

Acute ischemic stroke (AIS) remains a worldwide major cause of disability and mortality. Approximately 7-8 million people suffer from AIS every year, out of which almost one half dies and about 25-30% of stroke survivors remain disabled in basic activities (1,2).

The two treatment options for AIS are medical treatment with intravenous tissue plasminogen activator (alteplase or tenecteplase) and endovascular thrombectomy (EVT) (3). While the former is quite effective at opening smaller vessel occlusions, recanalizing medium-sized and large vessel occlusions almost always requires mechanical recanalization, i.e. EVT (4).

1.2 PATHOPHYSIOLOGY OF ACUTE ISCHEMIC STROKE

Acute occlusion of cerebral artery leads to immediate decrease in arterial blood flow in particular vessel territory resulting in alteration of cellular function. Interruption of arterial flow rich in oxygen and glucose results in disruption of the basal functions of electrically active neurons and supporting glial cells (5).

The normal cerebral blood flow (CBF) in adults is on average 50ml/min per 100g with lower values in the white matter (~20ml/min/100g) and greater values in the grey matter (~80ml/min/100g) (6). If the blood flow is above 20 ml/min/100g (40% of a normal flow), the cerebrovascular autoregulation leads to increased oxygen extraction (7). Below this level, the neurotransmission will cease and neurologic symptoms according to ischemia localization occur (8).

Immediately after the acute occlusion, the cerebrovascular and systemic compensatory mechanisms such as vasodilatation, blood pressure increase, collateral circulation recruitment etc., are activated in order to maintain the sufficient perfusion within the affected territory. First, the decline of blood perfusion pressure and an increase in CO₂ blood level causes an autoregulatory dilation of the resistance vessels. Subsequently, the stimulation of anaerobic metabolism results in lactacidosis and further pH-mediated vasodilation. Once the resistance vessels are fully dilated, CO₂ reactivity disappears and any further reduction of blood supply cannot be compensated (9). Neuron cells are able to survive for minutes, but unless the vessel is rapidly re-opened and the sufficient blood flow restored, the compensatory mechanisms fail. Together with the critical decrease in arterial perfusion, progression of hypoxia into ischemia

occurs, followed by neuronal death (1.9 million nerve cells per minute in average), infarct evolution and infarct growth (10).

1.1.1 Ischemic cascade

At the cellular level, more than 70% of all energy in the brain is used for the maintenance of the ionic gradient via facilitated transport of Na^+/K^+ that is fundamental for electrical and chemical signalling (11). During ischemia, oxygen insufficiency completely disrupts mitochondrial oxidative phosphorylation (the synthesis of ATP by phosphorylation of ADP in the mitochondria during aerobic respiration) and leads to intracellular ATP depletion within minutes. The lack of ATP hinders the physiological function of ion cell pumps causing the aberrant influx of sodium (Na^+) and calcium ions (Ca^{2+}) into the cell and efflux of potassium ions (K^+) out of the cell, resulting in the neuronal depolarization (12). The neuronal depolarization and the increase in intracellular Ca^{2+} triggers the release of glutamate, a neurotransmitter and a major contributor to ischemia-induced excitotoxicity in neurons and glial cells (13).

Glutamate binds to glutamate receptors, which opening leads to additional Ca^{2+} entry into the cell lumen. A sustained activation of Ca^{2+} -permeable channels due to an impaired glutamate uptake by astrocytes leads to a pathological increase in intracellular Ca^{2+} . The overexcited cells in turn release enzymes involved in the lysis of proteins, lipids and nucleic acids. This state of cellular excitation eventually leads to neuronal apoptosis, accompanied by formation of free radicals, edema, and inflammation (12).

1.1.2 Ischemic core and penumbra

The ischemic core is defined as irreversibly damaged tissue, consisting of apoptotic and/or necrotic cells. The threshold for irreversible neuronal death was identified as CBF of 8-10 ml/min/100g across the species (11,14–16), with grey matter demonstrating more vulnerability to ischemia than white matter (with a drop of CBF below ~10-12ml/min/100g in grey matter and below ~5ml/min/100g in white matter) (14). Nevertheless, even the brain tissue with CBF of 5-15ml/min/100g can regain function if the blood flow is restored within 30min (17,18).

The ischemic core is surrounded by electrically silent but still viable tissue of various extent – ischemic penumbra. Due to the decrease in the blood flow within this tissue, neurons are unable to transmit signals and clinical symptoms occur. However, the function of membrane cell pumps and therefore the retention of ionic gradients is preserved (11,19). The upper threshold for electrical silence and neuronal dysfunction was determined as CBF of ~22-

25 ml/min/100g (11,20). The ischemic penumbra eventually progresses into infarction if the blood flow is not restored. Opposite to that, with the prompt reperfusion, the tissue completely recovers and regains its function (10). Therefore, the duration of ischemia determines the brain tissue fate.

In contrast to the ischemic core and penumbra, benign oligemia represents the tissue that maintains its normal function regardless of reperfusion (21).

1.1.3 Role of leptomeningeal collaterals in acute ischemic stroke

Leptomeningeal collaterals, representing pial anastomoses between major cerebral arteries plays a pivotal role in sustaining the cerebral blood flow within the stroke affected territory, e.g. beyond the arterial occlusion.

Leptomeningeal vessels together with the ophthalmic arteries constitute the secondary brain collaterals, while the Circle of Willis represents the primary collateral pathway. The number and size of these anastomotic vessels are greatest between anterior cerebral artery (ACA) and middle cerebral artery (MCA), fewer connections exist between MCA and posterior cerebral artery (PCA) and even less terminal anastomoses could be identified between PCA and ACA (22). Despite this anatomical consideration, the interterritorial leptomeningeal collaterals between the PCA and MCA territory were shown to be functionally better than those between the ACA and MCA territory (23).

The robustness of the collateral pathways dictates the size of the ischemic core, ischemic core growth, and the size of the penumbra (24–26). It is a well-known fact that there is a large interindividual variability in the collateral robustness (23,27). The factors associated with the collateral morphology have been widely investigated. Evidence suggests that acute and as well as chronic hyperglycemia and diabetes are associated with poor collateral status (23,24,28). Variability in size is likely also related to genetic factors or to variability in autoregulatory mechanisms or myogenic tone of pial arteries (23).

Based on findings related to collateral recruitment during the ischemic stroke, leptomeningeal collaterals became an important prognostic factor in patients with AIS and the evaluation of their extent gained significant attention in acute stroke imaging.

1.3 CT IMAGING IN ACUTE ISCHEMIC STROKE

Diagnostic imaging has an irreplaceable role in the diagnosis and therapeutic management of AIS. Within the framework of AIS, computed tomography (CT) of the brain is still the most

widespread and used imaging method. CT represents a fast, simple, available and relatively inexpensive tool.

In contrary, magnetic resonance in the acute phase of stroke diagnostics is used only by the small number of stroke centres compared to CT (only one comprehensive stroke centre in the Czech Republic uses MR in the acute stroke setting). The main limitation of the routine MR use in the acute stroke management is a difficulty to maintain its availability in a 24/7 regime without restricting the remaining acute and/or routine care.

For the purpose of this thesis, the following chapters are dedicated to CT imaging in AIS.

1.2.1 Non-contrast CT

Non-contrast CT is a crucial imaging modality in all patients with suspected AIS. It helps to rule out other pathology, such as intracranial haemorrhage or mass lesion as well as to assess the presence and extent of ischemic changes. Early ischemic changes are manifested by the loss of grey-white differentiation on the basis of the developing cytotoxic edema. In some cases, these early changes can be expressed only as cortical swelling or sulcal effacement at the brain convexity (29).

In routine practice, the most common way of quantifying the extent of early ischemic changes is the ASPECTS score (Alberta Stroke Program Early CT Score) (30). Briefly, ASPECTS is a standardized quantitative scale assessing the extent of early ischemic changes in the brain parenchyma within the MCA territory, which distinguishes 10 anatomical areas (7 at the ganglionic and 3 at the supra-ganglionic level). Out of 10 points, one point is subtracted for each affected area, **Figure 1.1**.

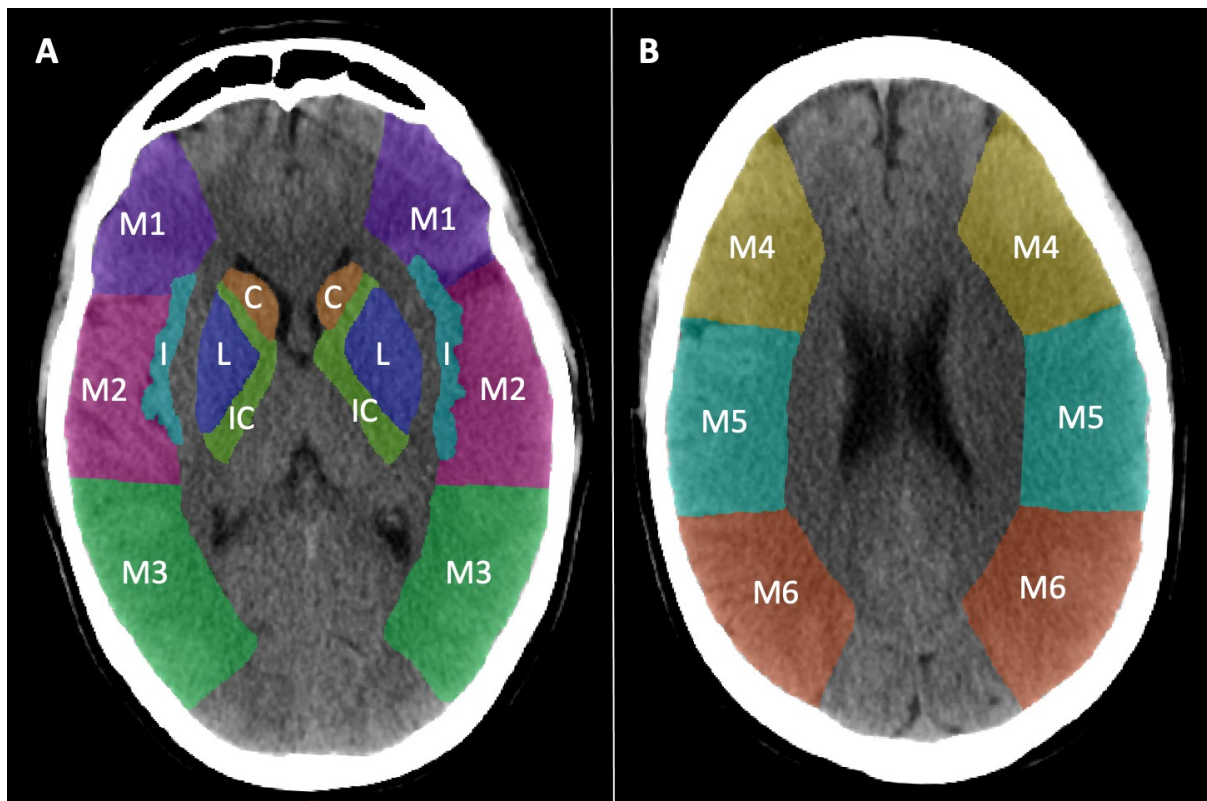
Although ASPECTS shows greater inter-rater reliability for assessing early ischemic changes in the MCA territory than the previously used method of $<1/3$ or $>1/3$ MCA territory involvement (30), the ASPECTS score is still prone to subjective error and varies among readers (31,32).

The automatic assessment of the ASPECTS is nowadays available (i.e. e-ASPECTS Brainomix, iSchemaView RAPID ASPECTS) demonstrating high reliability when compared to the experienced readers (33,34). The main benefit of the use of automatic software tools in clinical practice is the possibility of fastening the patient triage (34).

Another characteristics that can help in the differential diagnosis of a sudden neurological deficit is so-called “dense artery sign” which may reflect acute arterial occlusion by thrombus. On the non-contrast CT head, a higher density is detected within the arterial

lumen that varies between 60 and 90 HU and is due to the high erythrocyte content in the thrombus (35,36). However, the absence of this sign does not rule out the presence of a thrombus, therefore a subsequent CT angiography is required to identify the filling defect of the cerebral artery.

Figure 1.1. ASPECTS regions. The ten regions of the Alberta Stroke Program Early CT Score (ASPECTS) include the M1, M2, M3 territory, internal capsule (IC), caudate nucleus (C), lentiform nucleus (L), and insula (I) at the ganglionic level (A), and the M4, M5 and M6 territory at the supra-ganglionic level (B).



1.2.2 CT angiography

The detection of the arterial occlusion confirms the diagnosis of AIS and the thrombus localization guide the treatment decisions – occlusions of the large and medium vessels are less likely to recanalize with intravenous tPA alone (4). CT angiography (CTA) has a sensitivity and specificity of around 97% for large vessel occlusion detection, with high inter-observer reliability (37).

Vascular imaging of intra- and extracranial vasculature (arch-to-vertex) is routinely obtained in AIS patients, providing useful information on extracranial vessel tortuosity, atherosclerotic disease, and potential anatomic variants (4). In standard CTA, a bolus of iodinated contrast is injected, and a single angiography scan from aortic arch-to-vertex is obtained. In multiphase CTA (mCTA), the same contrast bolus is used to obtain two additional series during the peak-venous and late venous phase, the latter two phases covering only the area from the skull base to the vertex (intracranial vasculature) (38).

Several automated standalone acute stroke software platforms for detection of large vessel occlusion are available in the clinical practice, such as iSchemaView (RAPID CTA), Viz.ai (VIZ LVO), Brainomix (e-CTA), Canon (^{AUTO}Stroke Solution LVO) or StrokeViewer (NICO.LAB). These platforms use different artificial intelligence (AI) including machine-learning (ML) methods for automatic detection of LVOs. Strategies for computer-aided detection of LVO include the direct identification of occlusion site using local vascular features (i.e. detect the clot directly by identifying the discontinuity of the contrast-enhanced vessel), and the indirect identification of occlusion site based on the regional vessel density asymmetry between the affected hemisphere and the unaffected hemisphere (39).

In addition to localization of the occlusion, CTA also provides important information on the morphology of leptomeningeal collaterals. Standard CTA may underestimate the collateral extent as the CTA acquisition represents only a single snap-shot and the collateral anastomoses may not have been yet sufficiently opacified. The additional two phases of mCTA therefore overcomes this limitation and enable the better visualization of collaterals (38), **Figure 1.2.**

There are different scoring systems for CTA collateral assessment. The Miteff score (25) evaluates the degree of retrograde opacification of vessels within the affected MCA territory, the score by Tan et al. (40) considers percentage of the collateral filling within the affected territory compared to the contralateral hemisphere. Menon et al. first defined the collateral score using mCTA taking into account the delayed vessel opacification by one or two phases and, their prominence and overall extend compared to the contralateral unaffected hemisphere, **Table 1.1.**

Currently, various automatic software analysis for the collateral assessment are available. Brainomix e-CTA uses a percentage comparison of the collateral extent between the affected and healthy side with subsequent color marking (heat map) and a numerical score (0 = absence of collaterals or <10% collateral filling compared to the contralateral side; up to 3 = >90% collateral filling compared to the contralateral side) (41). RAPID e-CTA compares the

absolute density of the vasculature between the hemispheres. Based on the percentage difference in density, a color code is assigned to the affected territory (red = density <45%; yellow = density 45% to 60%; green = 60% to 74%; blue = 75% to 80%) (42).

Figure 1.2. Collateral scoring on multi-phase CT angiography in the axial plane. Top row: left-sided M1 middle cerebral artery segment occlusion with good collaterals (collaterals backfilling with one phase delay but normal extent); Middle row: left-sided M1 segment middle cerebral artery occlusion with intermediate collaterals (collaterals backfilling with one phase delay and decreased extent); Bottom row: left-sided M1 segment middle cerebral artery occlusion with poor collaterals (no backfilling of collaterals in the first phase and only very few collaterals visible in the second and third phases).

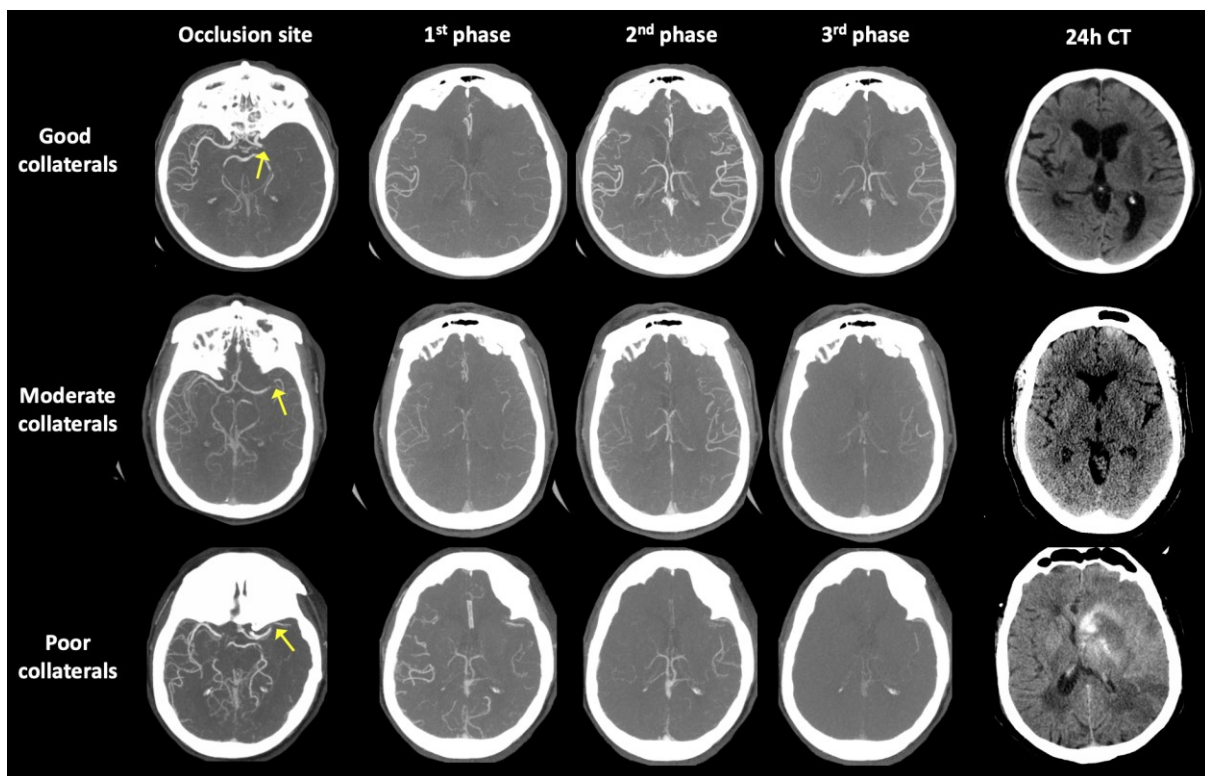


Table 1.1. Multiphase CTA collateral score

Multiphase CTA score		
Category	Score	Definition
Good	5	There is no delay and normal or increased prominence of pial vessels/normal extent within the ischemic territory in the symptomatic hemisphere compared to the asymptomatic contralateral hemisphere
	4	There is a one-phase delay in filling in of peripheral vessels, but prominence and extent is the same compared to the asymptomatic contralateral hemisphere
Moderate	3	There is a delay of two phases in filling in of peripheral vessels or there is a one-phase delay and significantly reduced number of vessels in the ischemic territory compared to the asymptomatic contralateral hemisphere
	2	There is a delay of two phases in filling in of peripheral vessels and decreased prominence and extent or a one-phase delay and some ischemic regions with no vessels compared to the asymptomatic contralateral hemisphere
Poor	1	there are just a few vessels visible in any phase within the occluded vascular territory compared to the asymptomatic contralateral hemisphere
	0	There are no vessels visible in any phase within the ischemic vascular territory compared to the asymptomatic contralateral hemisphere

1.2.3 CT perfusion

CT perfusion (CTP) is a functional examination of the brain tissue that characterizes the state of cerebral perfusion and thus informs about its functional state. The goal of perfusion analysis in the clinical use is to quantify tissue with significant hypoperfusion which is likely to infarct if reperfusion is not achieved (ischemic penumbra) and identify tissue that is likely irreversibly infarcted (ischemic core) (43).

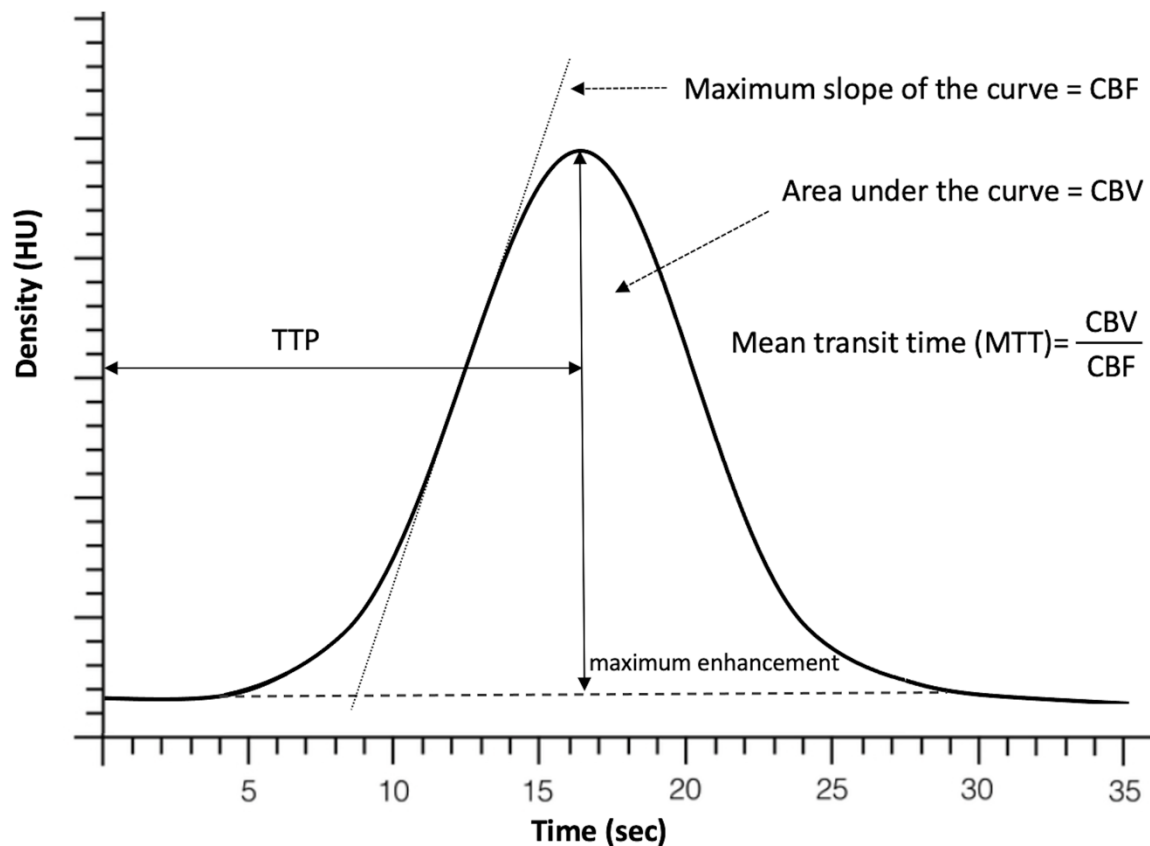
The essential hemodynamic parameters in CTP studies:

1. *Cerebral Blood Flow (CBF)* refers to the volume of blood flowing in a unit of brain mass during a unit of time, measured in milliliters/100 g/min (mL/100 g/min). CBF is often expressed proportionately (relative CBF) as normalized measure to a presumed normal reference region (in the contralateral hemisphere).

2. *Cerebral Blood Volume* (CBV) refers to the fraction of a tissue that is vascularized, expressed in the milliliters/100 g
3. *Mean Transit Time* (MTT) represents the average time that takes a contrast bolus to traverse the capillary bed; MTT is reported as an absolute in seconds.
4. *Time to maximum of the residual function* (Tmax) expresses the delay from the start of scan acquisition to the maximum intensity of contrast bolus in each voxel.

CBF, MTT, and CBV are mathematically related by the equation: $CBF = CBV/MTT$, known as the central volume principle (44). Therefore, measurement of any 2 of these parameters is sufficient to derive the third parameter (45), **Figure 1.3**.

Figure 1.3. Perfusion time attenuation curve. Time to peak (TTP) represents time it takes the contrast to achieve its maximum within the area of interest. Cerebral blood flow (CBF) is represented by the slope of the curve as contrast arrives into the brain and the cerebral blood volume (CBV) is expressed by the volume/area under the curve. Mean transit time (MTT) is then calculated as the ratio of CBV and CBF.



1.2.3.1 CT perfusion acquisition and postprocessing

CTP acquisition represents a dynamic capturing of a passing contrast bolus (its wash-in and wash-out) through the brain tissue (45,46). A slab of 8 to 16 cm of the brain is repeatedly scanned over 45 to 90 seconds. Based on the derived attenuation-time curves obtained for arterial input function (representing arterial flow/wash-in) and venous output function (representing venous flow/wash-out), perfusion parameters are calculated for each voxel. The results are displayed usually as color-coded maps (45).

The contrast passage and subsequent attenuation-time curves are dependent on arterial flow (expressed as arterial input function) and tissue characteristics. Among factors influencing the arterial flow of contrast media through the tissue belong impaired cardiac output, severe carotid stenosis or factors related to the contrast bolus injection (injection rate, saline chase). These factors may result in delay or dispersion of the contrast bolus which may introduce an error in the quantification of CBF (45).

Raw CTP data can be processed with 2 techniques to generate perfusion maps, non-deconvolution and deconvolution methods. Non-deconvolution methods are based on first-pass iodine extraction measurements resulting in a simplified and less computationally intensive processing algorithm. Deconvolution methods account for physiological variations in arterial flow, the collateral flow effect, and venous outflow components of cerebral perfusion (45) and correct for the inability to deliver a contrast bolus directly into the supplying artery of a tissue of interest (11).

There exist different deconvolution methods: singular value decomposition (SVD) (47), delay- and dispersion-corrected singular value deconvolution (dd-SVD) (48), and Bayesian methodologies (49). dd-SVD or Bayesian-estimated generate the arterial delay time in contrast T_{max} derived from SVD model. Use of different deconvolution methods may result in a the measurement variability of the core and penumbra based on the deconvolution algorithm (45).

1.2.3.2 Technical pitfalls

The technical factors influencing reliability of the perfusion maps are CT X-ray tube voltage, total duration of scan acquisition, contrast bolus injection, brain coverage, frame rate (time between frames in the scans) and scan order (46).

A well-known limitation of CT perfusion is its low contrast to noise ratio when compared to MR perfusion. To optimize contrast-to-noise and keep the radiation dose as low as reasonably achievable (ALARA principle), CTP scans are recommended to be acquired at 70–80 kV (46).

Optimization of timing parameters is required to capture the complete contrast passage and avoid excessively long scanning before or after the contrast passage. The optimal scan should capture a short baseline period (5–10 sec) with no contrast and the complete pass of the contrast bolus through a main cerebral vein (which follows the arterial contrast bolus pass) (46). This duration varies between patients. Empiric data showed that complete contrast passage was captured in >90% of patients with a scan duration of 60 sec (50). Based on this finding, an optimal scan duration should be planned for 60 to 70 sec (45).

The duration of the baseline is determined by the timing of the contrast bolus injection. Empiric data showed that a short (5–10 sec) baseline was obtained in most patients when acquisition starts 4s after start of the contrast injection. Administration of the contrast bolus with a power injector ensures consistency of acquisition. In general, it is recommended to administer 40mL contrast agent at 4–6 ml/s followed by 40 ml saline at 4–6 ml/s (46).

Z-axis brain coverage is primarily determined by the CT detector width and varies from 4 to 16 cm on most modern scanners. The minimal brain coverage of 4 cm obtained with narrow CT detectors may not be sufficient to capture the lesion with affected perfusion. It is therefore recommended obtaining at least 8 cm of z-axis coverage, extending rostrally from above the orbits (46).

The quality of the perfusion maps can be also impacted by low frame rates, and in order to generate reliable perfusion studies, frame sampling should be set to less than 2s when possible (46). It is beneficial to scan the patient with the head in a symmetrical position without any head tilt. The CTP software uses the contralateral side as reference for perfusion parameters calculations and significant asymmetry between the brain hemispheres could lead to incorrect results (45).

1.2.3.3 Interpretation of CT perfusion

There are few pitfalls hidden in the CTP interpretation. A variety of thresholds have been used to define ischemic core and penumbra by different software packages. These differences result in discrepancies in the size of the core and penumbra, ranging from 50 ml underestimation to >50 ml overestimation of core volumes compared to follow-up infarct volume (51). Such a differences may subsequently influence patient selection for reperfusion therapy.

Similarly to the use of automatic assessment of early ischemic changes on non-contrast CT or LVO detection on CTA, the automated perfusion analyses are nowadays used in clinical practice allowing for potential reduction of triage times by identifying the patients with potentially salvageable tissue who would benefit from treatment (10).

Several EVT trials used perfusion thresholds as imaging inclusion criteria (52–55) using RAPID-AI automatic software analysis. In this software, the ischemic core is defined as relative CBF <30% of the value in the contralateral hemisphere, and ischemic penumbra region is defined as Tmax delay of >6 sec compared to the contralateral hemisphere, **Figure 1.4**. The cut-off value of CBF for the RAPID-AI core was chosen to not significantly overestimate the size of the core, which would lead to undesirable patients over-selection. In contrary, a significant underestimation of the core would increase the risk of hemorrhagic transformation and reduce the probability of a good clinical outcome (56). With the chosen ischemic core threshold value of rCBF <30% allows, the expected core underestimation is approximately 10-15 ml (53).

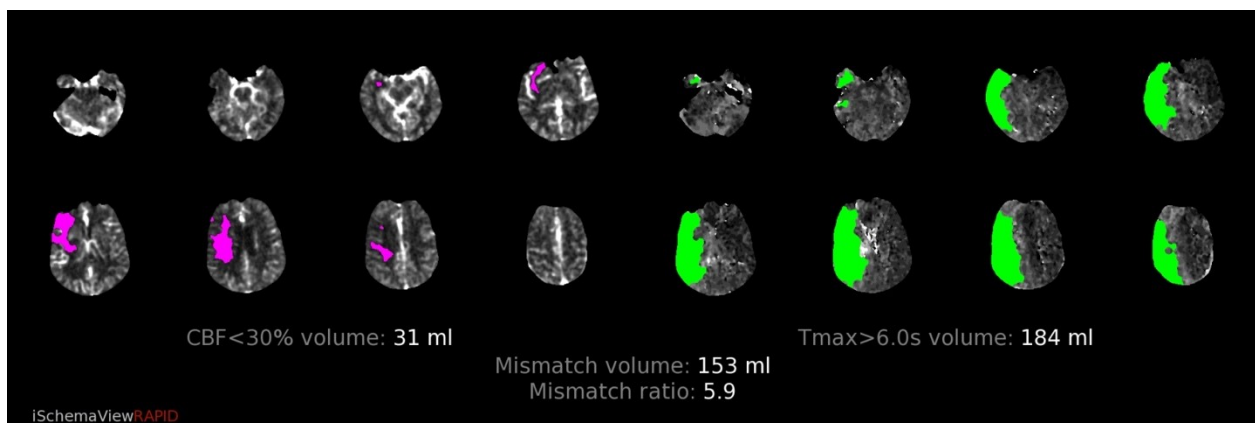
There are other automatic software for perfusion analysis, such as Olea Medical software (Brainomix) or Viz.ai. Olea software uses the Bayesian algorithm for perfusion parameters calculation that results in definition of the ischemic core as CBF <40% together with Tmax delay >2 sec, and penumbra as delay Tmax >6s (57). The potential advantages of using the Bayesian algorithm is the use of the half of the standard volume of the contrast media (58).

It is important to note that the CTP threshold are not absolute. It was shown that ischemic core may be overestimated if perfusion imaging is performed very early after the symptom onset (16), and the use of more strict thresholds should be considered, especially if the baseline imaging was performed within the first hour (“golden hour”) (59). The core overestimation was also demonstrated in patients with achieved rapid reperfusion (16).

Although it is known that the white matter is more resistant to the hypoperfusion and therefore more strict thresholds should be applied to distinguish grey and white matter at risk of infarction with a higher accuracy (60), this differentiation is not widely used in clinical practice and remains to be so far of a research interest.

The tissue fate prediction is also associated with the severity of hypoperfusion (43,61). Severely hypoperfused tissue defined as Tmax delay >10s tends to progress more rapidly than the tissue with better residual perfusion through collateral flow. The severity of hypoperfusion can be quantified by the hypoperfusion intensity ratio (HIR), which represents the proportion of Tmax >6s perfusion lesion with Tmax >10s perfusion lesion. The high HIR was proved to predict the poor collaterals and infarct progression (61).

Figure 1.4. CT perfusion analysis using RAPID-AI. Exemplary case of the overview perfusion map in patient with right MCA occlusion. Ischemic core defined as relative CBF <30% is displayed in purple color on the left side of the overview map (the core volume is 31ml in this particular case). The area in green on the right side of the map represents hypoperfused tissue with Tmax delay of > 6 sec compared to the contralateral hemisphere (184 ml). The difference between these volumes (mismatch volume) represents the penumbra volume, the mismatch ratio expresses how many times is the penumbra volume larger than the predicted ischemic core volume.



1.3. CURRENT STATE OF IMAGING IN ACUTE ISCHEMIC STROKE DIAGNOSIS AND TREATMENT DECISION

The indication of the particular CT modalities is currently based on the time from the symptom onset. In order to administer intravenous thrombolysis within 4.5 hours of onset, non-contrast CT scan is required to rule out intracranial hemorrhage or other non-vascular pathology (e.g. tumor). Beside excluding the hemorrhage, non-contrast scan is used to detect early ischemic changes. CTA is used not only to confirm the AIS by detecting the arterial occlusion, but it is also highly recommended in patients indicated for mechanical thrombectomy to evaluate the extracranial vascular anatomy.

CTP scan is primarily beneficial in patients presenting between 6 and 24 hours from the symptom onset or in cases where the time of onset is unclear. CTP enables to identify patients with potentially salvageable ischemic penumbra. In patients with unknown stroke onset (unclear time of onset or awakening with symptoms of CMP = “wake-up” stroke), the patient care is not strictly determined by the “time window” (“time is brain” concept (10)), but by so-called “tissue window” (“imaging is brain” concept (62,63)). Based on the results of the pooled data analysis from the EXTEND, ECASS4-EXTEND, and EPITHET clinical trials

(64), the treatment window for the intravenous thrombolysis has been extended beyond 4.5 hours in patients with mismatch profile (presence of ischemic penumbra). Another advantage of CTP even in early stages is the identification of perfusion lesion (hypoperfused area). This typically refers to situations when patients have small neurological deficit or repeated AIS with residual neurological deficit after the prior stroke, or when stroke-mimics are suspected.

1.4 FUTURE DIRECTIONS

The numerous different software solutions for image analysis and different imaging modalities are currently used in acute stroke imaging, however, lead to lack of standardization and comparability (4). For example, CTP thresholds should be harmonized throughout different vendors and software packages.

The expanding availability of the automatic software analysis enables primarily to fasten the patients' triage in the acute management and also reduce the inter-rater variability. For example, automated ASPECTS scoring based on machine-learning algorithms was shown to be reliable (33,34), and is expected to be soon used routinely in clinical practice.

Novel visual aids, such as time-variant mCTA maps or mCTA-derived CTP-like maps are promising tools that have been recently introduced and can help less experienced readers and thus potentially decrease the interpretation time (65,66). These can be obtained within seconds, with little computational effort and with no additional use of contrast or radiation dose compared to the CTP acquisition.

Time-variant (color-coded) mCTA display format encodes vascular information from all mCTA phases into a single color-coded map, combining the indicator effect of color with the technical advantages of mCTA. The assessment of the pial arterial filling using ColorViz is based on visual determination of the predominant vessel color (the color that is present in more than 40% of the vessels) in the affected vascular territory. Under standard circumstances, predominantly blue vessels indicate a 2-phase delay, green vessels a 1-phase delay and predominantly red vessels no delay. Differentiation of veins and arteries is based on their distinct flow characteristics (veins usually enhance in the peak venous and late venous phase and are therefore displayed in green or blue), filling direction, morphology and anatomical location (65).

mCTA-derived CTP-like maps are based on the machine learning technique to estimate infarct core and ischemic penumbra in patients with AIS. It has been shown that mCTA derived CTP-like maps demonstrated comparable accuracy to traditional CTP in predicting tissue fate (66).

1.5 AIMS AND OUTLINE OF THE THESIS

Despite the known applications of CTA and wide use of CTP as a part of the standard stroke management protocol, the main aim of this thesis was to further evaluate the utilization of these imaging modalities in the diagnosis and treatment decision in patients with acute ischemic stroke caused by the occlusion of the middle cerebral artery.

Part I of this thesis focuses on the assessment of correlations of different CT modalities. The correlation of the leptomeningeal collateral grading using mCTA and perfusion lesion volumes derived from the automatic CTP analysis was investigated in **Chapter 2**. In **Chapter 3**, we investigated the accuracy of different CT modalities including also automatically-derived CTP maps in the assessment of the early ischemic changes and their accuracy for the final infarct prediction.

Part II explores advanced applications and postprocessing of CTA. The machine learning based software tool for automated ICA and MCA occlusion detection in patients with suspected acute stroke using was validated and its high accuracy was demonstrated (**Chapter 4**). **Chapter 5** discusses the utility of time-variant mCTA maps in the prediction of the clinical outcome and final infarct volume compared to the conventional mCTA collateral grading. In **Chapter 6** investigates the accuracy of medium vessel occlusions (MeVO) on mCTA-derived tissue maps.

In **Chapter 7**, the general implications of the findings in this thesis and directions for the future research are discussed.

REFERENCES

1. Katan M, Luft A. Global burden of stroke. *Semin Neurol* 2018;38:208-211.
2. Tsao CW, Aday AW, Almarzooq ZI, et al. Heart disease and stroke statistics—2022 update: a report from the american heart association. *Circulation* 2022;145:e153-e639.
3. Powers WJ, Rabinstein AA, Ackerson T, et al. Guidelines for the early management of patients with acute ischemic stroke: 2019 update to the 2018 guidelines for the early management of acute ischemic stroke a guideline for healthcare professionals from the american heart association/american stroke association. *Stroke* 2019;50:E344-E418.
4. Ospel JM, Cimflova P, Goyal M. Stroke imaging. *Atlas Emerg Imaging from Head-to-Toe* 2021:1-14.
5. Cipolla MJ, Bullinger L V. Reactivity of brain parenchymal arterioles after ischemia and reperfusion. *Microcirculation* 2008;15:495.
6. Fantini S, Sassaroli A, Tgavalekos KT, Kornbluth J. Cerebral blood flow and autoregulation: Current measurement techniques and prospects for noninvasive optical methods. *Neurophotonics* 2016;3:031411.
7. Astrup J, Siesjö BK, Symon L. Thresholds in cerebral ischemia — the ischemic penumbra. *Stroke* 1981;12:723-725.
8. Cipolla M, Rafael S. Control of cerebral blood flow - the cerebral circulation - ncbi bookshelf. *The Cerebral Circulation*.
9. Hossmann KA. Pathophysiology and therapy of experimental stroke. *Cell Mol Neurobiol* 2006;26:1057-1083.
10. Saver JL. Time is brain—quantified. *Stroke* 2006;37:263-266.
11. d’Esterre CD. Improving acute stroke management with CT perfusion imaging: approaches to treatment guidance and braintissue salvage. *Univ West Ontario - Electron Thesis Diss Repos* 2013:Paper 1239.
12. Belov Kirdajova D, Kriska J, Tureckova J, Anderova M. Ischemia-triggered glutamate excitotoxicity from the perspective of glial cells. *Front Cell Neurosci* 2020;14.
13. Papazian I, Kyrargyri V, Evangelidou M, Voulgari-Kokota A, Probert L. Mesenchymal stem cell protection of neurons against glutamate excitotoxicity involves reduction of nmda-triggered calcium responses and surface glur1, and is partly mediated by tnf. *Int J Mol Sci* 2018;19.
14. Arakawa S, Wright PM, Koga M, et al. Ischemic thresholds for gray and white matter. *Stroke* 2006;37:1211-1216.
15. Røhl L, Østergaard L, Simonsen CZ, et al. Viability thresholds of ischemic penumbra

- of hyperacute stroke defined by perfusion-weighted MRI and apparent diffusion coefficient. *Stroke* 2001;32:1140-1146.
16. D'Esterre CD, Boesen ME, Ahn SH, et al. Time-dependent computed tomographic perfusion thresholds for patients with acute ischemic stroke. *Stroke* 2015;46:3390-3397.
 17. Goyal M, Ospel JM, Menon B, et al. Challenging the ischemic core concept in acute ischemic stroke imaging. *Stroke* 2020;3147-3155.
 18. Jones TH, Morawetz RB, Crowell RM, et al. Thresholds of focal cerebral ischemia in awake monkeys. *J Neurosurg* 1981;54:773-782.
 19. Symon L, FRCS. The relationship between CBF, evoked potentials and the clinical features in cerebral ischaemia. *Acta Neurol Scand* 1980;62:175-190.
 20. Hossmann K -A. Viability thresholds and the penumbra of focal ischemia. *Ann Neurol* 1994;36:557-565.
 21. Kamalian S, Kamalian S, Konstas AA, et al. CT perfusion mean transit time maps optimally distinguish benign oligemia from true "at-risk" ischemic penumbra, but thresholds vary by postprocessing technique. *Am J Neuroradiol* 2012;33:545-549.
 22. Liebeskind DS. Collateral circulation. *Stroke* 2003;34:2279-2284.
 23. Menon BK, O'Brien B, Bivard A, et al. Assessment of leptomeningeal collaterals using dynamic CT angiography in patients with acute ischemic stroke. *J Cereb Blood Flow Metab* 2013;33:365-371.
 24. Seifert K, Heit JJ. Collateral blood flow and ischemic core growth. *Transl Stroke Res* June 2022.
 25. Miteff F, Levi CR, Bateman GA, Spratt N, McElduff P, Parsons MW. The independent predictive utility of computed tomography angiographic collateral status in acute ischaemic stroke. *Brain* 2009;132:2231-2238.
 26. Menon BKK, Smith EEE, Modi J, et al. Regional leptomeningeal score on CT angiography predicts clinical and imaging outcomes in patients with acute anterior circulation occlusions. *AJNR Am J Neuroradiol* 2011;32:1640-1645.
 27. Brozici M, Van der Zwan A, Hillen B. Anatomy and functionality of leptomeningeal anastomoses: A review. *Stroke* 2003;34:2750-2762.
 28. Ribo M, Molina CA, Delgado P, et al. Hyperglycemia during ischemia rapidly accelerates brain damage in stroke patients treated with tPA. *J Cereb Blood Flow Metab* 2007;27:1616-1622.
 29. Cimflová P, Vališ K, Volný O, Vinklársek J, Haršány M, Mikulík R. Diagnostika ischemických CMP - přehled zobrazovacích metod a jejich využití v praxi. *Česká Radiol*

- 2019;73:150-159.
30. Barber PA, Demchuk AM, Zhang J, Buchan AM. Validity and reliability of a quantitative computed tomography score in predicting outcome of hyperacute stroke before thrombolytic therapy. ASPECTS study group. Alberta Stroke Programme Early Ct Score. *Lancet (London, England)* 2000;355:1670-1674.
 31. Gupta AC, Schaefer PW, Chaudhry ZA, et al. Interobserver reliability of baseline noncontrast CT Alberta Stroke Program Early CT score for intra-arterial stroke treatment selection. *AJNR Am J Neuroradiol* 2012;33:1046-1049.
 32. Naylor J, Churilov L, Rane N, Chen Z, Campbell BCV, Yan B. Reliability and utility of the Alberta Stroke Program Early Computed Tomography score in hyperacute stroke. *J Stroke Cerebrovasc Dis* 2017;26:2547-2552.
 33. Nagel S, Sinha D, Day D, et al. E-aspects software is non-inferior to neuroradiologists in applying the ASPECT score to computed tomography scans of acute ischemic stroke patients. *Int J Stroke* 2017;12:615-622.
 34. Herweh C, Ringleb PA, Rauch G, et al. Performance of e-aspects software in comparison to that of stroke physicians on assessing CT scans of acute ischemic stroke patients. *Int J Stroke* 2016;11:438-445.
 35. Kucinski T. Unenhanced CT and acute stroke physiology. *Neuroimaging Clin N Am* 2005;15:397-407.
 36. Puig J, Pedraza S, Demchuk A, et al. Quantification of thrombus hounsfield units on noncontrast CT predicts stroke subtype and early recanalization after intravenous recombinant tissue plasminogen activator. *Am J Neuroradiol* 2012;33:90-96.
 37. Amukotuwa SA, Straka M, Dehkharghani S, Bammer R. Fast automatic detection of large vessel occlusions on CT angiography. *Stroke* 2019;50:3431-3438.
 38. Menon BK, D'Este CD, Qazi EM, et al. Multiphase CT angiography: A new tool for the imaging triage of patients with acute ischemic stroke. *Radiology* 2015;275:510-520.
 39. Cimflova P, Golan R, Ospel JM, et al. Validation of a machine learning software tool for automated large vessel occlusion detection in patients with suspected acute stroke. *Neuroradiology* May 2022:1-11.
 40. Tan IYL, Demchuk AM, Hopyan J, et al. CT angiography clot burden score and collateral score: Correlation with clinical and radiologic outcomes in acute middle cerebral artery infarct. *Am J Neuroradiol* 2009;30:525-531.
 41. Seker F, Pfaff JAR, Mokli Y, et al. Diagnostic accuracy of automated occlusion detection in CT angiography using e-CTA. *Int J Stroke* February 2021.

42. Amukotuwa SA, Straka M, Smith H, et al. Automated detection of intracranial large vessel occlusions on computed tomography angiography a single center experience. *Stroke* 2019;50:2790-2798.
43. Demeestere J, Wouters A, Christensen S, Lemmens R, Lansberg MG. Review of perfusion imaging in acute ischemic stroke: From time to tissue. *Stroke* 2020;51:1017-1024.
44. MEIER P, ZIERLER KL. On the theory of the indicator-dilution method for measurement of blood flow and volume. *J Appl Physiol* 1954;6:731-744.
45. Vagal A, Wintermark M, Nael K, et al. Automated ct perfusion imaging for acute ischemic stroke: pearls and pitfalls for real-world use. *Neurology* 2019;93:888-898.
46. Christensen S, Lansberg MG. CT perfusion in acute stroke: practical guidance for implementation in clinical practice. *J Cereb Blood Flow Metab* 2019;39:1664-1668.
47. Fieselmann A, Kowarschik M, Ganguly A, Hornegger J, Fahrig R. Deconvolution-based CT and MR brain perfusion measurement: Theoretical model revisited and practical implementation details. *Int J Biomed Imaging* 2011;2011.
48. Bivard A, Levi C, Spratt N, Parsons M. Perfusion ct in acute stroke: A comprehensive analysis of infarct and penumbra. *Radiology* 2013;267:543-550.
49. Boutelier T, Kudo K, Pautot F, Sasaki M. Bayesian hemodynamic parameter estimation by bolus tracking perfusion weighted imaging. *IEEE Trans Med Imaging* 2012;31:1381-1395.
50. Kasasbeh AS, Christensen S, Straka M, et al. Optimal computed tomographic perfusion scan duration for assessment of acute stroke lesion volumes. *Stroke* 2016;47:2966-2971.
51. Austein F, Riedel C, Kerby T, et al. Comparison of perfusion CT software to predict the final infarct volume after thrombectomy. *Stroke* 2016;47:2311-2317.
52. Campbell BCV, Yassi N, Ma H, et al. Imaging selection in ischemic stroke: feasibility of automated CT-perfusion analysis. *Int J Stroke* 2015;10:51-54.
53. Saver JL, Goyal M, Bonafe A, et al. Stent-retriever thrombectomy after intravenous t-PA vs. t-PA alone in stroke. *N Engl J Med* 2015;372:2285-2295.
54. Nogueira RG, Jadhav AP, Haussen DC, et al. Thrombectomy 6 to 24 hours after stroke with a mismatch between deficit and infarct. *N Engl J Med* 2018;378:11-21.
55. Albers GW, Marks MP, Kemp S, et al. Thrombectomy for stroke at 6 to 16 hours with selection by perfusion imaging. *N Engl J Med* 2018;378:708-718.
56. Mokin M, Levy EI, Saver JL, et al. Predictive value of rapid assessed perfusion thresholds on final infarct volume in SWIFT PRIME (Solitaire With the Intention For

- Thrombectomy as Primary Endovascular Treatment). *Stroke* 2017;48:932-938.
57. Uwano I, Sasaki M, Kudo K, et al. Tmax determined using a bayesian estimation deconvolution algorithm applied to bolus tracking perfusion imaging: A digital phantom validation study. *Magn Reson Med Sci* 2017;16:32-37.
 58. Nael K, Mossadeghi B, Boutelier T, et al. Bayesian estimation of cerebral perfusion using reduced-contrast-dose dynamic susceptibility contrast perfusion at 3T. *AJNR Am J Neuroradiol* 2015;36:710-718.
 59. Najm M, Al-Ajlan FS, Boesen ME, et al. Defining CT perfusion thresholds for infarction in the golden hour and with ultra-early reperfusion. *Can J Neurol Sci* 2018;45:339-342.
 60. Chen C, Bivard A, Lin L, Levi CR, Spratt NJ, Parsons MW. Thresholds for infarction vary between gray matter and white matter in acute ischemic stroke: a CT perfusion study. *J Cereb Blood Flow Metab* 2019;39:536-546.
 61. Olivot JM, Mlynash M, Inoue M, et al. Hypoperfusion intensity ratio predicts infarct progression and functional outcome in the DEFUSE 2 cohort. *Stroke* 2014;45:1018-1023.
 62. Albers GW, Goyal M, Jahan R, et al. Ischemic core and hypoperfusion volumes predict infarct size in SWIFT PRIME. *Ann Neurol* 2016;79:76-89.
 63. Lansberg MG, Straka M, Kemp S, et al. MRI profile and response to endovascular reperfusion after stroke (DEFUSE 2): a prospective cohort study. *Lancet Neurol* 2012;11:860-867.
 64. Campbell BCV, Ma H, Ringleb PA, et al. Extending thrombolysis to 4·5–9 h and wake-up stroke using perfusion imaging: A systematic review and meta-analysis of individual patient data. *Lancet* 2019;394:139-147.
 65. Ospel JM, Volny O, Qiu W, et al. Displaying multiphase CT angiography using a time-variant color map: Practical considerations and potential applications in patients with acute stroke. *AJNR Am J Neuroradiol* 2020;41:200-205.
 66. Qiu W, Kuang H, Ospel JM, et al. Automated prediction of ischemic brain tissue fate from multiphase computed tomographic angiography in patients with acute ischemic stroke using machine learning. *J Stroke* 2021;23:234-243.

Part I

*Utilization of CT Angiography and CT Perfusion in
Acute Stroke Imaging*

2. Chapter 2 - Correlation of the multiphase CTA collateral score and the automatically-derived CT perfusion volumes

The contents of this chapter have been adapted from the journal article entitled “*Detection Correlation of the multiphase CTA collateral score and the automatically-derived CT perfusion volumes*”, submitted to Journal of Stroke and Cerebrovascular Diseases by P. Cimflova, K. Holikova, B.J. Kim, et al.

Background: Previous studies comparing collateral flow on CTA and CTP focused on good collaterals. While multiphase CTA (mCTA) enables visualization of delayed filling, intermediate collateral should still be considered as sufficient. Therefore, we evaluated the automatically-derived CTP lesion volumes (PLV) with mCTA collateral grades.

Methods: Imaging data of consecutive patients from Jan-2016 to Dec-2020 undergoing mechanical thrombectomy were retrospectively reviewed. Patients with terminal ICA and M1/M2-MCA occlusion and available baseline mCTA and CTP were included. Collaterals were assessed as good, intermediate or poor. PLV parameters were defined as Tmax delay >4s, >6s, >8s, >10s, CBF<30%. PLV and hypoperfusion intensity ratio (HIR) were compared across collateral score categories using Kruskal-Wallis and Wilcoxon rank-sum test. Correlation coefficients were calculated using Spearman’s rho. The cut-off values for PLV and HIR representing poor collaterals were derived from the receiver operating characteristic curve analysis.

Results: Out of 341 patients, 147 were included (44% women, mean age 71±14 years, median NIHSS 16, median ASPECTS 8). The median onset-to-CT time was 82.5 min. Sixty-three patients had good, 73 intermediate, and 11 poor collaterals. The PLV significantly differed between good and poor collaterals for Tmax>10s, >8s, >6s, CBF<30% and HIR. The highest correlation was demonstrated for Tmax >10s ($\rho=-.50$), followed by HIR ($\rho=-.47$) and CBF<30% ($\rho=-.42$). The poor collaterals were represented with CBF<30% of 31ml (AUC=0.77;sensitivity of 0.82;specificity 0.73), followed by Tmax>10s PLV of 114 ml (AUC=0.75;sensitivity of 0.64; specificity 0.84).

Conclusion: We demonstrated that mCTA collateral score corresponds to PLV with significant difference in PLV between good and poor collaterals .

2.1 INTRODUCTION

The quality of the leptomeningeal collateral flow in the acute ischemic stroke due to the large vessel occlusion in the anterior territory is associated with patients' clinical outcome (1,2), infarct growth and final infarct volume (3–5), and hemorrhagic transformation (6).

Various methods of collateral assessment have been developed over the past years. Besides the gold standard imaging of the collaterals on the digital subtraction angiography, CT/MR angiography are the most common methods of collateral evaluation, especially in the setting of the acute ischemic stroke where fast diagnostic tools are required (7). Multiphase CTA (mCTA) is a technique that generates time-resolved cerebral angiograms from skull base to vertex with two additional phases enabling evaluation of the delayed filling within the affected MCA territory (8).

Novel approaches suggested the collateral assessment based on the CT perfusion (CTP) parameters such as time-to-maximum-of-the-residual-function (Tmax) (9), hypoperfusion intensity ratio (HIR) (10,11) or CBV-index (12,13).

Previously published studies (10,12,14) comparing the collateral flow on CTA and CTP were predominantly focused on the associations related to the good collaterals. In the original publication by Menon et al. (8), in which the authors introduced mCTA, they highlighted a possibility of the underestimation of the leptomeningeal collateral flow on the standard (single-phase) CTA. That means that also intermediate collaterals (represented by delayed filling of the collaterals by 1 phase and some decrease in their extend or 2 phase delay but no decrease in extend compared to the unaffected side) should still be considered sufficient rather than poor. This assumption was followed by including both good and intermediate collateral flow grades into the imaging criteria of the randomized clinical trials such as ESCAPE (15), ESCAPE-NA1 (16) and currently ongoing ESCAPE-NEXT (NCT0446253). Therefore, the aim of the study was to evaluate perfusion lesion volumes (PLV) for each collateral grade and identify automatically derived CTP parameters associated with poor collateral flow as defined by Menon et al. (8)

2.2 MATERIALS & METHODS

2.2.1 Patient selection

Retrospective review of imaging data of consecutive patients who underwent mechanical thrombectomy at the comprehensive stroke center during the period from Jan 2016 to Dec 2020 was performed. Patients with intracranial terminal internal carotid artery occlusion (ICA) and middle cerebral artery occlusions (M1 and proximal M2 segments) with available baseline

imaging data including mCTA and CTP were included. Multiphase CTA is used as a stroke imaging standard at our center since 2013, and all patients with symptoms of AIS and no history of contrast allergy routinely undergo NCCT, mCTA and CTP in our institution.

Ethical approval was obtained from the local Institutional Review Boards (the Boards waived the need for patient consent).

2.2.2. Imaging protocol

The imaging protocol set up in our comprehensive stroke center consisted of NCCT, mCTA and CTP.

Multiphase CTA consists of three scanning phases after the contrast media injection (60ml of iodine contrast agent [Iomeron 300; Bracco Imaging, Konstanz, Germany] power-injected at 5ml/s followed by a saline chase of 40ml at 5ml/s) with a 0.625mm section thickness. The first phase from the aortic arch to the cranial vertex was followed by two additional phases from the skull base to the cranial vertex with a delay allowing the table repositioning between particular scanning phases and resulting in the performance of each phase 8s apart (120kv, Auto mA/Smart mA, rotation time 0.6s, pitch 0.98, collimation 64x0.625mm). Image acquisition was triggered by bolus tracking in the ascending aorta. According to the original protocol (8), each phase had increased noise index (13.86-15.84) in order to achieve lower total radiation dose.

For the CTP protocol, 40 ml of contrast agent (Iomeron 300; Mallinckrodt Pharmaceuticals; Dublin, Ireland) was power injected at 5 ml/s followed by a saline chase of 50 ml at 5 ml/s. Sections of 8cm thickness were acquired at 10 mm slice thickness. Scanning began after a delay of 5s from contrast injection in every 1.8s for 75s.

2.2.3 Image processing

CT perfusion studies were post-processed using the RAPID software (iSchemaView, Menlo Park, CA, USA) to generate perfusion maps of cerebral blood flow (CBF), cerebral blood volume (CBV), mean transit time (MTT), and time to the maximum of the residue function (Tmax). The RAPID software also automatically segmented and calculated volumes of the presumed ischemic core (defined as a relative regional CBF <30%) (17) and volumes of hypoperfused tissue with Tmax delay of >4s, >6s, >8s, and >10s.

2.2.4 Image review

The quality of leptomeningeal collaterals was assessed according to the original collateral score introduced by Menon et al. (8) by an experienced reader (PC, more than 8-year experience with stroke imaging evaluation). The collateral score was evaluated blindly to the patients' history and CTP maps. The collaterals were trichotomized into good (score = 4-5), intermediate (score = 2-3), and poor (score = 0-1).

The data regarding particular CTP volumes were extracted independently of the imaging and clinical data. Hypoperfusion intensity ratio (HIR), representing the proportion of Tmax delay > 10 s over Tmax delay > 6 s, was calculated (18).

2.2.5 Statistical Analysis

Clinical and imaging baseline characteristics were summarized using descriptive statistics. PLV parameters were defined as Tmax delay >4s, >6s, >8s, >10s, CBF<30%, and HIR. These parameters were compared across the collateral score categories using Kruskal-Wallis test and Wilcoxon rank-sum test. Spearman's coefficients were used to quantify correlations between the extent of collaterals and PLV or HIR. The cut-off values and their sensitivity and specificity for poor collaterals were calculated from area-under-the-curve of receiver operating characteristic curve analyses. Sensitivity analysis was performed for a subgroup with terminal ICA and M1 MCA occlusions only. All analyses were performed in Stata 16.1 (StataCorp LLC, College Station, TX, USA).

2.3 RESULTS

2.3.1 Baseline Characteristics

Mechanical thrombectomy was performed in 341 patients during the selected study period. Forty patients with the posterior circulation occlusions, 9 patients with isolated cervical ICA occlusion or ICA dissection, and 142 patients with no CTP baseline imaging were excluded. Additionally, 3 patients with poor CTP quality resulting in uninterpretable CTP maps were excluded. Data from 147 were analyzed, out of which 69 (44.2%) were women. The mean age was 71 ± 14 years, median baseline NIHSS was 16 [interquartile range (IQR) 12-19] and the median baseline ASPECTS was 8 (IQR 7-9). The median time from the onset to CT was 83 min (IQR 60-169 min), all included patients had the baseline CT <6h from the symptom onset. Leptomeningeal collaterals were scored as good in 63 (42.9%), intermediate in 73 patients (49.7%), and poor in 11 patients (7.5%). 20 patients had terminal ICA occlusion, 96 patients

(65.3%) had M1-MCA occlusion and 31 (21.1%) patients had M2-MCA occlusion. The collateral status differed between the occlusion sites ($p=0.002$) with the better collateral score in M2 occlusions [good collaterals in 21/31 (67.7%) in M2-MCA occlusions compared to 38/96 (39.6) and 4/20 (20%) in M1-MCA and terminal ICA occlusions, respectively].

2.3.2 Collateral score and hypoperfusion volumes

The PLVs significantly differed between good and poor collateral status in $T_{max} >10s$, $T_{max} >8s$, $T_{max} >6s$, and $CBF <30\%$; between good and intermediate collaterals in all evaluated perfusion parameters. The PLVs were similar between intermediate and poor collaterals except for the PLV from $CBF <30\%$, **Table 2.1 & Figure 2.1**.

Similar to perfusion lesion volumes, HIR was increasing with decreasing collateral grade and was significantly different between good and poor collateral grade ($p <0.001$) and between good and intermediate collateral grade ($p <0.001$).

The Spearman's rho demonstrated significant correlations between the collateral score and the perfusion lesion volumes and HIR, with the lowest coefficients for $T_{max} >10s$ ($\rho=-0.50$) and HIR ($\rho=-0.47$), **Table 2.2**.

Table 2.1. Hypoperfusion volumes in different collateral grades correlation.

Perfusion parameter	Hypoperfusion volumes (ml), median (IQR)			
	Good collaterals n=63	Intermediate collaterals n=73	Poor collaterals n=11	p-value*
$T_{max} >10s$	36 (11 – 56)	80 (57 – 110)	125 (59 – 149)	<0.001
$T_{max} >8s$	61 (29 – 90)	110 (94 – 138)	156 (81 – 172)	<0.001
$T_{max} >6s$	107 (59 - 141)	152 (127 – 210)	185 (89 – 216)	<0.001
$T_{max} >4s$	187 (126 – 282)	246 (198 – 316)	262 (157–350)	0.002
$CBF <30\%$	7 (0 – 19)	25 (12 – 40)	65 (33 – 103)	<0.001
HIR	0.33 (0.19-0.49)	0.52 (0.35-0.65)	0.63 (0.48-0.74)	<0.001

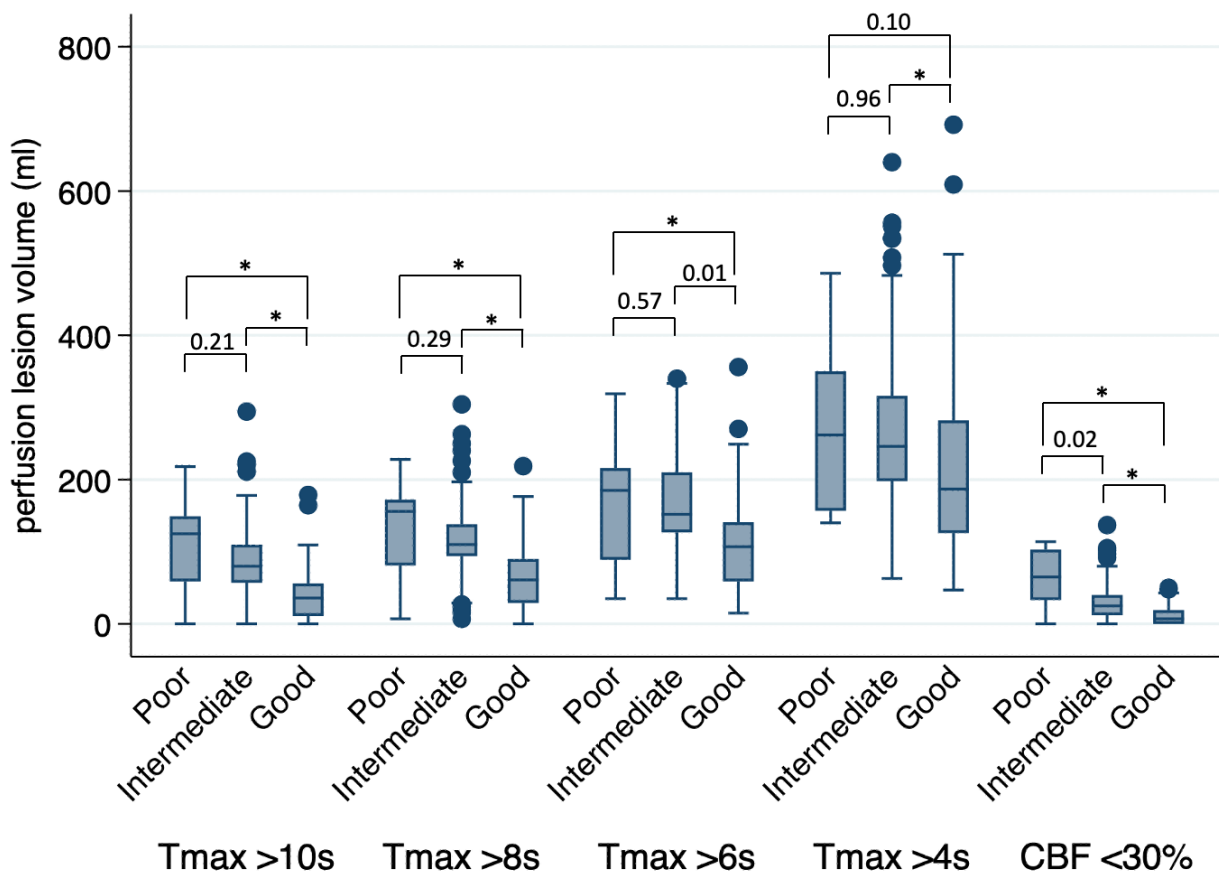
* Derived from Kruskal-Wallis test

Note: HIR – hypoperfusion intensity ratio, IQR – interquartile range

Table 2.2. Correlation coefficients for hypoperfusion lesion volumes and collateral score.

Perfusion parameter	Spearman's correlation	
	Spearman's rho	p-value
Tmax >10s	-0.50	<.001
Tmax >8s	-0.48	<.001
Tmax >6s	-0.40	<.001
Tmax >4s	-0.28	<.001
CBF <30%	-0.42	<.001
HIR	-0.47	<.001

Figure 2.1. mCTA collateral score versus CT perfusion lesion volumes. Comparison of perfusion lesion volumes defined as Tmax >10s, Tmax >8s, Tmax >6s, Tmax >4s and CBF <30% for different collateral grades (good, intermediate, poor). The values above the graph bars represent p-values derived from Wilcoxon rank sum test; * represents p < 0.01.



2.3.3 Optimal Cut-off values to representing poor collaterals

The highest AUC=0.75 for the cut-off value representing poor collaterals was shown for CBF <30% with the cut-off value of 31ml and sensitivity and specificity of 0.82 and 0.73, respectively, followed by Tmax >10s and HIR. The optimal cut-off value for Tmax >10s hypoperfusion volume was 114 ml with AUC, sensitivity and specificity of 0.75, 0.64 and 0.86, respectively. The optimal cut-off value of HIR associated with poor collaterals was 0.57 with AUC, sensitivity and specificity of 0.72, 0.73 and 0.72, respectively, **Table 2.3**.

Table 2.3. Optimal cut-off values defining poor collaterals

	Cut-off value	sensitivity	specificity	AUC
Tmax >10s	114 ml	0.64	0.86	0.75
Tmax >8s	146 ml	0.64	0.85	0.74
Tmax >6s	171 ml	0.64	0.76	0.70
Tmax >4s	229 ml	0.64	0.55	0.59
HIR	0.57	0.73	0.72	0.72
CBF <30%	31 ml	0.82	0.73	0.77

Note: AUC – area under the curve; HIR – hypoperfusion intensity ratio

2.3.4 Sensitivity analysis

Due to the significant difference in the collateral score based on the occlusion site, the sensitivity analysis was performed after excluding patients with M2-MCA occlusions. Baseline characteristics of this subgroup are listed in **Table 2.4**. In this subgroup, the collateral grades did not differ based on the clot localization (p=0.24).

Similar to the primary analysis, the gradual increase in the median perfusion lesion volume was observed with decreasing grade of the collateral score in all assessed perfusion parameters, **Table 2.5**. Compared to the main analysis, the significant difference in perfusion lesion volumes was also observed between good and poor collateral grades when perfusion lesion volume was defined as Tmax >10s, Tmax >8s, and CBF <30%, between good and intermediate collaterals in all evaluated perfusion parameters, and between intermediate and poor collaterals only when perfusion lesion was defined as CBF <30%, **Table 2.6**.

The Spearman's rho demonstrated direct correlation of the collateral score and the perfusion lesion volumes and HIR, with the strongest negative correlation for CBF <30% ($\rho=-0.46$), Tmax >10s ($\rho=-0.43$) and HIR ($\rho=-0.43$), **Table 2.7**.

Table 2.4. Baseline characteristics of the whole dataset and dataset used for the sensitivity analysis.

	All patients (n=147)	Patients with terminal ICA and M1-MCA occlusions (n=116)
Sex, female, n (%)	69 (44.2)	56 (48.3)
Age, years, mean (SD)	71 (14)	71 (15)
Baseline NIHSS, median (IQR)	16 (12 – 19)	16 (13 – 20)
Baseline ASPECTS, median (IQR)	8 (7 – 9)	8 (7 – 9)
Onset to CT time, min, median (IQR)	83 (60 – 169)	82 (59 – 162)
Collateral status, n (%)		
<i>Good</i>	63 (42.9)	42 (36.2)
<i>Intermediate</i>	73 (49.7)	63 (54.3)
<i>Poor</i>	11 (7.5)	11 (9.5)

Table 2.5. Comparison of hypoperfusion volumes for different collateral grades in patient with M1-MCA and terminal ICA occlusion.

Perfusion parameter	Hypoperfusion volumes (ml), median (IQR)			
	Good n=42	Intermediate n=63	Poor n=11	p-value*
Tmax >10s	41 (23 – 64)	87 (60 – 119)	125 (59 – 149)	<0.001
Tmax >8s	72 (53 – 101)	111 (95 – 147)	156 (81 – 172)	<0.001
Tmax >6s	128 (92 - 147)	154 (131 – 197)	185 (89 – 216)	0.002
Tmax >4s	196 (160 – 282)	246 (198 – 313)	262 (157–350)	0.049
CBF <30%	9 (0 – 22)	27 (12 – 41)	65 (33 – 103)	<0.001
HIR	0.33 (0.20-0.49)	0.56 (0.36-0.67)	0.63 (0.48-0.74)	<0.001

* Derived from Kruskal-Wallis test

Note: HIR – hypoperfusion intensity ratio, IQR – interquartile range

Table 2.6. Comparison of p-values derived from Wilcoxon rank sum test for perfusion lesion volumes and hypoperfusion intensity ratio.

	Tmax >10s	Tmax >8s	Tmax >6s	Tmax >4s	CBF <30%	HIR
Good vs. intermediate collaterals	<0.001	<0.001	<0.001	0.02	<0.001	<0.001
Good vs. poor collaterals	0.004	0.02	0.054	0.22	<0.001	0.001
Intermediate vs. poor collaterals	0.27	0.39	0.61	0.98	0.03	0.16

Note: HIR – hypoperfusion intensity ratio

Table 2.7. Correlation coefficients for hypoperfusion lesion volumes and collateral score in patient with M1-MCA and terminal ICA occlusion.

Perfusion parameter	Spearman's correlation	
	Spearman's rho	p-value
Tmax >10s	-0.43	<.001
Tmax >8s	-0.41	<.001
Tmax >6s	-0.31	<.001
Tmax >4s	-0.21	0.02
CBF <30%	-0.46	<.001
HIR	-0.43	<.001

2.4 DISCUSSION

We demonstrated that decreasing collateral score assessed on multiphase CTA inversely correlates with increasing perfusion lesion volumes with significant difference of PLV between good and poor collaterals, which is in concordance with the previous studies (10,12,14). As majority of smaller hospitals and primary stroke centers do not routinely use CTP, our findings suggest that evaluation of the collateral status can also provide estimation of the ischemic core volume and severely hypoperfused tissue.

Patients with poor collaterals had significantly larger ischemic core volumes defined as CBF <30% when compared to patient with good and intermediate collaterals and also had significantly larger areas of severe hypoperfusion defined as Tmax >10s compared to the patients with good collaterals. This association was reflected in the highest Spearman's rho correlation coefficient shown for Tmax >10s and for HIR, the known factor associated with infarct growth and worse clinical outcome (18).

Although CBF <30% did not show the strongest correlation with the collateral grading in the whole dataset, the correlation increased when only patients with terminal ICA and M1-MCA occlusions were involved. This might be explained by the additional collateral flow via patent ipsilateral MCA branches in patients with M2 occlusions and therefore smaller areas with significantly decreased cerebral blood flow.

We observed that poor collaterals were best represented by CBF <30% of >31ml identifies patients with the sensitivity and specificity of 0.82 and of 0.73, respectively, while Potreck et al. (12) reported that CBF <30% perfusion lesion volume of <14ml identified patients with good collaterals with sensitivity of 0.72 and specificity of 0.82. Accordingly, the cut-off volume of 114ml associated with poor collaterals was identified for Tmax >10s in our study with the sensitivity of 0.64 and sensitivity of 0.82, while cut-off value of 53ml for Tmax >10s demonstrated association with good collaterals with the sensitivity of 0.64 and specificity of 0.80 in the work by Potreck et al. (12) These findings are complimentary to each other and provide further insight on the correlation of particular grades of collateral score and perfusion parameters.

Compared to the prior studies evaluating the association of the collateral flow and perfusion parameters (10,12,14), we distinguished and evaluated the perfusion volumes in intermediate (score = 2-3) and poor collaterals (score = 0-1). Lyndon et al. proposed that HIR > 0.45 distinguishes poor collaterals (score = 0-3) from good collaterals with sensitivity of 0.78 and specificity of 0.76. Similarly, Potreck at al. and Guenego et al. identified HIR = 0.4 as a cut-off value distinguishing good (score = 4-5) and poor collaterals (score = 0-3), both merging

the subgroups of intermediate and poor collaterals. In our dataset, we found that poor collateral flow (score 0-1) was best characterized by $HIR > 0.57$ with the sensitivity of 0.64 and specificity of 0.86. The higher cut-off value in our study therefore likely reflects the higher severity of the poor collateral flow in patients with minimal (grade 1) or absent (grade 0) leptomeningeal collaterals.

Findings of this study supports the paradigm that the CT perfusion is not necessary in patients presenting during the first 6 hours from the symptom onset while the expected ischemic core (standardly defined as $CBF < 30\%$ (19)) remains relatively small even in patients with poor collateral flow. However, the fact that the severely hypoperfused area defined as $T_{max} > 10s$ was larger $> 100ml$ in patients with poor collaterals enhances the need for ultrarapid treatment in these patients as the large area of the brain is critically hypoperfused in contrast to the patients with good or intermediate collaterals, where the median of severely hypoperfused volumes were 36ml and 80ml, respectively.

The strength of our study is more detailed assessment of the collateral score on multiphase CTA that was acquired independently of the CTP source data and distinguishing poor collaterals from the good and intermediate collaterals. Our institution is one of the few centers that routinely performed mCTA and CTP in all patients with suspected AIS.

Our study has several limitations. This was a single center retrospective study including patient who underwent mechanical thrombectomy, therefore there is a potential selection bias of patients with higher baseline ASPECTS and better collateral flow. The patients with poor collateral flow represented only 7.5% of the dataset which may affect the validity of the results. Second, the collateral grades were assessed visually by one reader which may introduce some level of subjective bias despite the high expertise of the reader.

2.5 CONCLUSION

This study demonstrates that mCTA collateral score correlates well with automatically-derived perfusion lesion volumes with significant difference of PLV between good and poor collaterals. These findings suggest that evaluation of the collateral status on mCTA can provide estimation of the ischemic core volume and severely hypoperfused tissue.

REFERENCES

1. Menon BK, Qazi E, Nambiar V, et al. Differential effect of baseline computed tomographic angiography collaterals on clinical outcome in patients enrolled in the Interventional Management of Stroke III trial. *Stroke* 2015;46:1239-1244.
2. Berkhemer OA, Jansen IGH, Beumer D, et al. Collateral status on baseline computed tomographic angiography and intra-arterial treatment effect in patients with proximal anterior circulation stroke. *Stroke* 2016;47:768-776.
3. Bang OY, Saver JL, Buck BH, et al. Impact of collateral flow on tissue fate in acute ischaemic stroke. *J Neurol Neurosurg Psychiatry* 2007;79:625-629.
4. De Havenon A, Mlynash M, Kim-Tenser MA, et al. Results from DEFUSE 3: Good collaterals are associated with reduced ischemic core growth but not neurologic outcome. *Stroke* 2019;50:632-638.
5. Lin L, Yang J, Chen C, et al. Association of collateral status and ischemic core growth in patients with acute ischemic stroke. *Neurology* 2021;96:e161-e170.
6. Bang OY, Saver JL, Kim SJ, et al. Collateral flow averts hemorrhagic transformation after endovascular therapy for acute ischemic stroke. *Stroke* 2011;42:2235-2239.
7. Menon BK, Campbell BC V., Levi C, Goyal M. Role of imaging in current acute ischemic stroke workflow for endovascular therapy. *Stroke* 2015;46:1453-1461.
8. Menon BK, d'Esterre CD, Qazi EM, et al. Multiphase CT angiography: A new tool for the imaging triage of patients with acute ischemic stroke. *Radiology* 2015;275:510-520.
9. Lee MJ, Son JP, Kim SJ, et al. Predicting collateral status with magnetic resonance perfusion parameters: Probabilistic approach with a tmax-derived prediction model. *Stroke* 2015;46:2800-2807.
10. Guenego A, Fahed R, Albers GW, et al. Hypoperfusion intensity ratio correlates with angiographic collaterals in acute ischaemic stroke with M1 occlusion. *Eur J Neurol* 2020;27:864-870.
11. Wang CM, Chang YM, Sung PS, Chen CH. Hypoperfusion index ratio as a surrogate of collateral scoring on CT angiogram in large vessel stroke. *J Clin Med* 2021, Vol 10, Page 1296 2021;10:1296.
12. Potreck A, Scheidecker E, Weyland CS, et al. RAPID CT perfusion-based relative CBF identifies good collateral status better than hypoperfusion intensity ratio, CBV-index, and Time-to-maximum in anterior circulation stroke. *AJNR Am J Neuroradiol* June 2022. doi:10.3174/ajnr.A7542

13. Mlynash M, Lansberg MG, Kemp S, et al. Abstract wp79: Combination of Tmax and relative CBV perfusion parameters more accurately predicts CTA collaterals than a single perfusion parameter in DEFUSE 3. *Stroke* 2019;50.
14. Lyndon D, van den Broek M, Niu B, Yip S, Rohr A, Settecase F. Hypoperfusion intensity ratio correlates with CTA collateral status in large-vessel occlusion acute ischemic stroke. *Am J Neuroradiol* 2021;42:1380-1386.
15. Goyal M, Demchuk AM, Menon BK, et al. Randomized assessment of rapid endovascular treatment of ischemic stroke. *N Engl J Med* 2015;372:1-12.
16. Hill MD, Goyal M, Menon BK, et al. Efficacy and safety of nerinetide for the treatment of acute ischaemic stroke (ESCAPE-NA1): A multicentre, double-blind, randomised controlled trial. *Lancet* 2020;395:878-887.
17. Mokin M, Levy EI, Saver JL, et al. Predictive value of rapid assessed perfusion thresholds on final infarct volume in SWIFT PRIME (Solitaire With the Intention For Thrombectomy as Primary Endovascular Treatment). *Stroke* 2017;48:932-938.
18. Olivot JM, Mlynash M, Inoue M, et al. Hypoperfusion intensity ratio predicts infarct progression and functional outcome in the DEFUSE 2 cohort. *Stroke* 2014;45:1018-1023.
19. Demeestere J, Wouters A, Christensen S, Lemmens R, Lansberg MG. Review of perfusion imaging in acute ischemic stroke: From time to tissue. *Stroke* 2020:1017-1024.

Chapter 3 - Detection of ischemic changes on baseline multimodal computed tomography: expert reading vs. Brainomix and RAPID software

The contents of this chapter have been adapted from the journal article entitled “*Detection of ischemic changes on baseline multimodal computed tomography: expert reading vs. Brainomix and RAPID software*”, published in *J Stroke Cerebrovasc Dis* 2020;29:104978 by P. Cimflova, O. Volny, R. Mikulik, et al.

Purpose: The aim of the study was to compare the assessment of ischemic changes by expert reading and available automated software for non-contrast CT (NCCT) and CT perfusion on baseline multimodal imaging and demonstrate the accuracy for the final infarct prediction.

Methods: Early ischemic changes were measured by ASPECTS on the baseline neuroimaging of consecutive patients with anterior circulation ischemic stroke. The presence of early ischemic changes was assessed a) on NCCT by two experienced raters, b) on NCCT by e-ASPECTS, and c) visually on derived CT perfusion maps (CBF<30%, Tmax>10s). Accuracy was calculated by comparing presence of final ischemic changes on 24-hour follow-up for each ASPECTS region and expressed as sensitivity, specificity, positive predictive value (PPV), and negative predictive value (NPV). The subanalysis for patients with successful recanalization was conducted.

Results: Of 263 patients, 81 fulfilled inclusion criteria. Median baseline ASPECTS was 9 for all tested modalities. Accuracy was 0.76 for e-ASPECTS, 0.79 for consensus, 0.82 for CBF<30%, 0.80 for Tmax>10s. e-ASPECTS, consensus, CBF<30%, and Tmax>10s had sensitivity 0.41, 0.46, 0.49, 0.57, respectively; specificity 0.91, 0.93, 0.95, 0.91, respectively; PPV 0.66, 0.75, 0.82, 0.73, respectively; NPV 0.78, 0.80, 0.82, 0.83, respectively. Results did not differ in patients with and without successful recanalization.

Conclusion: This study demonstrated high accuracy for the assessment of ischemic changes by different CT modalities with the best accuracy for CBF<30% and Tmax>10s. The use of automated software has a potential to improve the detection of ischemic changes.

3.1. INTRODUCTION

The Alberta Stroke Program Early CT Score (ASPECTS) quantifies the extent of early ischemic changes in the middle cerebral artery territory on baseline non-contrast (NCCT) scans (1). ASPECTS has been proven to be a significant predictor of clinical outcome in patients with acute ischemic stroke (AIS) in the anterior circulation (2,3). It is also used to select patients for endovascular therapy (4). It represents a validated grading system (3) but the inter-rater variability has been questioned. Even experienced clinicians show only a 39% agreement in the identification of ischemic changes on NCCT involving more than one-third of the MCA territory(5). Hence, there is a trend to develop reliable software tools to help stroke physicians in acute scan reading and subsequent decision making (6,7).

The e-ASPECTS software (Brainomix, Oxford, UK) is a fully-automated ASPECT scoring tool for NCCT, which has previously demonstrated a scoring on expert level (8–10). The advantage of e-ASPECTS is its potential to eliminate the inter-rater variability (8,10). CT perfusion (CTP) has a potential to discriminate between irreversibly damaged tissue, infarct core, and tissue at risk of infarction, penumbra (11,12). It has been demonstrated that visual applying of ASPECTS into CTP parametric maps has a strong correlation with good clinical outcome (defined as modified Rankin scale/mRS 0-2), with a prognostic value greater than NCCT ASPECTS (13–16). All previous studies have shown the highest correlation of good clinical outcome with CBV ASPECTS (13–16).

The most accurate prediction of irreversibly ischemic changes by automatic software post-processing with RAPID was shown for relative cerebral blood flow (CBF) less than 30% in comparison to the mean CBF of normally perfused brain parenchyma (17,18). This threshold was used in the randomized trials with patient selection based on perfusion mismatch (SWIFT-PRIME, EXTEND-AI, DAWN, DEFUSE III) to define ischemic core (19–22).

Severe hypoperfusion has been associated with irreversible necrosis of the ischemic lesion even after reperfusion (23). In the DEFUSE and EPITHET meta-analysis, large regions of severe delay (>10 s) have been associated with poor outcome after reperfusion (24). This finding suggests that higher Tmax may identify tissue with more severely reduced cerebral blood flow, which may have a substantial impact on the evolution of the acute ischemic lesion (23).

The main aim of our study was to evaluate how accurate the different CT modalities with and without software processing (consensus reading, e-ASPECTS, CBF $<$ 30%, Tmax $>$ 10s) assess early ischemic changes at baseline and what is their accuracy for final ischemia prediction.

3.2 MATERIALS & METHODS

3.2.1 Patient selection

Ethical approval was obtained from the local Institutional Review Boards (the Boards waived the need for patient consent). All patients with symptoms of AIS and no history of contrast allergy routinely underwent NCCT, multiphase CTA (mCTA) from the aortic arch to the vertex (25) and CTP in our institution. If the diagnosis of AIS was confirmed by this neuroimaging protocol, NCCT was repeated within 24-32 hours to determine the extent and location of ischemia and diagnose potential complications such as hemorrhagic transformation. Radiological data of consecutive patients from March 2017 to September 2017 presenting with symptoms of AIS in the anterior circulation within 6 hours of last seen normal (symptom onset) were retrospectively reviewed. This time period was chosen in order to compare the reliability of the detection of early ischemic changes while the software for automatic detection of early ischemic changes, Brainomix e-ASPECTS, was implemented into our institutional system. Inclusion criteria were: 1) availability of baseline NCCT with automatic software analysis, baseline CTP and follow-up 24-hour NCCT. Exclusion criteria were: 1) evidence of any intracranial hemorrhage or non-ischemic lesion, 2) negative findings on baseline diagnostic imaging and no ischemic changes on follow-up CT.

We defined patients with successful reperfusion/recanalization angiographically as TIC1 2b-3 (in patients treated with mechanical thrombectomy (MT) or as >40% decrease in the 24-hour NIHSS score in patients treated with intravenous thrombolysis (IVT) only (26). Subanalysis of this subgroup was conducted.

3.2.2 Imaging protocol

The imaging protocol set up in our stroke center combines NCCT, mCTA and CTP and both software programs were available during the study period for automatic analysis (Brainomix for NCCT and RAPID for CTP).

NCCT was acquired on a multi-detector scanner (120kV, 328 mAs (419mAs/slice), Brilliance iCT 256; Philips Healthcare, Cleveland, OH) with a section thickness of 0.9mm and an image reconstruction of 3mm.

For the CTP protocol, 40 ml of contrast agent (Iomeron 300; Mallinckrodt Pharmaceuticals; Dublin, Ireland) was power injected at 5 ml/s followed by a saline chase of 50 ml at 5 ml/s. Sections of 8cm thickness were acquired at 10 mm slice thickness. Scanning began after a delay of 5s from contrast injection in every 1.8s for 75s. After 24 hours, a NCCT was acquired for final infarct delineation in all patients.

3.2.3 Image processing

NCCT scans were automatically analysed by the e-ASPECTS software (version 6.0, Brainomix, Oxford, UK). The e-ASPECTS software is a standardized, fully-automated, CE mark-approved ASPECTS scoring tool for NCCT, which has previously demonstrated scoring on an expert level (8–10). The e-ASPECTS software is based on a combination of advanced image-processing and machine-learning algorithms. Its scoring module operates on the standardized 3D images, classifying signs of ischemic damage and assigning them to ASPECTS regions (9).

CT perfusion studies were post-processed using the RAPID software (iSchemaView, Menlo Park, CA, USA) to generate perfusion maps of CBF, CBV, MTT, and Tmax. The RAPID software also automatically segmented and calculated volumes of the ischemic core (relative regional CBF<30%) and the critically hypoperfused tissue (Tmax>6s) (27).

3.2.4 Image review

Early ischemic changes were assessed on baseline NCCT by two experienced readers (a consultant neuroradiologist, PC, and a stroke neurologist, OV)* using the ASPECTS score defined by Barber et al. (3) previously, blind to the results of the e-ASPECTS analysis, as well as to other baseline imaging modalities and follow-up NCCT.

Automatic segmentations of ASPECTS regions on e-ASPECTS derived scans were visually checked to avoid any severe inaccuracy. Otherwise, the given e-ASPECTS score were not modified and the original e-ASPECTS was noted.

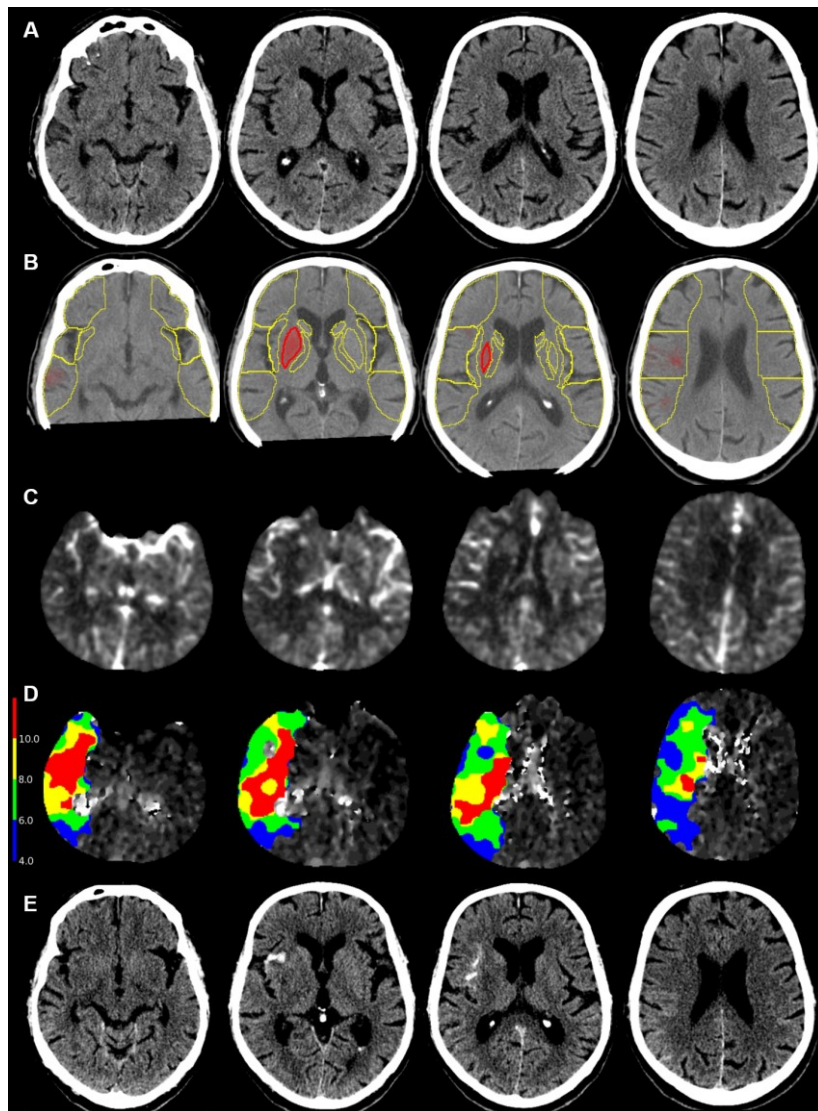
CTP maps were superposed on the CT-ASPECTS template and visually assessed by an experienced reader (PC). Ischemic changes on CTP maps were evaluated using the ASPECTS as follows: 1) on the CBF map as the area with CBF<30 % when compared to the contralateral hemisphere and 2) on the Tmax map as the area with Tmax>10s delay in the maximum contrast filling within the region of interest when compared to the contralateral hemisphere, **Figure 3.1**. The reader was blind to findings on NCCT, perfusion baseline scans available in the summary of RAPID analysis were visually controlled to exclude any false positive CTP findings (e.g. chronic infarction).

The final infarction was assessed on a 24-hour follow-up NCCT with consensus of the two readers, during a different session, one month after the previous assessment of the early ischemic changes on baseline NCCT.

To support the reliability of the consensus reading, two radiologists evaluated ASPECTS of 40 random admission NCCT and 40 follow-up scans (of different patients). The

inter-rater agreement with the consensus was counted using weighted kappa (κ_w) and Krippendorff's alpha (α) (28). The moderate agreement between raters was demonstrated for baseline NCCT ($\kappa_w=0.53-0.54$; $\alpha=0.72$) and good to excellent agreement for follow-up imaging ($\kappa_w=0.78-0.88$; $\alpha=0.94$).

Figure 3.1. Comparison of CT imaging modalities and evaluation of early ischemic changes. Baseline ASPECTS was assessed as follows: 10 points on NCCT by expert reading (A), 9 (lentiform) by automatic e-ASPECTS (B), 0 points on CBF <30% CTP map, and 6 (M2, M3, insula, lentiform) on Tmax>10s CTP map (C). Follow-up CT (D) shows the ischemic changes within insula, lentiform and M5 (ASPECTS 7); and hemorrhagic transformation within the right insula.



3.2.5 Statistical Analysis

Clinical and imaging baseline characteristics were summarized using descriptive statistics. The accuracy, sensitivity, specificity, positive predictive value (PPV) and negative predictive value (NPV) were calculated for particular ASPECTS regions (81 patients x 10 ASPECTS regions) at baseline imaging (e-ASPECTS, expert consensus reading, CBF<30%, Tmax>10s) in comparison with ASPECTS regions at the follow-up CT. The Bland-Altman plots were calculated to compare the differences between each baseline imaging method and follow-up ASPECTS.

The sensitivity analysis of pooled data for the group with determined successful reperfusion/recanalization was conducted; clinical and imaging baseline characteristics were summarized using descriptive statistics and compared to the group with non-determined recanalization/reperfusion using Wilcoxon rank sum test; the accuracy, sensitivity, specificity, PPV, NPV as well as Bland-Altman plots were calculated. To compare the two subgroups, we calculated residuals between follow-up ASPECTS and each baseline ASPECT score method (e-ASPECTS, expert consensus reading, CBF<30%, Tmax>10) and analysed these residuals using Wilcoxon rank sum test.

This study provides hierarchically structured data with 3 levels: subject ID, imaging modalities (e-ASPECTS, expert consensus reading, CBF<30%, Tmax>10s, and follow-up ASPECTS); and ASPECTS regions (M1-M6, Insula, Lentiform, Capsula, Caudate). We regarded regions as a fixed effect. The generalized estimating equation accommodating clustering at the subject ID level was used (PROC GENMOD; SAS Institute Inc, Cary, NC). LS-means estimates of fixed effect “region” computed from generalized mixed model were graphically illustrated.

All analyses were performed in Stata 16.1 (StataCorp LLC, College Station, TX, USA) and SAS 9.3 (SAS Institute, Cary, NC, USA).

3.3 RESULTS

Baseline scans of 263 patients were retrospectively reviewed; 16 patients with intracranial hemorrhage and 166 patients with either negative findings on all imaging modalities or missing follow-up imaging were excluded. Overall, 81 patients met all the criteria and were included into the analysis.

Mean age was 70 years (standard deviation [SD] 14 years, range 30-92 years), 38 (46,9%) were women. Median baseline NIHSS was 9 (interquartile range [IQR]=4 – 17). The median time interval from symptom onset to CT was 156 mins (IQR=71-220); there were

12 patients with the unknown time of symptom onset or wake-up stroke. Median baseline ASPECTS was 9 for all tested modalities (IQR=8-10 for e-ASPECTS, IQR=7-10 for consensus, IQR=7-10 for CBF<30%, IQR 6-10 for Tmax>10s, median ASPECTS on follow-up NCCT was 8, IQR=5-9), left hemisphere was affected in 44 cases (54.3%). Fifty patients received intravenous thrombolysis and 19 patients had mechanical thrombectomy. Reperfusion was achieved in 11 patients in the mechanical thrombectomy group and in 22 patients in the IVT group, the data from mechanical thrombectomy and intravenous thrombolysis groups were pooled for further analysis (as determined recanalization).

Accuracy of baseline ASPECTS and follow-up ASPECTS was 0.76 for e-ASPECTS, 0.79 for expert consensus, 0.81 for CBF<30% and 0.8 for Tmax>10s. Sensitivity and specificity were 0.41 and 0.91 for e-ASPECTS; 0.46 and 0.93 for expert consensus; 0.49 and 0.95 for CBF<30%; 0.57 and 0.91 for Tmax>10s respectively. PPV and NPV were 0.66 and 0.78 for e-ASPECTS; 0.75 and 0.8 for expert consensus; 0.82 and 0.81 for CBF<30%; 0.73 and 0.83 for Tmax>10s, respectively, **Table 3.1, Figure 3.2.**

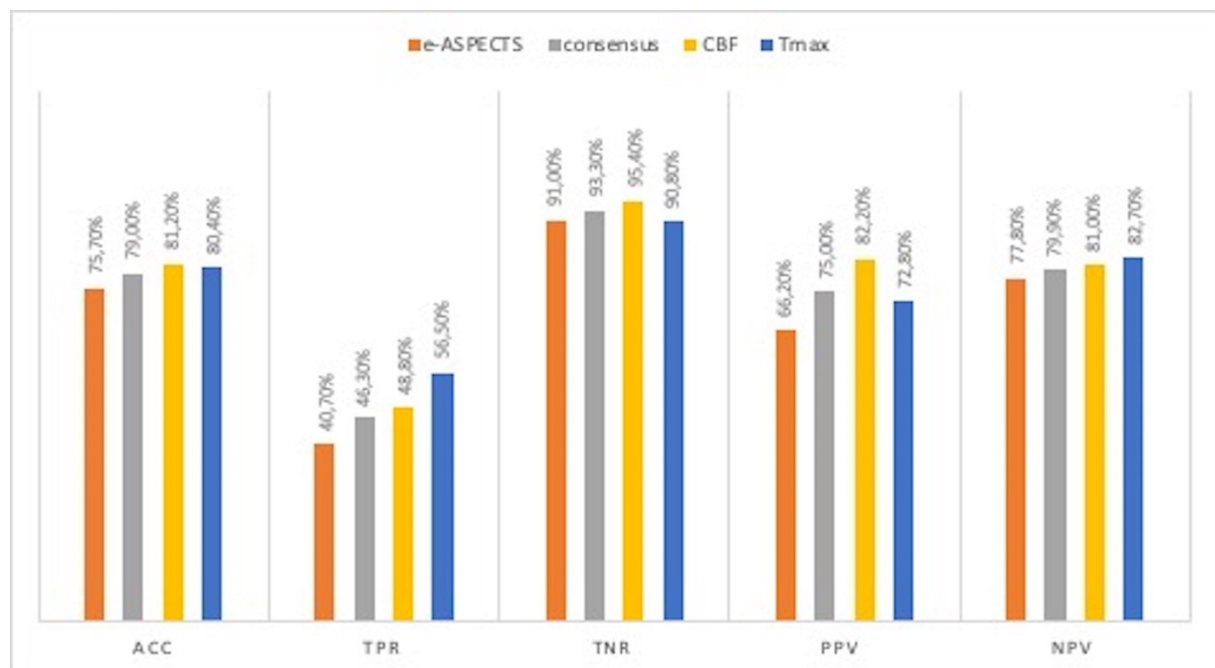
Bland-Altman plots comparing differences in scores of baseline ASPECTS and follow-up ASPECTS are demonstrated in **Figure 3.3.** The mean difference between e-ASPECTS and follow-up was -1.16 ± 2.52 (median undercall of ASPECTS was -1), expert consensus and follow-up -1.16 ± 2.23 (median undercall was -1), CBF<30% and follow-up -1.15 ± 1.77 % (median undercall was -1), and Tmax>10s and follow-up -0.59 ± 1.86 (median undercall was 0). The ASPECTS was rated as lower on baseline imaging in 15/81 cases for e-ASPECTS, 11/81 for expert consensus, 6/81 for CBF<30, and in 15/81 cases for Tmax>10s.

Table 3.1. Accuracy, sensitivity, specificity, PPV and NPV of baseline ASPECTS (e-ASPECTS, consensus, CBF<30% and Tmax>10s) vs. follow-up imaging.

	Accuracy	Sensitivity	Specificity	PPV	NPV
e-ASPECTS vs. follow-up	0.76	0.41	0.91	0.66	0.78
Consensus vs. follow-up	0.79	0.46	0.93	0.75	0.8
CBF<30% vs. follow-up	0.81	0.49	0.95	0.82	0.81
Tmax>10 s vs. follow-up	0.80	0.57	0.91	0.73	0.83

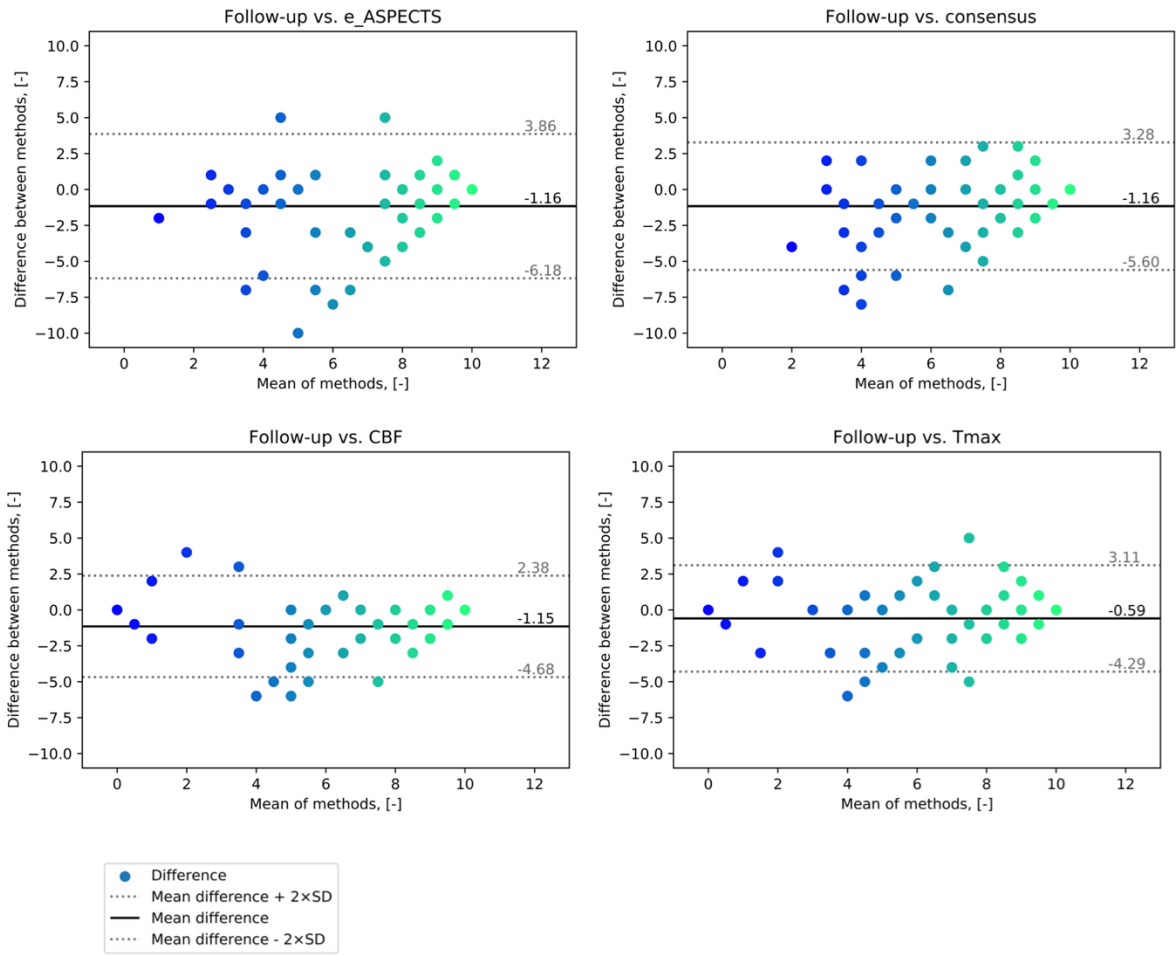
Legend: ASPECTS = Alberta Stroke Program Early CT Score; CBF = cerebral blood flow; NPV = negative predictive value; PPV = positive predictive value; Tmax = time to maximum.

Figure 3.2. Accuracy, sensitivity, specificity, positive predictive value, negative predictive values of baseline ASPECTSs evaluated by e-ASPECTS, consensus (expert reading), CBF<30% and Tmax>10s)



Legend: ACC – accuracy; TPR – true positive value/sensitivity, TNR – true negative value/specificity, PPV – positive predictive value, NPV – negative predictive value

Figure 3.3. Bland-Altman plots. Bland-Altman plots illustrating the level of agreement between the baseline and follow-up ASPECTS for different baseline CT modalities and means of evaluation (software vs. expert reading). Solid line indicates the mean difference between the baseline and follow-up, dashed lines indicate the limits of the agreement.



3.3.1 Sensitivity analysis

Clinical and imaging baseline characteristics for patients with determined successful recanalization were not significantly different in comparison to the subgroup of patients with non-determined recanalization **Table 3.2**. The results of the subgroup analysis in patients with successful reperfusion/recanalization are graphically demonstrated in **Table 3.3, Figure 3.4**. Accuracy of baseline ASPECTS and follow-up ASPECTS was 0.79 for e-ASPECTS, 0.81 for expert consensus, 0.83 for CBF<30% and 0.82 for Tmax>10s. Sensitivity and specificity were 0.51 and 0.90 for e-ASPECTS; 0.53 and 0.92 for expert consensus; 0.55 and 0.94 for CBF<30%; 0.66 and 0.89 for Tmax>10s, respectively. PPV and NPV were 0.67 and 0.82 for e-ASPECTS; 0.73 and 0.83 for expert consensus; 0.77 and 0.84 for CBF<30%; 0.7 and 0.87 for Tmax>10s, respectively.

Bland-Altman plots for the subgroup analysis comparing differences in scores of baseline ASPECTS and follow-up ASPECTS are demonstrated in **Figure 3.5**. The mean difference between e-ASPECTS and follow-up was -0.70 ± 2.48 (median undercall of ASPECTS was -1), expert consensus and follow-up -0.79 ± 2.33 (median undercall was 0), CBF<30% and follow-up -0.82 ± 1.77 (median undercall was -1), and Tmax>10s and follow-up -0.21 ± 1.74 (median undercall was 0). The ASPECTS was lower on baseline imaging in 7/33 cases for e-ASPECTS, 6/33 for expert consensus, 5/33 for CBF<30% , and in 9/33 cases for Tmax>10s.

There was no significant difference between residuals of the follow-up ASPECTS and each baseline ASPECTS for the two subgroups (determined recanalization versus non-determined recanalization group), the median under-call of baseline ASPECT scores was -1 point in comparison to the follow-up ASPECTS for the baseline methods in the subgroup with non-determined recanalization and for CBF<30% and e-ASPECTS in the subgroup with determined recanalization. There was a trend observed for Tmax>10s that show a higher precision in the subgroup with determined successful recanalization with the median under-call of 0 points, **Table 3.4**.

Results from generalized mixed model are illustrated in **Figure 3.6**.

Table 3.2. Baseline characteristics. Comparison of patient baseline characteristics for the whole dataset (n=81) and a subgroup of patients with determined successful recanalization (n=33).

	Dataset N= 81	Recanalization subgroup N=33	P-value*
Female sex – n (%)	38 (46.9)	13 (39.4)	0.26
Age – median (IQR)	71 (62 – 81)	69 (62 – 80)	0.54
Affected left side – n (%)	44 (54.3)	18 (54.55)	0.97
Baseline NIHSS – median (IQR)	9 (4 – 17) ¹	14 (7 – 17.5) ¹	0.002
Baseline ASPECTS – median (IQR)	9 (7 – 10)	9 (6.5 – 10)	0.41
Onset to baseline CT in min – median (IQR)	156 (71-220) ²	110 (67-216) ²	0.41

Note: IQR = interquartile range, NIHSS = National Institutes of Health Stroke Scale, ASPECTS = Alberta Stroke Program Early CT Score, EVT = endovascular treatment

*Derived from Wilcoxon rank sum test for two subgroups – determined successful recanalization versus non-determined recanalization

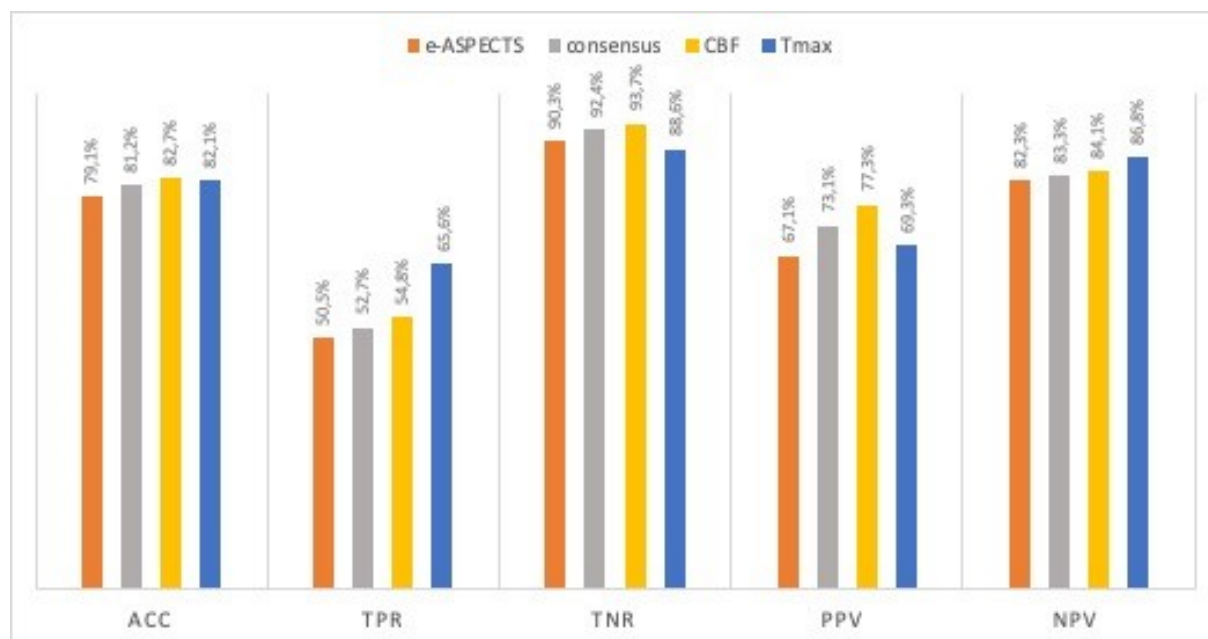
¹ computed for n=79 and subgroup n=32; ² computed for n=69 and subgroup n=31

Table 3.3. Subgroup analysis of patients with successful reperfusion/recanalization. Accuracy, sensitivity, specificity, PPV and NPV of baseline ASPECTSs (e-ASPECTS, consensus, CBF<30% and Tmax>10s) vs. follow-up imaging.

	Accuracy	Sensitivity	Specificity	PPV	NPV
e-ASPECTS vs. follow-up	0.79	0.51	0.93	0.67	0.82
Consensus vs. follow-up	0.81	0.53	0.92	0.73	0.83
CBF<30% vs. follow-up	0.83	0.55	0.94	0.77	0.84
Tmax>10 s vs. follow-up	0.82	0.66	0.89	0.69	0.87

Note: ASPECTS = Alberta Stroke Program Early CT Score; CBF = cerebral blood flow; NPV = negative predictive value; PPV = positive predictive value; Tmax = time to maximum.

Figure 3.4. Subgroup analysis of patients with successful reperfusion. Accuracy, sensitivity, specificity, positive predictive value and negative predictive value for baseline assessment (e-ASPECTS, consensus, CBF<30% and Tmax>10s) and final ischemic changes on follow-up NCCT.



Legend: ACC – accuracy; TPR – true positive value/sensitivity, TNR – true negative value/specificity, PPV – positive predictive value, NPV – negative predictive value

Table 3.4. Comparison of residuals for the follow-up ASPECTS and the baseline ASPECTS for the subgroups of patients with determined successful recanalization versus non-determined recanalization.

	Determined recanalization n=33	Non-determined recanalization n=48	P-value*
e-ASPECTS – median (IQR)	-1 (-3 – 0)	-1 (-1 – 0)	0.54
Consensus – median (IQR)	-1 (-2.5 – 0)	0 (-2 – 0)	0.15
CBF <30% – median (IQR)	-1 (-2 – 0)	-1 (-2 – 0)	0.26
Tmax >10s – median (IQR)	-1 (-2 – 0)	0 (-1 – 1)	0.03

Note: ASPECTS = Alberta Stroke Program Early CT Score; CBF = cerebral blood flow; Tmax = time to maximum.

*Derived from Wilcoxon rank sum test

Figure 3.5. Bland-Altman plots for the subgroup analysis of patients with successful recanalization/reperfusion (MT and IVT group pooled data). Bland-Altman plots compare the baseline ASPECTS and follow-up ASPECTS for baseline CT modalities and different means of assessment. Solid line indicates the mean difference between baseline and follow-up, dashed lines indicate the limits of the agreement.

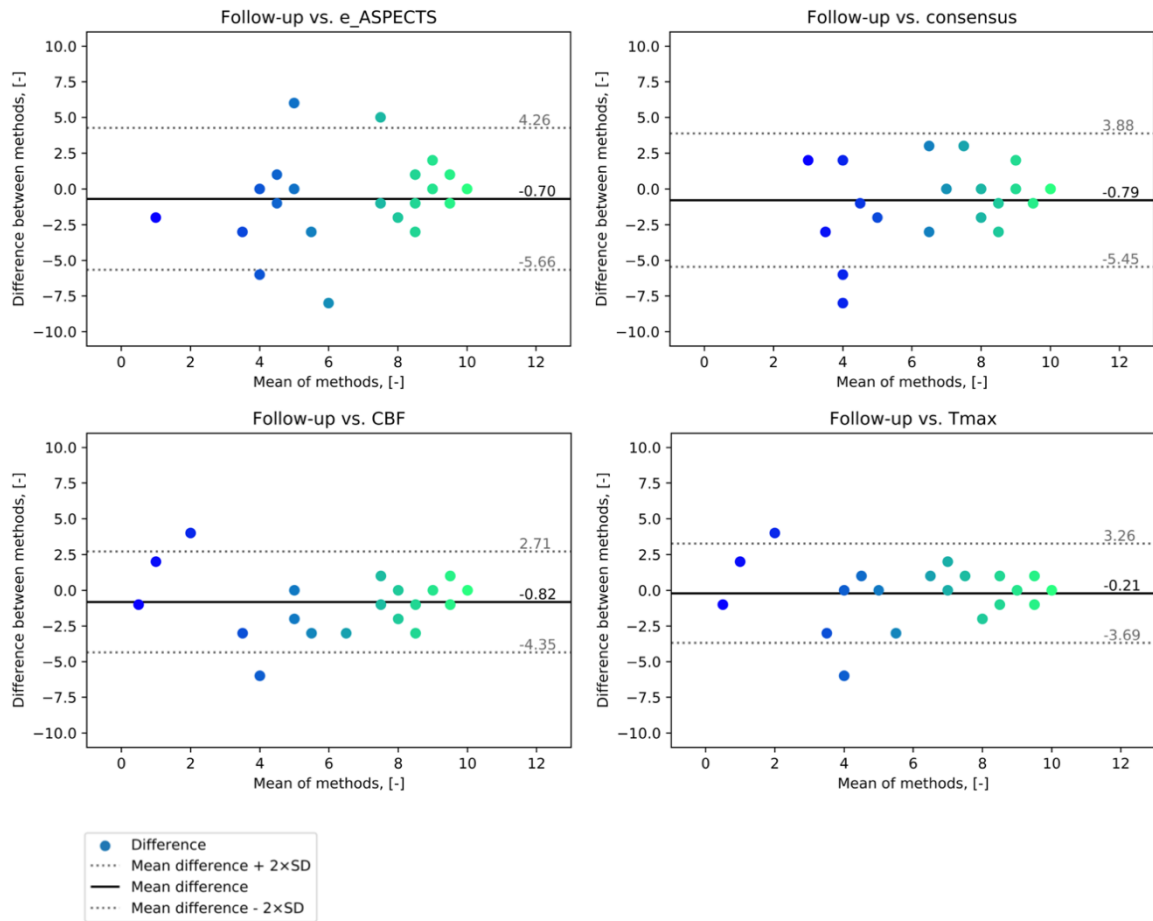
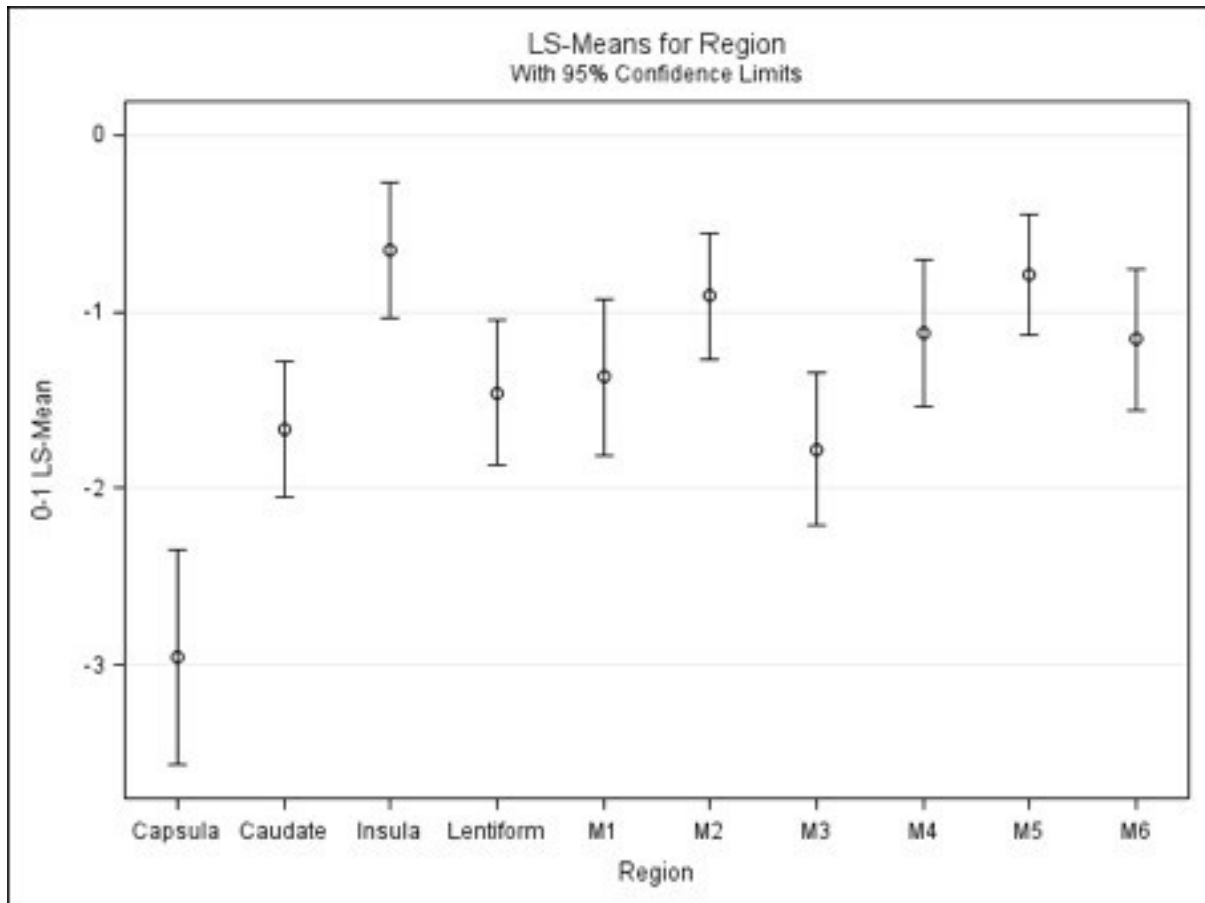


Figure 3.6. Least square means estimates of fixed effect “region” computed from generalized mixed model. The least square means (Ls-means) estimates were computed from a generalized mixed model (fixed effect was ASPECTS region). Follow-up NCCT was used as a reference grid. Results expressed on a logit scale demonstrate the highest agreement for final ischemia in insula and M5 region regardless the used CT modality and scoring approach. The lowest odds were demonstrated for internal capsule, which also showed the highest variability in scoring.



3.4 DISCUSSION

In this study we demonstrated high sensitivity and specificity for detection of acute ischemic changes for CT imaging modalities including assessment of acute ischemic changes by experienced readers and clinically available software. Unlike in previous studies, we have focused on CTP parameters representing either ischemic core (CBF<30%) or severely hypoperfused tissue (Tmax>10s), parameters that were not analyzed previously in the perspective of ASPECT scoring. CBF <30% is nowadays widely accepted to represent the ischemic core with the high sensitivity and specificity and with low overestimation of the core, that could result in unwarranted exclusion of patients who could benefit from reperfusion (17). In contrast to Tmax>6s, which is used to define penumbra, we evaluated a more severe delay, Tmax>10s, representing the critically hypoperfused tissue, which is associated with irreversible necrosis of the ischemic lesion even after reperfusion (23).

The highest specificity was observed for CTP parameter, rCBF<30%, assessed visually on CTP maps processed by RAPID software. This CTP parameter also showed the highest positive predictive value for final ischemic changes.

Moreover, the CTP parameter of Tmax delay >10s, representing a severe hypoperfusion, showed the highest sensitivity and high accuracy for prediction of final ischemic lesion (within the whole dataset as well as in the subgroup analysis of successful reperfusion/recanalization). Tmax delay >10s was studied previously – the association of large Tmax>10s lesion and malignant MCA profile was showed in previous studies (18,29). Tmax volumes at a delay of >8s and >10s were strongly correlated with clinical outcome.(30) Our findings support the importance of this parameter in the detection of irreversible ischemic changes on baseline neuroimaging. We demonstrated that both CBF <30% and Tmax>10s have high accuracy in detection of early ischemic changes as shown previously for CBV (13–16) and these changes could be easily assessed on the derived perfusion maps from RAPID analysis.

The Blant-Altman plots showed the lowest difference in baseline ASPECTS and follow-up ASPECTS for Tmax>10s. The other baseline methods showed similar differences in baseline and follow-up ASPECTS with the median undercall of the baseline score of 1 point (these findings did not differ when we analyzed the residuals between follow-up ASPECTS and baseline ASPECTS for the subgroups with determined/non-determined recanalization). The CBF <30% and Tmax>10s also demonstrated the lowest data dispersion for baseline and follow-up ASPECTS. This indicates that these perfusion parameters may represent irreversibly affected tissue with higher accuracy in comparison to detectable changes on baseline NCCT.

Nevertheless, the semi-automated analysis showed similar results with expert reading. This finding suggests a comparable diagnostic value of the software evaluation and expert reading in the acute stroke management.

Although e-ASPECTS showed the lowest accuracy and sensitivity among the tested baseline methods, the accuracy of 0.76 could still be considered as good, the sensitivity analysis also did not show any significant difference between baseline methods for the tested subgroups. The comparable findings for e-ASPECTS and other studied imaging methods implicates the benefit of software evaluation for less experienced readers.

We observed a certain level of variability in assessment of particular ASPECTS regions. The highest odds for agreement in evaluation of baseline ischemic changes and final ischemia was demonstrated for insula regardless the baseline imaging modality and the way of ASPECT scoring. It was demonstrated previously that the insular ribbon sign represented a very early ischemic change in the middle cerebral artery strokes (31). Contrarily, the lowest odds for agreement between multimodal baseline and follow-up imaging was observed in the internal capsule. That might be explained by difficulties in the visual assessment of hypoattenuation within this region as the internal capsule is naturally less hypodense on NCCT (32). This small subcortical region might also be challenging to be distinguished on the CTP maps as hypoperfused. Additionally, there was low variability demonstrated for all cortical ASPECTS regions, caudate and lentiform. It may reflect that early ischemic changes of the insula are easy to detect even with the low experience, but assessment of early ischemic changes within the internal capsule might be problematic also for experienced readers.

We are aware of some limitations of this study. First of all, this was a single center observational study. The patients were not selected according to the recanalization rate. Information about the recanalization status was available only in patients indicated to mechanical thrombectomy. Nevertheless, due to a limited (6-months) period when the e-ASPECTS software was available at our institution, we decided to include all patients meeting our inclusion criteria regardless of the treatment or recanalization status. We also did not focus on the correlation of ASPECTS and final clinical outcome, as this relationship has been studied in other work (33). The main purpose of this work was to evaluate the accuracy of ASPECTS assessment on baseline multimodal imaging.

We are also aware of a possible misinterpretation of particular regions caused by visual application of ASPECTS regions into the CTP maps processed by RAPID software. At the time of the patient recruitment, the RAPID CTP software presented only the volumes of impaired tissue perfusion (not co-registered within the ASPECTS regions). The automatic

segmentation of ASPECTS regions on e-ASPECTS scans also has its limitations and beside the visual control to avoid any severe inaccuracy we did not tend to correct the automatic segmentation and given ASPECTS scoring as we aimed to test the accuracy of commercially available version of the software.

There are a few potential pitfalls in regard of the detection of acute ischemic changes with automatic analysis. There might be a false positive finding on CTP maps in patients with a subacute or chronic infarction. The RAPID software automatically segments and removes areas with very low CBF, such as CSF spaces and other extra-parenchymal tissue, so in most cases subacute/chronic infarction is also excluded. Another known pitfall is that CTP maps do not display an infarcted area if the reperfusion was achieved ahead of the imaging, even though there is evidence of the infarction on NCCT (34). These potential pitfalls highlight the necessity of a visual control of CTP derived maps with NCCT or other available imaging as well as a control of the correct placement of arterial input function and venous output function.

3.5 CONCLUSION

Our study demonstrated high accuracy for the evaluation of early ischemic changes by different CT modalities with the best accuracy for $CBF < 30\%$ and $T_{max} > 10s$. The use of automated software in everyday clinical practice has a potential to improve detection of extent of early ischemic changes.

REFERENCES

1. Puetz V, Dzialowski I, Hill MD, Demchuk AM. The Alberta Stroke Program Early CT Score in clinical practice: What have we learned? *Int J Stroke*. 2009;4(5):354-364.
2. Wardlaw JM, Mielke O. Early signs of brain infarction at CT: Observer reliability and outcome after thrombolytic treatment—systematic review. *Radiology*. 2005;235(2):444-453.
3. Barber PA, Demchuk AM, Zhang J, Buchan AM. Validity and reliability of a quantitative computed tomography score in predicting outcome of hyperacute stroke before thrombolytic therapy. ASPECTS Study Group. Alberta Stroke Programme Early CT Score. *Lancet (London, England)*. 2000;355(9216):1670-1674.
4. Hill MD, Demchuk AM, Goyal M, et al. Alberta Stroke Program early computed tomography score to select patients for endovascular treatment: Interventional Management of Stroke (IMS)-III Trial. *Stroke*. 2014;45(2):444-449.
5. Grotta JC, Chiu D, Lu M, et al. Agreement and variability in the interpretation of early CT changes in stroke patients qualifying for intravenous rtPA therapy. *Stroke*. 1999;30(8):1528-1533.
6. Goyal M, Menon BK, van Zwam WH, et al. Endovascular thrombectomy after large-vessel ischaemic stroke: a meta-analysis of individual patient data from five randomised trials. *Lancet*. 2016;387(10029):1723-1731.
7. Nogueira RG, Jadhav AP, Haussen DC, et al. Thrombectomy 6 to 24 hours after stroke with a mismatch between deficit and infarct. *N Engl J Med*. 2018;378(1):11-21.
8. Pfaff J, Herweh C, Schieber S, et al. e-ASPECTS correlates with and is predictive of outcome after mechanical thrombectomy. *Am J Neuroradiol*. 2017;38(8):1594-1599.
9. Herweh C, Ringleb PA, Rauch G, et al. Performance of e-ASPECTS software in comparison to that of stroke physicians on assessing CT scans of acute ischemic stroke patients. *Int J Stroke*. 2016;11(4):438-445.
10. Nagel S, Sinha D, Day D, et al. e-ASPECTS software is non-inferior to neuroradiologists in applying the ASPECT score to computed tomography scans of acute ischemic stroke patients. *Int J Stroke*. 2017;12(6):615-622.
11. Murphy BD, Fox AJ, Lee DH, et al. Identification of penumbra and infarct in acute ischemic stroke using computed tomography perfusion-derived blood flow and blood volume measurements. *Stroke*. 2006;37(7):1771-1777.
12. Wintermark M, Flanders AE, Velthuis B, et al. Perfusion-CT assessment of infarct core and penumbra: receiver operating characteristic curve analysis in 130 patients suspected

- of acute hemispheric stroke. *Stroke*. 2006;37(4):979-985.
13. Aviv RI, Mandelcorn J, Chakraborty S, et al. Alberta Stroke Program Early CT Scoring of CT perfusion in early stroke visualization and assessment. *AJNR Am J Neuroradiol*. 2007;28(10):1975-1980.
 14. Sillanpaa N, Saarinen JT, Rusanen H, et al. CT perfusion ASPECTS in the evaluation of acute ischemic stroke: Thrombolytic therapy perspective. *Cerebrovasc Dis Extra*. 2011;1(1):6-16.
 15. Padroni M, Bernardoni A, Tamborino C, et al. Cerebral blood volume ASPECTS is the best predictor of clinical outcome in acute ischemic stroke: A retrospective, combined semi-quantitative and quantitative assessment. Chang AYW, ed. *PLoS One*. 2016;11(1):e0147910.
 16. Naylor J, Churilov L, Rane N, Chen Z, Campbell BCV, Yan B. Reliability and utility of the alberta stroke program early computed tomography score in hyperacute stroke. *J Stroke Cerebrovasc Dis*. 2017;26(11):2547-2552.
 17. Mokin M, Levy EI, Saver JL, et al. Predictive value of RAPID assessed perfusion thresholds on final infarct volume in SWIFT PRIME (Solitaire With the Intention for Thrombectomy as Primary Endovascular Treatment). *Stroke*. 2017;48(4):932-938.
 18. Albers GW, Goyal M, Jahan R, et al. Ischemic core and hypoperfusion volumes predict infarct size in SWIFT PRIME.
 19. Saver JL, Goyal M, Bonafe A, et al. Stent-retriever thrombectomy after intravenous t-PA vs. t-PA alone in stroke. *N Engl J Med*. 2015;372(24):2285-2295.
 20. Campbell BCV, Mitchell PJ, Kleinig TJ, et al. Endovascular therapy for ischemic stroke with perfusion-imaging selection. *N Engl J Med*. 2015:150211090353006.
 21. Nogueira RG, Haussen DC, Dehkharghani S, et al. Large volumes of critically hypoperfused penumbral tissue do not preclude good outcomes after complete endovascular reperfusion: redefining malignant profile. *Stroke*. 2016;47(1):94-98.
 22. Albers GW, Marks MP, Kemp S, et al. Thrombectomy for stroke at 6 to 16 hours with selection by perfusion imaging. *N Engl J Med*. 2018;378(8):708-718.
 23. Olivot JM, Mlynash M, Inoue M, et al. Hypoperfusion intensity ratio predicts infarct progression and functional outcome in the DEFUSE 2 Cohort. *Stroke*. 2014;45(4):1018-1023.
 24. Mlynash M, Lansberg MG, De Silva DA, et al. Refining the definition of the malignant profile: insights from the DEFUSE-EPITHET pooled data set. *Stroke*. 2011;42(5):1270-1275.

25. Menon BK, d'Esterre CD, Qazi EM, et al. Multiphase CT Angiography: A new tool for the imaging triage of patients with acute ischemic stroke. *Radiology*. 2015;275(2):510-520.
26. Kharitonova T, Mikulik R, Roine RO, et al. Association of early national institutes of health stroke scale improvement with vessel recanalization and functional outcome after intravenous thrombolysis in ischemic stroke. *Stroke*. 2011;42(6):1638-1643.
27. Mokin M, Levy EI, Saver JL, et al. Predictive value of RAPID assessed perfusion thresholds on final infarct volume in SWIFT PRIME (Solitaire With the Intention for Thrombectomy as Primary Endovascular Treatment). *Stroke*. 2017;48(4):932-938.
28. Hayes AF, Krippendorff K. Answering the call for a standard reliability measure for coding data. *Communication Methods and Measures*. 2007;1(1):77-89.
29. Inoue M, Mlynash M, Straka M, et al. Patients with the malignant profile within 3 hours of symptom onset have very poor outcomes after intravenous tissue-type plasminogen activator therapy. *Stroke*. 2012;43(9):2494-2496.
30. Seker F, Pfaff J, Potreck A, et al. Correlation of Tmax volumes with clinical outcome in anterior circulation stroke. *Brain Behav*. 2017;7(9):e00772.
31. Nakano S, Iseda T, Kawano H, Yoneyama T, Ikeda T, Wakisaka S. Correlation of early CT signs in the deep middle cerebral artery territories with angiographically confirmed site of arterial occlusion. *AJNR Am J Neuroradiol*. 2001;22(4):654-659.
32. Finlayson O, John V, Yeung R, et al. Interobserver agreement of ASPECT score distribution for noncontrast CT, CT angiography, and CT perfusion in acute stroke. *Stroke*. 2013;44(1):234-236.
33. Sundaram VK, Goldstein J, Wheelwright D, et al. Automated ASPECTS in acute ischemic stroke: a comparative analysis with CT perfusion. *AJNR Am J Neuroradiol*. 2019;40(12):2033-2038.
34. Laughlin B, Chan A, Tai WA, Moftakhar P. RAPID automated CT perfusion in clinical practice. *Pract Neurol*. 2019;(9):39-55.

Part II

*CT Angiography Advanced Postprocessing and
Machine Learning*

4. Chapter 4 - Validation of a machine learning software tool for automated large vessel occlusion detection in patients with suspected acute stroke

The contents of this chapter have been adapted from the journal article entitled “*Validation of a machine learning software tool for automated large vessel occlusion detection in patients with suspected acute stroke*”, published in *Neuroradiology* in May 2022 (*ahead of print*) by P. Cimflova, R. Golan, J.M. Ospel, et al. doi:10.1007/s00234-022-02978-x

Reproduced with permission from Springer Nature

Background: CT Angiography (CTA) is the imaging standard for large vessel occlusion (LVO) detection in patients with acute ischemic stroke. Stroke*SENS* LVO is an automated tool that utilizes a machine learning algorithm to identify anterior large vessel occlusions (LVO) on CTA. The aim of this study was to test the algorithm’s performance in LVO detection in an independent dataset.

Methods: A total of 400 studies (217 LVO, 183 other/no occlusion) read by expert consensus were used for retrospective analysis. The LVO was defined as intracranial internal carotid artery (ICA) occlusion and M1 middle cerebral artery (MCA) occlusion. Software performance in detecting anterior LVO was evaluated using receiver operator characteristics (ROC) analysis, reporting area under the curve (AUC), sensitivity and specificity. Subgroup analyses were performed to evaluate if performance in detecting LVO differed by subgroups namely M1 MCA and ICA occlusion sites and in data stratified by patient age, sex, and CTA acquisition characteristics (slice thickness, kilovoltage tube peak and scanner manufacturer).

Results: AUC, sensitivity and specificity overall, were as follows: 0.939, 0.894 and 0.874, respectively, in the full cohort; 0.927, 0.857 and 0.874, respectively, in the ICA occlusion cohort; 0.945, 0.914 and 0.874, respectively, in the M1 MCA occlusion cohort. Performance did not differ significantly by patient age, sex or by CTA acquisition characteristics.

Conclusion: The Stroke*SENS* LVO machine learning algorithm detects anterior LVO with high accuracy from a range of scans in a large dataset.

4.1 INTRODUCTION

Patients with acute ischemic stroke due to large vessel occlusions (LVO), on average, may account for around 15-20% of all acute ischemic stroke patients (1). However, LVO strokes contribute to 90% of stroke mortality and severe clinical disability if left untreated (2). Recent advances in endovascular stroke treatment (EVT) have led to significant reduction in disability in these patients in comparison to best medical management.(3) Because of the robust evidence from clinical trials confirming its efficacy and safety, EVT has become the standard of care in patients with anterior circulation stroke due to LVO (3).

Contrast-enhanced CT Angiography (CTA) has been widely adopted as the imaging standard for LVO detection in order to identify eligible patients for endovascular treatment (4–6). Timely CTA interpretation and LVO detection remains challenging especially in smaller, more rural hospitals where physicians with experience in stroke imaging are not always available (7). Since any delay in the treatment of patients with LVO directly affects patient outcomes (8), automated detection and notification of suspected LVO can help improve patient outcomes by directly reducing time to diagnosis and clinical decision making (6).

Stroke*SENS* LVO (Circle Neurovascular Imaging, Calgary, Canada) is a computer-aided triage and notification tool which utilizes machine learning to automatically detect LVO on CTA head images. The automated software is intended to notify clinicians of patients with suspicious LVO via pre-determined communication protocols, thus allowing them to get involved in the case sooner than they may have been able to if using standard diagnostic workflows. The aim of this retrospective cohort study was to evaluate the software's performance in LVO detection, when compared to a neuroradiologist expert consensus assessment on imaging data from a large multi-center image database.

4.2 METHODS

4.2.1 Software development dataset

The Stroke*SENS* LVO algorithm was developed using a dataset of 874 CTA cases (development dataset) of pooled de-identified imaging data from three clinical trials initiated from within the University of Calgary (INTERRSeCT (9), PRove-IT (10), ESCAPE (11)). The primary goal for the software development was a reliable detection of the anterior LVO including intracranial ICA and M1 MCA occlusions. The subset of data used for development was selected from the pooled database according to the following inclusion criteria: age of 18 years or older who underwent baseline CTA imaging for suspected acute stroke with image slice thickness between 0.5 mm to 2.5mm.

The imaging data for development were acquired from multiple institutions and multiple CT scanners, manufactured by four different CT vendors (GE, Siemens, Philips, Toshiba). Scans determined to be technically inadequate (e.g., invalid DICOM image or inappropriate head coverage or no contrast) or with significant patient motion were excluded. Images in the development dataset included 553 subjects with anterior LVO (ICA and the M1 MCA segment) and 321 subjects with other/no occlusions [negative cases (non-occlusions), distal occlusions (i.e., M2, M3 MCA), and non-anterior circulation occlusions (i.e., occlusions in the vertebrobasilar territory)]. There was no scan with intracranial hemorrhage (ICH) in the development dataset. The manually labeled data points annotating the occlusion were used for the algorithm development.

4.2.2 Image pre-processing and convolutional neural network

A pre-processing pipeline was used to transform the raw CTA volume into a normalized space suitable for using as inputs to a convolutional neural network. This is required so that the network is always presented with images of the same resolution, field of view, and range of intensity values; and so, does not have to account for these factors of variation as they are standardized. To this end, the volumes were cropped 181 mm from the top of the raw volume and then resampled to a voxel spacing of 1.13 mm³, leading to an input shape of 160x192x160 voxels. Furthermore, the image intensities were clipped to the range of 0 to 1000 Hounsfield Units (HU).

A 3D Convolutional Neural Network (CNN) (12) was used to extract valuable features from the normalized volume and to perform the detection of LVO. It was composed of 4 down blocks, each of which was composed of 2 convolutional layers with 8 kernels. The activation function for each convolutional layer was the rectified linear unit function (13). At the end of each down block, a batch normalization operation was performed (14). After the last convolutional layer, all nodes were flattened, and a single fully connected layer was applied to compute the output layer. The output layer encoded information about both the existence of an LVO and the location of the clot from the manually labeled data points on the source scans.

The training of the model was performed using an Adam optimizer (15) with a learning rate of 1e-3 and a batch size of 16 for 2700 epochs. In each epoch, the entire training set was backpropagated through the model. During training, several data augmentation operations were performed. These include 1) rotation of up to +/-45 degrees on the axial plane, 2) rotation of +/-20 degrees in the coronal/sagittal planes, 3) flipping along the x axis only, and 4) translation of up to +/-40 voxels in all axes.

The loss function was necessary to guide the training process of the model and was not used during the deployment of the model. It was based on the softmax cross entropy function between the output layer and the reference encoding, both of which contained information about the existence of an LVO and the location of the clot. (Of note, the occlusion location was used for the software development, but only to a limited extent and the information about the occlusion location is not provided to the end-users).

4.2.3 Software validation dataset

This test data was independent of the development dataset and was retrospectively selected from the following studies, namely, ESCAPE-NA1 (16), ALIAS (17), TEMPO-1 (18) and PREDICT (19). Additional inclusion criteria for the test set included subjects aged 18 years or older, who underwent baseline CTA imaging for acute stroke with image slice thickness between 0.5 mm to 2.5mm. Similar to the derivation dataset, the imaging data for the test set were acquired from multiple CT scanner models, manufactured by four different CT scanner vendors (GE, Siemens, Philips, Toshiba), as well as from multiple hospital sites and geographies. Scans determined to be technically inadequate (e.g., invalid DICOM image or inappropriate head coverage or no contrast) or with significant patient motion were excluded.

Based on data from similar marketed devices, it was determined that a lower bound 95% confidence interval (CI) of 80% for both sensitivity and specificity is required to demonstrate the clinical utility of the device. Using the normal approximation interval, and assuming that the sensitivity/specificity point estimates would be at 85% (5% above the acceptance criteria), a sample size of 200 LVO and 200 other/no occlusion was deemed necessary to meet this performance goal.

Random selection with purposive sampling was performed to achieve a balanced number of LVO and other/no occlusion cases, and to ensure representation of cases acquired on multiple scanner manufacturers. The sampling was automated and informed by patient-level meta data which included only the scanner manufacturer and the clinical reference label (LVO yes/no) from the originating clinical study.

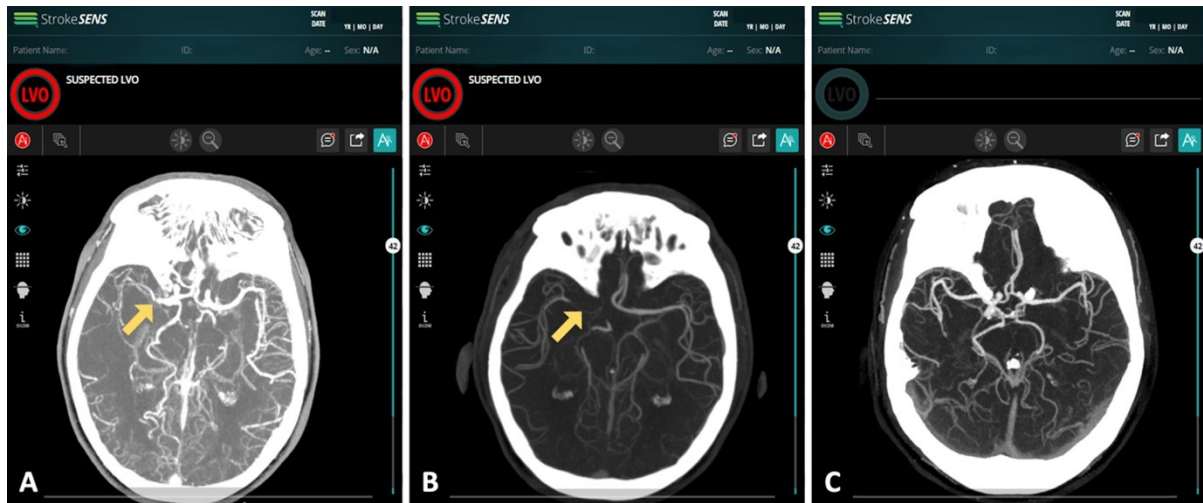
Expert-consensus was used as ground truth to establish the reference dataset labels. Three board-certified neuroradiologists (with >5 years of experience in stroke imaging) independently read all CTA images. A LVO scan was defined as containing an ICA or M1 MCA occlusion. A other/no occlusion scan was defined as any scan that does not contain an LVO, i.e., it may either have other more distally located intracranial occlusions or no occlusions at all. In addition to reporting “LVO” vs “other/no occlusion”, the readers were also asked to

report the site of occlusion (anatomical location including any intracranial ICA segment, M1 MCA segment and/or other occlusion/distal occlusions; the MCA bifurcation/trifurcation was used as the anatomical cut off between M1 and M2 MCA segments) as well as the presence of any intracranial hemorrhage (ICH). The readers interpreted the scans blinded to any clinical information. Consensus was determined when at least two of three readers agreed on the presence or absence of LVO. This study was approved by the University of Calgary Conjoint Health Research Ethics Board.

4.2.4 StrokeSENS LVO detection and notification

StrokeSENS generates a binary prediction of the presence or absence of LVO on CTA images of the brain. CTA head scans were automatically routed to the StrokeSENS LVO processing engine where they were processed and analyzed. In the case of a positive finding, i.e., a LVO detection by the software, the StrokeSENS user interface stated that a LVO was suspected, **Figure 4.1**. In the case of a positive finding, the system also automatically generates a notification which is sent to a prespecified email list. In a typical clinical scenario, the notification would be configured to be sent to physicians at a treating hospital parallel to the standard of care workflow. In the current setting, the notifications are sent only for suspected LVO cases.

Figure 4.1. Exemplary cases of StrokeSENS™ LVO software performance. In case A and B StrokeSENS LVO correctly detected a large vessel occlusion (demonstrated as a red circle in the upper left corner) in the right M1 middle cerebral artery (A, yellow arrow) and right terminal internal carotid artery (B, yellow arrow). In case C, StrokeSENS™ LVO correctly predicted that no large vessel occlusion was present. (Of note, the occlusion sites are marked with yellow arrows for clarity, it is not part of the software analysis)



4.2.5 Statistical analysis

Baseline characteristics of patients with LVO vs. other/no occlusion were compared using a chi-square test or Wilcoxon rank-sum test as appropriate. Expert reads on presence or absence of LVO was considered as the ground truth. Software performance for LVO detection was assessed using ROC analysis, reporting area under the curve (AUC), sensitivity, and specificity. The level of softmax cross entropy was used to calculate the AUC. False negative and false positive cases were retrospectively analyzed and the reason for the false negative/false positive result was identified.

Subgroup analyses were performed to evaluate software performance in detection of M1 and ICA segment occlusions separately. Software performance was also tested on data stratified by patient sex (female versus male), age (<70 years or ≥ 70 years or), slice thickness (<1.0 mm or ≥ 1.0 mm), kilovoltage tube peak (<120 kVp or ≥ 120 kVp) of the scan, and scanner manufacturer (GE Medical, Siemens, Philips, Toshiba). As no cases with ICH were used for the development, a sensitivity analysis to evaluate an impact of the ICH presence on the software performance was performed. Separate logistic regression models were used to test if the association between software prediction and ground truth (expert reads of LVO vs. not)

were modified by either patient age, sex, presence or absence of ICH, slice thickness, kVp or scanner manufacturer. Additionally, the mean, the maximum and the minimum processing times for positive cases (both true positive and false positive) were reported as a representative measure of time-to-notification (representing the time from the moment the scan is received in StrokeSENS to the notification send to the end-user). No imputation was performed for missing data since there were no missing data. Data analysis was performed using Stata 16.1 (Stata LLC Corp).

The Checklist for AI in Medical Imaging (CLAIM) guidelines were followed (20).

4.3 RESULTS

Out of 2779 eligible stroke cases, 1205 cases with identified baseline CTA and initial core lab reading were included into the preliminary dataset (excluded scans: 1339 cases with no baseline CTA, 52 scans with missing age information, and 183 scans with missing initial core lab read). Scans with inappropriate head coverage (n=12), no contrast (n=11), or corrupted DICOM (n=4) were additionally excluded and 400 cases randomly selected for expert consensus read (200 scans allocated in the primary LVO cohort and 200 scans allocated to the primary other/no occlusion cohort). Seventeen scans were re-classified by the consensus as LVO and a total of 400 cases (217 allocated to LVO cohort and 183 allocated to other/no occlusion cohort) were included in the test set, **Figure 4.2**.

Baseline characteristics of patients stratified by presence or absence of LVO are shown in **Table 4.1**. Patients with LVO presented with more severe stroke symptoms (expressed with higher NIHSS and had lower ASPECTS on non-contrast CT. The distribution of intracranial occlusion site in patients with LVO was terminal ICA (35.5%, n=77) and M1 MCA (64.5%, n=140). In the patients without LVO, there were 183 scans with either no occlusion (21.3%), a more distally located MCA occlusion (15.8%), or an occlusion in the posterior circulation (2.7%). The intracranial haemorrhage was present in 110 cases (60.1% of other/no occlusion cohort).

Of the 217 LVO cases evaluated, 194 (89.4%) were correctly identified as LVO by the software. Of 23 falsely negative cases, there were seven cases with ICA occlusion but normally opacified terminal ICA through the circle of Willis, six cases with short-segment M1 MCA occlusions and good collaterals, three with M1 MCA occlusion and one case with ICA occlusion demonstrated good collaterals and also early venous opacification that may contributed to “richer” vasculature beyond the occlusion, four cases demonstrated a distal M1 MCA occlusion with a prominent anterior temporal artery, one case had a nonocclusive M1

MCA thrombus. Poor contrast opacification was present in one case.

Of the 183 other/no occlusion cases, 23 (12.6%) were incorrectly identified as LVO by the software. A review identified multiple possible reasons for the false positive findings: scan asymmetry at the level of the circle of Willis was present in six cases; four cases had an M2 segment occlusion and either relatively short M1 MCA segment or a dominant M2 MCA branch occlusion; three cases had M1 MCA segment stenosis; beam hardening artifact obscured the ICA/MCA segment in three cases; one case was with a M1 MCA aneurysm adjacent to the M1 segment occlusion; and two cases had low quality scans (poor contrast filling, incomplete study). No obvious reason for the false positive finding was found in the remaining four cases.

The sensitivity and specificity for LVO detection were 0.894 (95% CI: 0.854–0.932) and 0.874 (95% CI: 0.817–0.919), respectively, and the AUC was 0.939 (95% CI: 0.915–0.962). Results of subgroup analyses for the M1 and ICA segment occlusion detection were comparable to the main analysis, **Table 4.2**. In analysis stratified by patient sex, age, presence of hemorrhage, slice thickness, kVp and scan manufacturer, the sensitivity, specificity, and AUC ranged from 0.843–0.945, 0.83–1.0, and 0.924–0.970, respectively, **Table 4.2**. There was also no difference found in the software performance when the cases with ICH were excluded from the other/no occlusion cohort. No statistically significant interactions were noted between age, sex, presence/absence of ICH, slice thickness, kVp and software prediction of LVO in logistic regression models testing for association between software prediction and ground truth (all $p > 0.05$).

The mean processing time for the sum of 217 true and false positive cases was 44.5 seconds (standard deviation \pm 11 seconds), the minimum time was 18.4 seconds, the maximum time was 77.9 seconds.

Figure 4.2. Diagram of scan selection. Scan selection of the test set that was used for evaluation of large vessel occlusion detection with Stroke*SENS* LVO.

Note: ICA – internal carotid artery, LVO – large vessel occlusion, M1 MCA – M1 segment of the middle cerebral artery

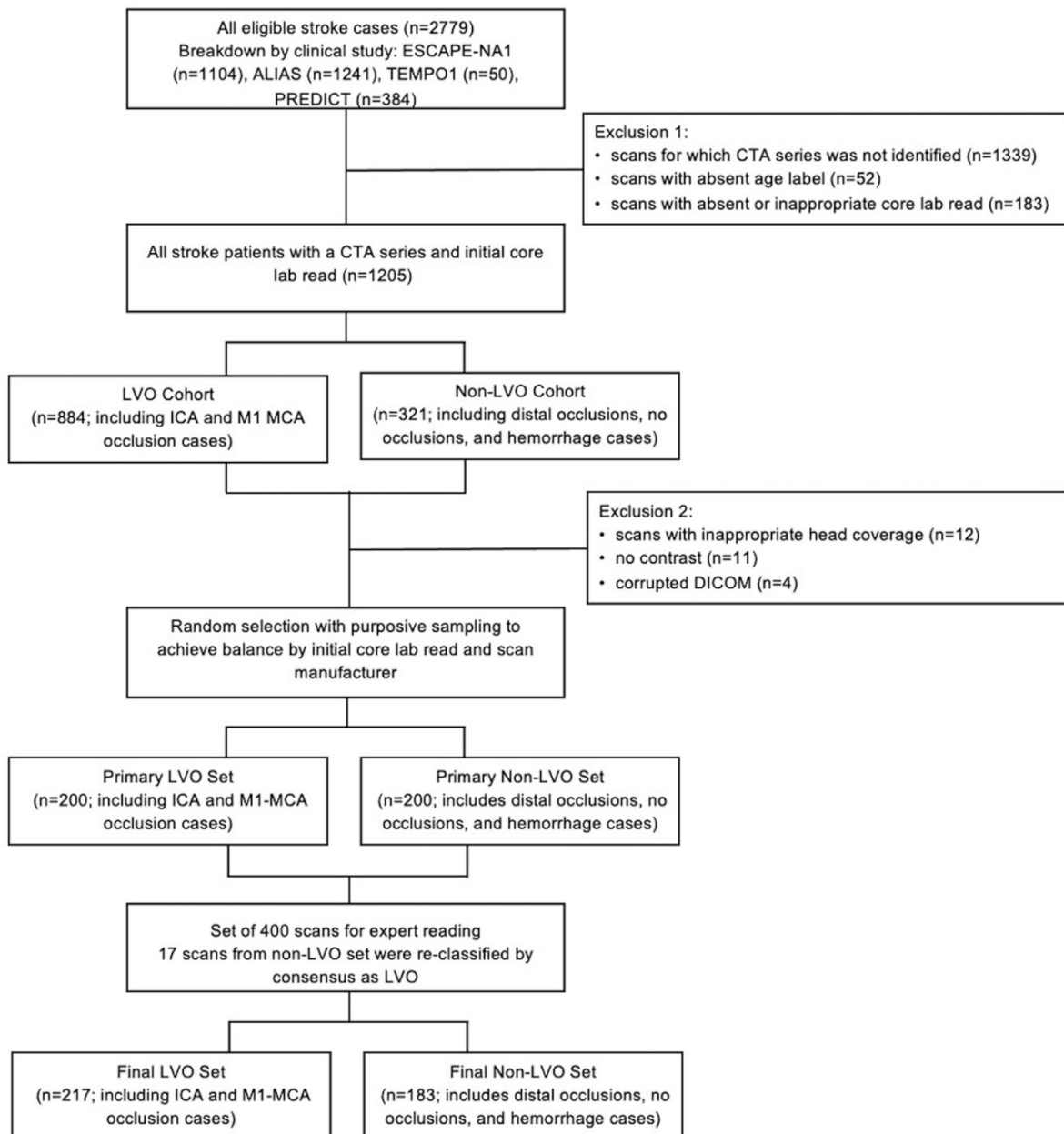


Table 4.1. Baseline clinical and imaging characteristics of subjects in the test set.

Baseline characteristic	LVO (n=217)	other/no occlusion (n=183)	p-value
Age, median (IQR)	70 (61 – 78)	69 (58 – 78)	0.671a
Sex, female, n (%)	97 (44.7)	86 (46.7)	0.687b
Baseline NIHSS, median (IQR)	17 (11 – 21)	8 (6 – 16)	<0.001a
Baseline ASPECTS, median (IQR)	8 (7 – 9)	10 (9 – 10)	<0.001a
Onset to CT, min, median (IQR)	134 (71 – 253)	115 (72 – 195)	0.261a

a derived from Wilcoxon rank sum test

b derived from chi-square test

Note: ASPECTS – Alberta Stroke Programme Early CT Score, IQR – interquartile range, LVO – large vessel occlusion; NIHSS - National Institutes of Health Stroke Scale

Table 4.2. Area under the curve, sensitivity and specificity for automated LVO detection using the machine learning-based algorithm.

Group	# of LVO	# of other/no occlusion	Total	Sensitivity [95% CI]	Specificity [95% CI]	AUC [95% CI]
Full cohort	217	183	400	0.894 [0.854, 0.932]	0.874 [0.817, 0.919]	0.939 [0.915, 0.962]
Site of Occlusion						
ICA + other/no occlusion	77	183	260	0.857 [0.759, 0.927]	0.874 [0.817, 0.919]	0.927 [0.888, 0.965]
M1 MCA + other/no occlusion	140	183	323	0.914 [0.855, 0.955]	0.874 [0.817, 0.919]	0.945 [0.918, 0.972]
Age						
<70 years	108	95	203	0.843 [0.760, 0.901]	0.916 [0.841, 0.963]	0.928 [0.891, 0.965]
≥70 years	109	88	197	0.945 [0.884, 0.980]	0.83 [0.735, 0.901]	0.951 [0.923, 0.980]
Sex						
Male	120	97	217	0.875 [0.802, 0.928]	0.866 [0.782, 0.927]	0.936 [0.905, 0.968]
Female	97	86	183	0.918 [0.844, 0.964]	0.884 [0.797, 0.943]	0.940 [0.903, 0.977]
Hemorrhage						
LVO + Hemorrhage	217	110	327	0.894 [0.845, 0.932]	0.891 [0.817, 0.942]	0.944 [0.920, 0.968]
LVO + Non-Hemorrhage	217	73	290	0.894 [0.845, 0.932]	0.849 [0.746, 0.922]	0.930 [0.899, 0.961]
Slice thickness						
<1.0 mm	120	100	220	0.883 [0.812, 0.935]	0.850 [0.765, 0.914]	0.936 [0.904, 0.967]
≥1.0 mm	97	83	180	0.939 [0.849, 0.983]	0.924 [0.832, 0.975]	0.939 [0.902, 0.977]

Tube voltage						
<120 kVp	76	4	80	0.908 [0.819, 0.962]	1.0 [0.398, 1.0]	0.970 [0.923, 1.0]
≥120 kVp	141	179	320	0.887 [0.822, 0.934]	0.872 [0.814, 0.917]	0.935 [0.905, 0.965]
Scanner manufacturer						
GE Medical	62	84	146	0.903 [0.801, 0.964]	0.869 [0.778, 0.933]	0.956 [0.924, 0.987]
Siemens	63	80	143	0.857 [0.746, 0.933]	0.90 [0.812, 0.956]	0.924 [0.875, 0.972]
Other (Philips, Toshiba)	92	19	11	0.913 [0.836, 0.962]	0.79 [0.544, 0.94]	0.927 [0.871, 0.983]

Note: AUC – area under the curve, CI – confidence interval, ICA – internal carotid artery, kVp- kilovoltage peak, LVO – large vessel occlusion, M1 MCA – M1 segment of the middle cerebral artery

4.4 DISCUSSION

In this study, we test the ability of Stroke*SENS* LVO in detecting LVO of the anterior circulation automatically in patients presenting with acute stroke. The accuracy (sensitivity and specificity of 0.894 and 0.874 overall, with similar results across various subgroups, **Figure 4.3**) and speed of detection of the software in a large dataset from multiple centers and geographies, using a variety of vendor machines and protocols for CTA image acquisition supports the generalizability of the software's use in routine clinical practice.

In general, sensitivity is important metrics to indeed capture as many positive cases as possible and consider them for lifesaving EVT treatment; on the flip side, specificity is very important, especially in hospital sites in which the prevalence of LVOs is very low, since the positive predictive value (precision) is directly influenced by it. In turn, low PPV values can lead clinicians to not trust the tool which can, in turn, lead them to ignore the notifications of the tool entirely (21). Given that, we aimed at maximizing both the sensitivity and specificity of the model equally.

The test set in this analysis was purposively sampled to include a higher prevalence of common pathologies (i.e., ICH, distal occlusions, and posterior circulation occlusions) than is typically encountered in consecutive suspected acute stroke cases in the anterior circulation. The objective of the purposive sampling was to test the model's diagnostic performance in a dataset with a large representation of less straightforward cases (i.e. ICH & "other" occlusions) that are expected to be encountered by the algorithm in the clinical practice. A high proportion of hemorrhagic scans in the other/no occlusion cohort was included in order to test the consistency of the software's performance in LVO detection and verified the consistency of the tool. We considered this to be a valid feature of the software tool as the presence of the ICH or other pathologies such as intracranial tumors can lead to false positive finding due to tissue distortion resulting in a change of the vessel course (22). Although ICH cases can be detected on NCCT scan and will most likely be excluded from further imaging in many diagnostic settings, the fact that other settings include a CTA after NCCT in patients with ICH (for detection of neurovascular abnormalities or spot sign identification) means that even with diagnostic pathways including such cases being sent to the algorithm, the performance continues to be good.

Several automated standalone acute stroke software platforms are available for use in the clinical practice, such as iSchemaView (RAPID CTA), Viz.ai (VIZ LVO), Brainomix (e-CTA), Canon (^{AUTO}Stroke Solution LVO) or StrokeViewer (NICO.LAB). These platforms use different artificial intelligence including machine-learning methods for automatic detection of

LVOs. Strategies for computer-aided detection of LVO include the direct identification of occlusion site using local vascular features (i.e. detect the clot directly by identifying the discontinuity of the contrast-enhanced vessel), and the indirect identification of occlusion site based on the regional vessel density asymmetry between the affected hemisphere and the unaffected hemisphere. The 3D-CNN that is at the core of Stroke*SENS* LVO was trained using information about the existence of LVO and the location of the clot, which allows it to extract both global (image-level) features as well as local features of the clot. Additional analysis is required to assess the trade-off between these two strategies, but it is expected that an ideal device will take both strategies into consideration, similar to how a clinician typically reviews a CTA scan. More specifically, it is well known that in LVO cases with good collateral flow, the downstream effect of the occlusion on the opacification of the peripheral vasculature might not be easily detectable; in contrast, a bundle of vessels around the site of occlusion in LVO cases, or an intracranial MCA stenosis or aneurysm in other/no occlusion cases, may influence a detection of the clot features and result in false negative/positive findings.

Different methodologies for the computer-aided detection of LVO are discussed in a systematic review by Murray, et al. (23) published in 2019. Of the previously mentioned commercial LVO detection platforms, most have undergone validation studies that describe the software's performance in LVO (ICA and M1 MCA) occlusion detection, **Table 4.3**. The reported sensitivity and specificity of the software tools ranged from 0.72-0.97 and 0.74-0.96, respectively. The performance of the software tools was tested on various datasets and therefore a direct comparison is not possible. However, with regard to this limitation, the available data suggest that Stroke*SENS* with its sensitivity and specificity of 0.89 and 0.87, respectively, is likely comparable to the currently available tools.

The retrospective review of false negative cases revealed imaging characteristics that the algorithm did not overcome such as normally opacified terminal ICA segment in the presence of more proximally located ICA occlusion or presence of short-segment occlusion and good collaterals. The same reasons for the false negative finding were mentioned by authors of the RAPID CTA validation study (24). This suggests that an early opacification of the vasculature beyond the occlusion through collateral flow remains a challenge for automatic software. Similar to the previously reported reasons for false positive findings in literature (22,24), intracranial MCA stenosis or the presence of an MCA aneurysm lead to falsely positive result also in our dataset. However, the most common reason identified in this study that likely lead to false positive results was an asymmetric projection of the circle of Willis on the axial scan caused by lateral tilt. This is important information that could be incorporated into the

further development of the software tool. In three cases, M2 occlusions were identified as LVO and marked as false positive result while the validated software version was primarily developed to identify ICA and M1 MCA occlusions.

Automated software systems utilizing AI for detection of stroke signs can potentially accelerate the triage, diagnosis and treatment initiation of stroke patients significantly (25). Current methods of notifying the treating physician results in delays in treatment that negatively impact patient outcomes (26). A recent study showed that utilizing an automated LVO detection software together with a notification system resulted in an average reduction of 22.5 minutes in triage and transfer times between the spoke primary stroke center and the hub comprehensive stroke center (27). A tool for automated LVO detection and notification that would streamline the clinical workflow and aid in accurate and timely patient selection for rapid EVT at spoke hospitals. The *StrokeSENS* LVO showed excellent performance in speed of potential notification with a mean processing/notification time of 44.5 seconds in this study. Although a short processing time is a promising feature, time for data transfer from the CT machine to the processing computer needs to be evaluated in the real-world.

This study has some limitations. First, the current version of the software has been developed to identify only LVOs in the anterior circulation and its primary evaluation was therefore focused only on detection of such LVOs. With increasing evidence of endovascular treatment benefit in more distally located occlusions and occlusions in the posterior territory, further software development is warranted to reliably identify such intracranial occlusions. Second, the software performance was evaluated in a retrospective fashion on data from clinical studies that may have excluded patients with stroke mimics and other non-stroke pathologies that are detected routinely in real life practice. Our study dataset consisted of an artificially high LVO prevalence (54%) as we optimized the model with as many LVO cases as possible while matching those with an equal number of examples of other/no occlusion findings. The real-world LVO prevalence is approximately 15%-30%, therefore, the evaluation of the software performance in real-world data is warranted. The *StrokeSENS* LVO's performance in LVO detection and potential speed of notification in this validation dataset will need to be supported by tests in real life conditions done in a prospective manner. Such studies are planned. Finally, the impact of tools such as *StrokeSENS* will need to be compared with current standard workflow in a randomized manner for us to understand the true benefit of such tools on the population of acute stroke patients.

Figure 4.3. Areas under the receiver operating characteristic curves (AUC) for the StrokeSENSLVO. Model performance is demonstrated in the full dataset and in data stratified by occlusion site (ICA and M1 MCA segment), age (<70 years and \geq 70 years), sex and presence/absence of intracranial hemorrhage

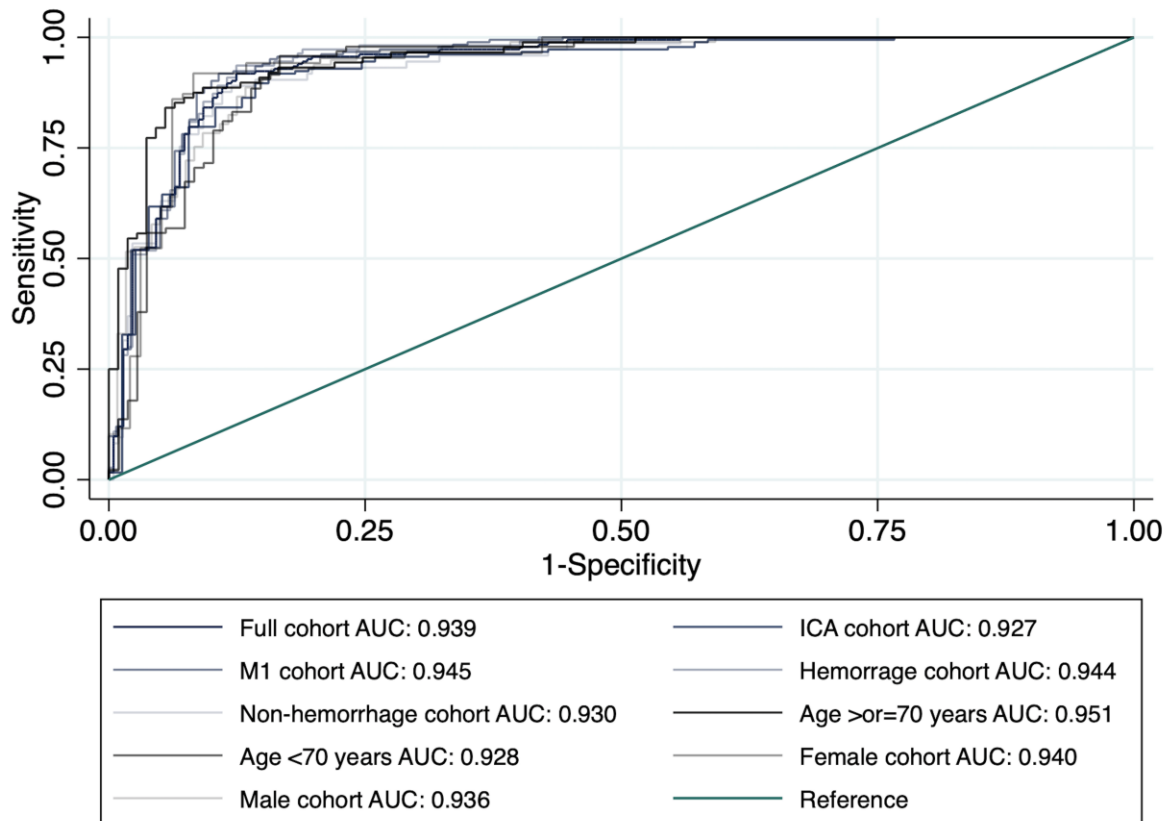


Table 4.3. The summary of available automatic software tools for LVO detection.

Software	Number of cases (LVO/all)	Detected occlusion site	Sensitivity	Specificity	AUC	False negative	False positive	Processing time, seconds
StrokeSENS	217/400	ICA & M1 MCA	0.894	0.874	0.939	23 (6 ICA occlusions with normally opacified terminal ICA segment; 6 short-segment occlusions; 4 distal M1 MCA occlusion with prominent ATA; 3 good collaterals and arterio-venous phase; 1 non-occlusive thrombus; 1 poor contrast filling)	23 (6 axial scan asymmetry; 4 M2 occlusions; 3 MCA stenosis; 3 beam hardening artifact; 1 MCA aneurysm; 5 unclear reason)	44.5 (mean)
Viz LVO (Viz.ai)[28]	163/2544	Not specified	0.963	0.938				345 (median)
Viz LVO (Viz.ai)[22]	75/1167	ICA & M1 MCA	0.81	0.96	0.91	14	56 (12 M2 and M3 MCA occlusions; 12 hemorrhage; 9 >50% MCA stenosis; 4 scans with tumor; 19 no pathology)	
<i>Stroke protocol</i>	72/404	ICA & M1 MCA	0.82	0.90		13	-	
RAPID CTA[24] (iSchemaView)	320/926	ICA & M1 MCA	0.969	0.743	0.941	9 (3 short-segment occlusions; 5 robust collaterals; 1 ICA at skull base)	11 (4 variant MCA anatomy; 1 subdural hematoma with severe midline shift; 1 MCA aneurysm; 3 M2 MCA stenosis; 1 incomplete TICI 2b reperfusion after MT)	158 (median)
e-CTA (Brainomix)[29]	(160/301)	ICA & M1 MCA,	0.92	0.98		26		
Stroke Solution LVO (Canon)[30]	202/303	ICA / M1 MCA	0.90/0.77	0.98/0.98		55	2	71.5 (for LVO cohort)

StrokeViewer (NICO.LAB)[31] <i>MR CLEAN Registry</i>	952 ^a	ICA / M1 MCA	0.88/0.94			65 (8 ICA occlusions; 13 M1 occlusions; 44 incorrect location marked)	0	299 (mean)
<i>PRESTO</i>	76/581 ^a	ICA/M1 MCA	0.80/0.95	-	-	6 (2 ICA occlusions; 4 incorrect location marked)	55 (24 no occlusion; 2 extracranial ICA, 29 unknown data)	

^a Data from the sensitivity analysis with excluded M2 MCA occlusions

^b Mean processing time for the pooled dataset of patients from MR CLEAN Registry and PRESTO study

Note: ATA – anterior temporal artery; AUC – area under the curve, CI – confidence interval, ICA – internal carotid artery, LVO – large vessel occlusion, MCA – middle cerebral artery, MT – mechanical thrombectomy; NPV – negative predictive value, PPV – positive predictive value

4.5 CONCLUSION

Automated LVO detection and notification can aid in acute stroke management by quickly and accurately detecting patients with LVO who may likely require immediate medical attention and benefit from EVT. However, a further development including the full range of clinically relevant intracranial occlusions is as well as prospective studies exploring the impact of the software tools on acute stroke workflow and patient outcomes is warranted.

REFERENCES

1. Duloquin G, Graber M, Garnier L, et al. Incidence of acute ischemic stroke with visible arterial occlusion. *Stroke* 2020;51:2122-2130.
2. Malhotra K, Gornbein J, Saver JL. Ischemic strokes due to large-vessel occlusions contribute disproportionately to stroke-related dependence and death: a review. *Front Neurol* 2017;8.
3. Goyal M, Menon BK, Van Zwam WH, et al. Endovascular thrombectomy after large-vessel ischaemic stroke: a meta-analysis of individual patient data from five randomised trials. *Lancet* 2016;387:1723-1731.
4. Powers WJ, Rabinstein AA, Ackerson T, et al. Guidelines for the early management of patients with acute ischemic stroke: 2019 update to the 2018 guidelines for the early management of acute ischemic stroke a guideline for healthcare professionals from the american heart association/american stroke association. *Stroke* 2019;50:E344-E418.
5. Demchuk AM, Menon BK, Goyal M. Comparing vessel imaging: noncontrast computed tomography/computed tomographic angiography should be the new minimum standard in acute disabling stroke. *Stroke* 2016;47:273-281.
6. Menon BK. Neuroimaging in acute stroke. *Contin Lifelong Learn Neurol* 2020;26:287-309.
7. Almekhlafi MA, Kunz WG, Menon BK, et al. Imaging of patients with suspected large-vessel occlusion at primary stroke centers: available modalities and a suggested approach. *Am J Neuroradiol* 2019;40:396-400.
8. Saver JL. Time is brain—quantified. *Stroke* 2006;37:263-266.
9. Menon BK, Al-Ajlan FS, Najm M, et al. Association of clinical, imaging, and thrombus characteristics with recanalization of visible intracranial occlusion in patients with acute ischemic stroke. *JAMA - J Am Med Assoc* 2018;320:1017-1026.
10. Menon BK, d’Esterre CD, Qazi EM, et al. Multiphase ct angiography: a new tool for the imaging triage of patients with acute ischemic stroke. *Radiology* 2015;275:510-520.
11. Goyal M, Demchuk AM, Menon BK, et al. Randomized assessment of rapid endovascular treatment of ischemic stroke. *N Engl J Med* 2015;372:1-12.
12. O’Shea K, Nash R. An introduction to convolutional neural networks. November 2015.
13. Agarap AF. Deep learning using rectified linear units (relu). March 2018.
14. Ioffe S, Szegedy C. Batch normalization: accelerating deep network training by reducing internal covariate shift. *32nd Int Conf Mach Learn ICML 2015* 2015;1:448-456.
15. Kingma DP, Ba JL. Adam: a method for stochastic optimization. *3rd Int Conf Learn*

Represent ICLR 2015 - Conf Track Proc December 2015.

16. Hill MD, Goyal M, Menon BK, et al. Efficacy and safety of nerinetide for the treatment of acute ischaemic stroke (escape-na1): a multicentre, double-blind, randomised controlled trial. *Lancet* 2020;395:878-887.
17. Ginsberg MD, Palesch YY, Hill MD, et al. High-dose albumin treatment for acute ischaemic stroke (alias) part 2: a randomised, double-blind, phase 3, placebo-controlled trial. *Lancet Neurol* 2013;12:1049-1058.
18. Coutts SB, Dubuc V, Mandzia J, et al. Tenecteplase-tissue-type plasminogen activator evaluation for minor ischemic stroke with proven occlusion. *Stroke* 2015;46:769-774.
19. Demchuk AM, Dowlatshahi D, Rodriguez-Luna D, et al. Prediction of haematoma growth and outcome in patients with intracerebral haemorrhage using the ct-angiography spot sign (predict): a prospective observational study. *Lancet Neurol* 2012;11:307-314.
20. Mongan J, Moy L, Kahn CE. Checklist for artificial intelligence in medical imaging (claim): a guide for authors and reviewers. *Radiol Artif Intell* 2020;2:e200029.
21. Walach E. Lies, damned lies and ai statistics - medcity news.
22. Dovrat AY, Saban M, Merhav G, et al. Evaluation of artificial intelligence-powered identification of large-vessel occlusions in a comprehensive stroke center. *Am J Neuroradiol* 2021;42:247-254.
23. Murray NM, Unberath M, Hager GD, Hui FK. Artificial intelligence to diagnose ischemic stroke and identify large vessel occlusions: a systematic review. *J Neurointerv Surg* 2020;12:156-164.
24. Amukotuwa SA, Straka M, Dehkharghani S, Bammer R. Fast automatic detection of large vessel occlusions on ct angiography. *Stroke* 2019;50:3431-3438.
25. Amukotuwa SA, Straka M, Smith H, et al. Automated detection of intracranial large vessel occlusions on computed tomography angiography a single center experience. *Stroke* 2019;50:2790-2798.
26. Froehler MT, Saver JL, Zaidat OO, et al. Interhospital transfer before thrombectomy is associated with delayed treatment and worse outcome in the stratis registry (systematic evaluation of patients treated with neurothrombectomy devices for acute ischemic stroke). *Circulation* 2017;136:2311-2321.
27. Hassan AE, Ringheanu VM, Rabah RR, Preston L, Tekle WG, Qureshi AI. Early experience utilizing artificial intelligence shows significant reduction in transfer times and length of stay in a hub and spoke model. *Interv Neuroradiol* 2020;26:615-622.

5. Chapter 5 - Utility of time-variant multiphase CTA color maps in outcome prediction for acute ischemic stroke due to anterior circulation large vessel occlusion

The contents of this chapter have been adapted from the journal article entitled “*Utility of time-variant multiphase CTA color maps in outcome prediction for acute ischemic stroke due to anterior circulation large vessel occlusion*”, published in Clin Neuroradiol 2021;31:783-790 by J.M. Ospel, P. Cimflova, O. Volny, et al.

Reproduced with permission from Springer Nature

Background Multiphase CTA (mCTA) is an established tool for endovascular treatment decision-making and outcome prediction in acute ischemic stroke, but its interpretation requires some degree of experience. We aimed to determine whether mCTA-based prediction of clinical outcome and final infarct volume can be improved by assessing collateral status on time-variant mCTA color maps rather than using a conventional mCTA display format.

Methods Patients from the PROve-IT cohort study with anterior circulation large vessel occlusion were included in this study. Collateral status was assessed with a three-point scale using the conventional display format. Collateral extent and filling dynamics were then graded on a three-point scale using time-variant mCTA color-maps (FastStroke, GE Healthcare, Milwaukee, WI, USA). Multivariable logistic regression was performed to determine the association of conventional collateral score, color-coded collateral extent and color-coded collateral filling dynamics with good clinical outcome and final infarct volume (volume below vs. above median infarct volume in the study sample).

Results A total of 285 patients were included in the analysis and 53% (152/285) of the patients achieved a good outcome. Median infarct volume on follow-up was 12.6ml. Color-coded collateral extent was significantly associated with good outcome (adjusted odds ratio [adjOR] 0.53, 95% confidence interval [CI]:0.36–0.77) while color-coded collateral filling dynamics (adjOR 1.30 [95%CI:0.88–1.95]) and conventional collateral scoring (adjOR 0.72 [95%CI:0.48–1.08]) were not. Both color-coded collateral extent (adjOR 2.67 [95%CI:1.80–4.00]) and conventional collateral scoring (adjOR 1.84 [95%CI:1.21–2.79]) were significantly

associated with follow-up infarct volume, while color-coded collateral filling dynamics were not (adjOR 1.21 [95%CI:0.83–1.78]).

Conclusion: In this study, collateral extent assessment on time-variant mCTA maps improved prediction of good outcome and has similar value in predicting follow-up infarct volume compared to conventional mCTA collateral grading.

5.1 INTRODUCTION

Acute ischemic stroke (AIS) due to large vessel occlusion (LVO) is a highly time-critical disease. A typical LVO patient loses 1.9 million neurons per minute (1). In 2015, endovascular treatment (EVT) has become standard of care for LVO strokes presenting within 6 hours from symptom onset (2). EVT is a powerful treatment, and its effect is highly time-dependent (3). The overarching goal when performing EVT is therefore to treat the patient as fast as possible. However, not all patients will benefit from EVT, and selecting the right patients is crucial, in order not to cause harm. Currently, patient selection is based on 2 pillars: clinical characteristics (symptom severity, pre-morbid functional status) and brain imaging (2). Imaging is used to determine how much brain tissue is already irreversibly damaged, since in patients with extensive ischemic changes, tissue is unlikely to be salvaged by EVT, and the risk of reperfusion hemorrhage is high. There are many ways of identifying irreversibly damaged tissue; the most commonly used imaging techniques are CT perfusion (CTP) and multiphase CTA (mCTA). Both techniques have been successfully used for EVT patient selection in randomized controlled trials (4-7), and both have their advantages/disadvantages: CTP maps can be quickly and easily interpreted even with limited imaging experience, because the color-coded display format is a clear visual indicator of pathology. On the other hand, CTP is susceptible to patient motion and post-processing artifacts, and generating postprocessed maps takes some time. mCTA is more robust against patient motion, and requires less contrast and radiation dose. It is equally reliable to CTP as an EVT selection and outcome prediction tool, and because it can easily be implemented without any additional technical requirements, it is particularly attractive for smaller hospitals and places in which it is not possible to afford additional hardware and software (8). However, the standard display format of mCTA consists of 3 separate gray-scale images of the cerebral vessels, and evaluating the collaterals requires the reader to assess all three of them simultaneously. The interpretation of mCTA therefore requires some degree of experience and is often perceived to be less intuitive than CTP interpretation. Novel color-coded mCTA display format, was recently described, in which all 3 mCTA series are consolidated in a single color-coded map, thereby potentially facilitating and improving mCTA interpretation (9).

The purpose of this study is to compare prediction of clinical outcome and final infarct volume in acute ischemic stroke due to LVO using a conventional mCTA display format vs. time-variant color maps.

5.2 MATERIALS & METHODS

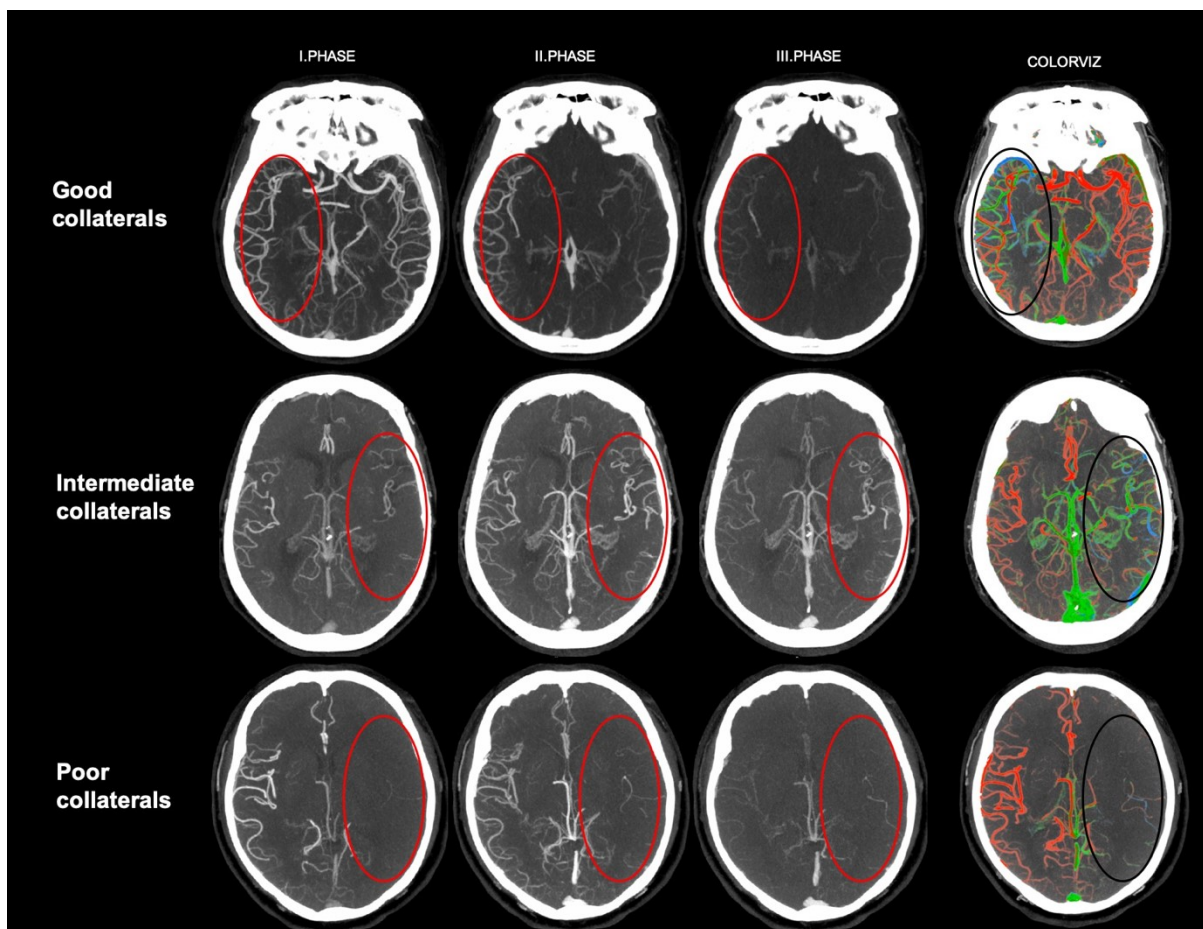
5.2.1 Patient population

The Precise and Rapid Assessment of Collaterals Multi-phase CTA in the Triage of Patients With Acute Ischemic Stroke for IA Therapy (Prove-IT) study (10) was a prospective multi-center cohort study that enrolled 464 patients who presented with symptoms consistent with AIS (NCT02184936). Patients were eligible for the study if they presented to the emergency department with symptoms consistent with AIS, were older than 18 years, and mCTA and CTP were performed within 12 hours of symptom onset and before recanalization therapy. Detailed inclusion and exclusion criteria have been published previously (8). We included patients with anterior circulation LVO (internal carotid artery, M1 or proximal M2 occlusions) in this study. Patients in which baseline mCTA images were incomplete or not interpretable were excluded.

5.2.2 Image acquisition

Non contrast head CT (NCCT) and mCTA: NCCT was acquired with 5 mm slice thickness. mCTA consisted of three phases, with arch to vertex coverage in the first (arterial) and skull base to vertex coverage the second (peak venous) and third (late venous) phases. Detailed mCTA acquisition parameters have been published previously (8). Axial images with 1 mm overlap and multiplanar axial, coronal and sagittal reconstructions with 3 mm thickness, 1 mm intervals and 1 mm overlap for the first phase were then generated, as well as axial maximum intensity projections (MIPs) for all three phases. Time variant mCTA color maps were generated with the FastStroke research prototype (GE Healthcare, Milwaukee, Wisconsin) and displayed as axial, coronal, sagittal, and oblique MIP reformations. Color-coding of the collaterals based on a per-patient adaptive threshold technique (9); vessels with maximum enhancement in the pre-venous phase are displayed in red; those with maximum enhancement in the peak-venous phase and late-venous phase are displayed in green and blue, respectively, **Figure 5.1.**

Figure 5.1. Conventional and color-based collateral scoring. Top row: good collaterals. Most collaterals are opacified on the first mCTA phase and appear red on the color-map, which is consistent with a zero-phase delay. The vessel extent is nearly identical to the contralateral side. Middle row: Intermediate collaterals. Most collaterals are opacified on the second mCTA phase and appear green on the color-map, which is consistent with a one-phase delay. The vessel extent is slightly reduced compared to the the contralateral side. Bottom row: Poor collaterals. The few visible collaterals are mostly opacified on the third mCTA phase and appear blue on the color-map, which is consistent with a two-phase delay. The vessel extent is markedly reduced compared to the contralateral side.



5.2.3 Image interpretation

All images were assessed in a consensus read (by a neurologist and neuroradiologist).

ASPECTS: ASPECTS was scored on 5 mm reconstructed axial unenhanced NCCT images.

Occlusion site: Occlusion site determined on axial mCTA MIP images and was reported as either terminal internal carotid artery, M1 segment or proximal M2 segment. We decided to

include the proximal M2 segment in our analysis, since most physicians consider proximal M2 occlusions “large vessel occlusions” and as appropriate target lesions for EVT (10). Proximal M2 occlusions were hereby defined as Sylvian segment M2 occlusions located within 1 cm from the middle cerebral artery bifurcation.

Conventional mCTA collateral grading: The delay and extent of collateral filling was graded on axial MIPs of the three mCTA phases. A trichotomized collateral scale as used in the ESCAPE (6) and ESCAPE NA1 (11) trial was used:

- 1) Poor collaterals: no or only few vessels visible in any phase within the occluded vascular territory compared to the asymptomatic contralateral hemisphere.
- 2) Intermediate collaterals: delay of two phases in filling in of peripheral vessels with or without decreased prominence and extent or a one-phase delay and some ischemic regions with only few or no vessels compared to the asymptomatic contralateral hemisphere.
- 3) Good collaterals: no delay or 1 phase delay in filling of peripheral vessels with identical or increased prominence of vessels compared to the asymptomatic contralateral hemisphere.

Collateral grading on time-variant color maps: Both delay and extent of collateral filling were graded on a trichotomized scale on axial color-coded MIPs.

Collateral extent was graded as follows:

- 1) Normal or almost normal extent (>90%) of visible vessels within the occluded vascular territory compared to the contralateral hemisphere.
- 2) Vessel extent 50 – 90% compared within the occluded vascular territory to the contralateral hemisphere.
- 3) Vessel extent <50% compared within the occluded vascular territory to the contralateral hemisphere.

Collateral delay was graded as follows:

- 1) Predominantly no delay (most vessels are displayed in red) within the occluded vascular territory.
- 2) Predominantly 1 phase delay (most vessels are displayed in green) within the occluded vascular territory.
- 3) Predominantly 2 phase delay or no collaterals (most vessels are displayed in blue/no vessels visible at all) within the occluded vascular territory.

Final infarct volume: Final infarct volumes were measured by summation of manual planimetric demarcation of infarct on axial NCCT or DWI-MRI follow-up imaging at 24 hours.

5.2.4 Interrater agreement

To determine interrater agreement for scoring of collateral extent and filling dynamics on time-variant mCTA color maps, a neuroradiologist and a medical student independently reviewed 30 cases in two separate reading sessions with a 1-week break between the two sessions (session 1: conventional collateral scoring, session 2: assessment of collateral extent and filling dynamics on time-variant color maps). The reader had access to the site of occlusion, age and baseline NIHSS, but were blinded to all other baseline information and patient outcomes.

5.2.5 Statistical analysis

Patient baseline characteristics were described using descriptive statistics. Uni- and multivariable logistic regression was used to determine the association of conventional and color-coded collateral scores and a) good outcome, defined mRS 0-2 at 90 days (primary outcome), and b) follow-up infarct volume (secondary outcome). Follow-up infarct volume was hereby included in the models as binary variable (infarct volume below or equal to/above the median infarct volume in the study sample). Information loss across models was compared using the Akaike and Bayesian information criterion (AIC, BIC) and the area under the curve (AUC). Adjustment was performed for patient age, sex and baseline NIHSS. Inter-rater agreement was assessed using the Kappa statistic. All statistical tests were two-sided and conventional levels of significance ($\alpha = 0.05$) were used for interpretation. All analysis was performed using Stata 15.1.

5.3 RESULTS

Out of 464 patients, 285 were included in the analysis. **Figure 5.2** shows a flow chart of included and excluded patients. Patient baseline characteristics are shown in **Table 5.1**.

When using the trichotomized grading system on conventional display format, 60.7% (173/285) patients had good collaterals, 30.2% (86/285) had intermediate and 9.1% (26/285) poor collaterals. Collateral extent on time-variant color maps was normal or almost normal in 50.9% (145/285) patients, a collateral extent of 50-90% compared to the contralateral hemisphere was seen in 34.0% (97/285), and a collateral extent of less than 50% compared to the contralateral hemisphere in 15.1% (43/285). When using time-variant color maps, there was

mostly no delay in 14.4% (41/285), mostly a one phase delay in 56.5% (161/285) and mostly a two phase delay in 29.1% (83/285).

5.3.1 Collateral grading and clinical outcome

Overall, 53.3% (152/285) patients achieved a good outcome at 90 days. **Table 5.2** shows unadjusted and adjusted measures of effect size for the association of conventional collateral grade, color-coded collateral extent, color-coded collateral filling dynamics and good clinical outcome, as well as the respective AIC, BIC, and AUC values for the multi-variable models.

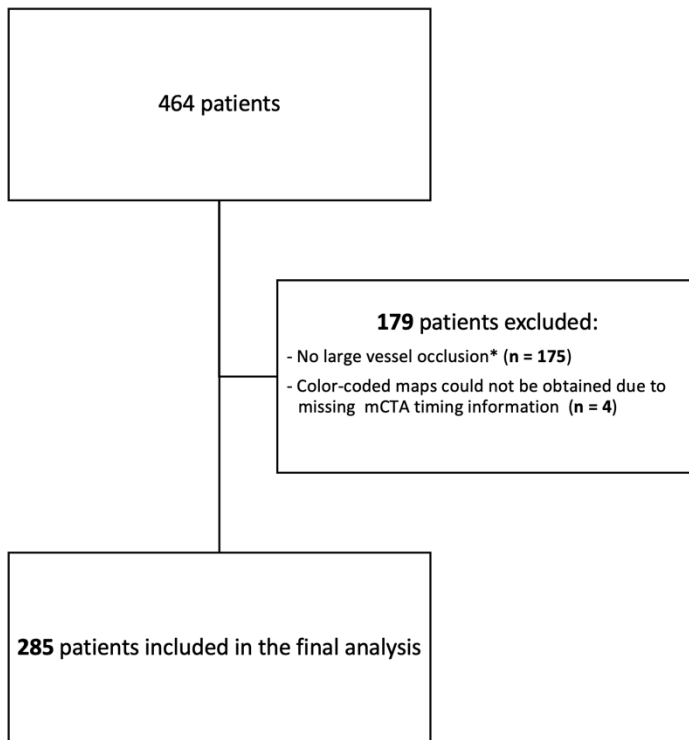
5.3.2 Collateral grading and final infarct volume

Infarct volume was available for 93.0% (265/285) patients. Median final infarct volume was 12.6 ml (IQR 1.7 – 49.2). **Table 5.3** shows unadjusted and adjusted measures of effect size for the association of conventional collateral grade, color-coded collateral filling dynamics, color-coded collateral extent and follow-up infarct volume (infarct volume below vs. above the median infarct volume), as well as the respective AIC, BIC, and AUC values for the multi-variable models.

5.3.3 Inter-rater agreement

Inter-rater agreement for color-coded grading of collateral filling dynamics and collateral extent was substantial (Kappa = 0.69 and 0.74 respectively).

Figure 5.2. Flowchart of included and excluded patients.



* Patients with proximal M2 occlusions (Sylvian segment M2 occlusions located within 1 cm from the middle cerebral artery bifurcation) were considered large vessel occlusions. mCTA = multiphase CT angiography

Table 5.1. Patient baseline characteristics (n = 285).

Female sex – n (%)	152 (53.3)
Age – median (IQR)	74 (64 – 81)
Co-morbidities – n (%)	
<i>Coronary artery disease</i>	50/284 (17.6)
<i>Chronic heart failure</i>	31/284 (10.9)
<i>Valvular disease</i>	20/284 (7.0)
<i>Hypertension</i>	188/284 (66.2)
<i>Previous stroke</i>	52 (18.3)
<i>Dyslipidemia</i>	122/284 (43.0)
<i>Atrial Fibrillation</i>	108/283 (38.2)
<i>Diabetes</i>	42/281 (14.9)
<i>Smoking</i>	107/276 (38.8)
Heart rate/min – median (IQR)	77 (66 – 92), n = 270
Systolic blood pressure – median (IQR)	148 (130 – 170), n = 282
Blood glucose in mmol/l – median (IQR)	6.5 (5.7 – 7.7), n = 281
Baseline NIHSS – median (IQR)	17 (11 – 22)
Baseline ASPECTS – median (IQR)	9 (8– 10), n = 284
EVT – n (%)	193 (67.7)
Intravenous alteplase – n (%)*	192 (67.4)
Occlusion Site – n (%)	
<i>Intracranial internal carotid artery</i>	56 (19.7)
<i>M1 segment</i>	184 (64.6)
<i>Proximal M2 segment**</i>	45 (15.8)
Onset to baseline CT in min – median (IQR)	124 (80 – 245)

Note: IQR = interquartile range, NIHSS = National Institutes of Health Stroke Scale, ASPECTS = Alberta Stroke Program Early CT Score, EVT = endovascular treatment

* Including six patients who received intravenous tenecteplase

** Proximal M2 occlusions were defined as occlusions in the horizontal M2 segment within one cm from the middle cerebral artery bifurcation.

Table 5.2. Association of conventional and color-map based collateral grade and good clinical outcome (n = 285).

Collateral score	Unadjusted (95% CI)	OR	Adjusted (95% CI)	OR*	AIC**	BIC**	AUC**
Conventional score	0.62 (0.43 – 0.89)		0.72 (0.48 – 1.08)		350.0	368.2	0.74
Color-map based collateral extent	0.54 (0.39 – 0.75)		0.53 (0.36 – 0.77)		340.9	359.2	0.76
Color-map based filling delay	1.21 (0.84 – 1.74)		1.30 (0.88 – 1.95)		350.8	369.1	0.74

*Adjusted for patient age, sex and baseline National Institutes of Health Stroke Scale.

**Derived from adjusted models

Note: OR = odds ratio, 95% CI = 95% confidence interval, AIC = Akaike information criterion, BIC = Bayesian information criterion, AUC = Area under the curve

Table 5.3. Association of conventional and color-map based collateral grade and final infarct volume (n = 265).

Collateral score	Unadjusted (95% CI)	OR	Adjusted (95% CI)	OR*	AIC**	BIC**	AUC**
Conventional score	2.05 (1.37 – 3.07)		1.84 (1.21– 2.79)		354.2	372.1	0.67
Color-map based collateral extent	2.99 (2.04 – 4.40)		2.67 (1.80 – 4.00)		336.4	354.3	0.72
Color-map based filling delay	1.29 (0.89 – 1.87)		1.21 (0.83 – 1.78)		361.7	379.6	0.63

*Adjusted for patient age, sex and baseline National Institutes of Health Stroke Scale.

**Derived from adjusted models

Note: Final infarct volume was coded as a binary variable in this analysis (volume below vs. above the median infarct volume)

OR = odds ratio, 95% CI = 95% confidence interval, AIC = Akaike information criterion, BIC = Bayesian information criterion, AUC = Area under the curve

5.4 DISCUSSION

Our study has the following main findings: 1) Color-coded mCTA grading of collateral extent improves prediction of good outcome at 90 days, and its performance in predicting follow-up infarct volume is similar compared to conventional collateral grading, 2) Color-coded mCTA grading of collateral filling dynamics performs worse than conventional collateral grading, and 3) inter-rater agreement for color-coded mCTA grading of collateral extent and filling dynamics is substantial.

Assessing collateral status on mCTA using a conventional display format, i.e. three separate series that are usually linked by the reader and then assessed in conjunction, takes both collateral filling dynamics and extent into account (13). When using time-variant mCTA color maps, collateral extent and filling dynamics are graded separately. When color-coded collateral extent was used to predict good outcome and follow-up infarct volume in our study, information loss was lower and discrimination better compared to conventional mCTA collateral scoring and color-coded scoring of filling dynamics. These results potentially indicate that collateral extent reflects tissue viability more accurately compared to collateral filling dynamics. In a previous study, D'Esterre et al assessed collateral extent and filling dynamics on conventional mCTA images and found that the former was not independently associated with follow-up infarction, while washout, a parameter that partly reflects filling dynamics, was associated with follow-up infarction (14). The apparently contradictory findings between their and our study could be explained by the fact that in the current study, the entire hemisphere was assessed, while d'Esterre and colleagues evaluated brain tissue per ASPECTS region. Both the current study and the study by d'Esterre et al relied on visual assessment of collaterals, which will always be subject to some degree of inter-rater variability. This variability could also explain the different results. Automation of collateral scoring could mitigate this problem, but the automated assessment would have to be available instantaneously, and integration of the technology into routine clinical practice will probably take some time (15). Software to generate time-variant mCTA maps on the other hand is already available, and the color-maps can be generated within a few seconds. mCTA color-maps therefore constitute a good alternative to facilitate interpretation of collateral status until fully-automated collateral assessment is routinely available, particularly for less experienced readers. Indeed, when comparing a non-expert to an expert reader, inter-rater agreement for color-map based collateral grading in our study was substantial. Agreement was higher for color-map based grading of collateral extent compared to filling dynamics. This suggests that

the latter is more challenging, which could be the reason for the lacking association of collateral filling dynamics and clinical outcome /follow-up infarct volume.

The predictive utility of conventional collateral assessment, while it was still good overall, was slightly lower when compared to color-map based grading of collateral extent. It is possible that complications that happened after treatment in the 3-month follow-up period have influenced the association with clinical outcomes, while the efficacy of treatment (either EVT or intravenous alteplase) might have influenced the association of collateral grade and final infarct volumes, although the latter two points would in theory affect both conventional and color-map based collateral grading. The exact reasons for the differences in predictive power remain therefore unknown at the time being.

Our study has several limitations: First, assessing infarct volume on NCCT can be challenging, since the infarct is often not clearly demarcated. In order to account for this possibility, we performed sensitivity analysis by stratifying patients according to their follow-up imaging modality. Second, we restricted our analysis to patients with LVO (including proximal M2 occlusions); our findings can thus not be generalized to more distal occlusion sites. Third, reperfusion status is an important predictor of infarct volume and outcome, but since vascular imaging was not available in all patients, we could not stratify our analysis by reperfusion status. Fourth, recanalization data were missing in a relatively large number of patients, partly because it was impractical to obtain follow-up vascular imaging in many local institutional settings, and partly because it does not have a therapeutic consequence in the vast majority of cases. Fifth, we showed that color-map based assessment of collateral extent is significantly associated with good outcome and infarct volume in LVO patients, but we could not assess in our study whether and how this alters clinical decision-making. Doing so would warrant a diagnostic randomized controlled trial. Such trials generally require very large sample sizes and are difficult to conduct for various reasons (16). Thus, no randomized diagnostic trials have so far been conducted for any acute stroke imaging paradigm and we suspect that this will remain true in the near future as well. Sixth, the current GE FastStroke™ Software does not allow the user to change the color-coding scheme; this might be confusing for some users who are used to different color schemes and is something that could be improved on in subsequent iterations of the software.

5.5. CONCLUSION

In this study, collateral extent, assessed on time-variant mCTA maps improved prediction of good outcome and has similar utility in predicting follow-up infarct volume compared to conventional mCTA collateral grading.

REFERENCES

1. Saver JL. Time is brain--quantified. *Stroke*. 2006;37:263-266
2. Powers WJ, Rabinstein AA, Ackerson T, Adeoye OM, Bambakidis NC, Becker K, et al. Guidelines for the early management of patients with acute ischemic stroke: 2019 update to the 2018 guidelines for the early management of acute ischemic stroke: A guideline for healthcare professionals from the American Heart Association/American Stroke Association. *Stroke*. 2019:STR0000000000000211
3. Goyal M, Menon BK, van Zwam WH, Dippel DW, Mitchell PJ, Demchuk AM, et al. Endovascular thrombectomy after large-vessel ischaemic stroke: A meta-analysis of individual patient data from five randomised trials. *Lancet*. 2016;387:1723-1731
4. Albers GW, Marks MP, Kemp S, Christensen S, Tsai JP, Ortega-Gutierrez S, et al. Thrombectomy for stroke at 6 to 16 hours with selection by perfusion imaging. *N Engl J Med*. 2018;378:708-718
5. Campbell BC, Mitchell PJ, Kleinig TJ, Dewey HM, Churilov L, Yassi N, et al. Endovascular therapy for ischemic stroke with perfusion-imaging selection. *N Engl J Med*. 2015;372:1009-1018
6. Goyal M, Demchuk AM, Menon BK, Eesa M, Rempel JL, Thornton J, et al. Randomized assessment of rapid endovascular treatment of ischemic stroke. *N Engl J Med*. 2015;372:1019-1030
7. Nogueira RG, Jadhav AP, Haussen DC, Bonafe A, Budzik RF, Bhuva P, et al. Thrombectomy 6 to 24 hours after stroke with a mismatch between deficit and infarct. *N Engl J Med*. 2018;378:11-21
8. Menon BK, d'Este CD, Qazi EM, Almekhlafi M, Hahn L, Demchuk AM, et al. Multiphase CT angiography: A new tool for the imaging triage of patients with acute ischemic stroke. *Radiology*. 2015;275:510-520
9. Ospel JM, Volny O, Qiu W, Najm M, Kashani N, Goyal M, et al. Displaying multiphase CT angiography using a time-variant color map: Practical considerations and potential applications in patients with acute stroke. *AJNR Am J Neuroradiol*. 2020;41:200-205
10. Ospel JMVO, Qiu W, Najm M, Hafeez M, Abdalrahman S, Fainardi E, Rubiera M, Khaw A, Shankar J, Hill M, Almekhlafi M, Demchuk A, Goyal M, Menon BK. CT perfusion vs. multiphase CTA in endovascular treatment decision-making for acute ischemic stroke. 2020.

11. Almekhlafi M, Ospel JM, Saposnik G, Kashani N, Demchuk A, Hill MD, et al. Endovascular treatment decisions in patients with m2 segment mca occlusions. *AJNR Am J Neuroradiol*. 2020;41:280-285
12. Hill MD, Goyal M, Menon BK, Nogueira RG, McTaggart RA, Demchuk AM, et al. Efficacy and safety of nerinetide for the treatment of acute ischaemic stroke (escape-na1): A multicentre, double-blind, randomised controlled trial. *Lancet*. 2020
13. Tan IY, Demchuk AM, Hopyan J, Zhang L, Gladstone D, Wong K, et al. Ct angiography clot burden score and collateral score: Correlation with clinical and radiologic outcomes in acute middle cerebral artery infarct. *AJNR Am J Neuroradiol*. 2009;30:525-531
14. d'Este CD, Trivedi A, Pordeli P, Boesen M, Patil S, Hwan Ahn S, et al. Regional comparison of multiphase computed tomographic angiography and computed tomographic perfusion for prediction of tissue fate in ischemic stroke. *Stroke*. 2017;48:939-945
15. Grunwald IQ, Kulikovski J, Reith W, Gerry S, Namias R, Politi M, et al. Collateral automation for triage in stroke: Evaluating automated scoring of collaterals in acute stroke on computed tomography scans. *Cerebrovasc Dis*. 2019;47:217-222

6. Chapter 6 - Multiphase CTA-derived tissue maps aid in detection of medium vessel occlusions

The contents of this chapter have been adapted from the journal article entitled “*Multiphase CTA-derived tissue maps aid in detection of medium vessel occlusions*”, published in *Neuroradiology* 2022;64(5):887-896 by R. McDonough, W. Qiu, ... P. Cimflova, et al.

Reproduced with permission from Springer Nature

Background: Medium vessel occlusions (MeVOs) can be challenging to reliably and quickly detect on imaging due to their smaller vessel caliber and relatively distal location. Multiphase computed-tomography angiography (mCTA) has been shown to improve large vessel occlusion (LVO) detection and endovascular treatment (EVT) selection. The aims of this study were to determine if mCTA-derived tissue maps can 1) accurately detect MeVOs; and 2) predict infarction on 24h follow-up imaging with comparable accuracy to CT perfusion (CTP) maps.

Methods: Two readers assessed mCTA tissue maps of 116 AIS patients (58 MeVO, 58 non-MeVO [49 LVO, 4 from the vertebrobasilar circulation, and 5 cases without any occlusion]) and determined by consensus: 1) the presence of MeVO (yes/no) and 2) occlusion site, blinded to clinical or imaging data. Sensitivity, specificity, and area under the curve (AUC) for MeVO detection were estimated in comparison to the reference standards of 1) expert core lab reading of baseline mCTA and 2) CTP maps. Volumetric and spatial agreement between predicted infarcts based on mCTA and CTP was assessed using concordance correlation coefficient and intraclass correlation coefficient. Interrater agreement for MeVO detection on mCTA tissue maps was estimated with Cohen’s Kappa.

Results: MeVO detection based on mCTA-derived tissue maps had a sensitivity of 91% (95%CI: 80-97), specificity of 82% (95%CI: 70-90), and AUC of 0.87 (95%CI:0.80-0.93) compared to expert reads of baseline mCTA. Compared to CTP maps, sensitivity was 87% (95%CI 75-95), specificity was 78% (95%CI 65-88), and AUC of 0.83 (95%CI:0.76-0.90). The mean difference between mCTA and CTP predicted final infarct volume was 4.8 mL (limits of agreement: -58.5 to 68.1) with a Dice coefficient of 33.5%. Interrater reliability (Cohen’s kappa) was good (0.72, 95%CI: 0.60-0.85) for the presence of MeVO.

Conclusion: mCTA tissue maps can be used to reliably detect MeVO stroke and predict tissue fate.

6.1 INTRODUCTION

Endovascular treatment (EVT) has become the standard of care patients with acute ischemic stroke (AIS) due to large vessel occlusion (LVO) (1-6). LVOs, however, constitute only 10-30% of all AIS cases; 25-40% are caused by so-called medium vessel occlusions (MeVOs), which are defined as occlusion of the M2, M3, A2, A3, P2, or P3 segments with disabling deficits(7,8). Due to the smaller caliber, varied vascular anatomy, and more distal location from the arterial tree compared with LVOs, MeVOs can be challenging to diagnose on imaging, particularly for trainees (9). Indeed, MeVOs are approximately five times more likely to be overlooked compared to LVOs, with physicians failing to detect occlusions of the M2 segment in up to one third of cases (9). This is important within the context of the time-critical nature of AIS, where it is crucial to identify the occluded vessel and assess the extent of tissue damage quickly and reliably to establish the diagnosis and initiate rapid treatment.

CT perfusion (CTP) is commonly used during admission imaging to select patients most likely to benefit from EVT. The color-coded output maps facilitate detection of occlusion location. The disadvantages, however, are longer acquisition and post-processing times, and overestimation of infarct core, particularly in the ultra-early time window(10,11), which may cause physicians to forego EVT in patients who may have otherwise benefitted from treatment. Multiphase computed-tomography angiography (mCTA) is an alternative advanced imaging technique that provides time-resolved, whole brain imaging of the cerebral vasculature, without the requirement for postprocessing (12). During mCTA, an initial aortic arch-to-vertex CTA is obtained in an analogous fashion to single-phase CTA, followed by the acquisition of two additional series during the peak-venous and late-venous phases using the same contrast bolus. These latter two phases cover only the intracranial vasculature from the skull base to the vertex. Patient selection for treatment based on mCTA collateral status has been shown to identify patients that are likely to benefit from EVT, without being overly restrictive (12). However, while mCTA has been proven to be a valid EVT selection tool in LVO stroke (3,13), imaging selection criteria for MeVO EVT have yet to be established.

Recently, mCTA-derived tissue maps with color indicator effect, analogous to CTP perfusion maps, were developed using machine learning methods (14). In contrast to CTP, they require a lower radiation dose, less contrast, and do not result in prolonged imaging times. Despite their slightly lower signal-to-noise ratios (due to the comparatively limited temporal resolution), mCTA tissue maps were able to predict infarct core, penumbra, and perfusion status with comparable accuracy to CTP (14). However, the majority of included images were

from patients with LVOs; it currently remains unclear whether mCTA-based tissue maps are capable of aiding in the detection of the more subtle imaging findings of MeVO stroke.

To this end, we sought to determine the accuracy of mCTA-derived tissue maps for the detection of MeVOs. In a secondary analysis, we quantitatively compared mCTA-based core and penumbra maps to those generated from CTP in their ability to predict final infarct volume in patients with definite MeVOs.

6.2 MATERIALS & METHODS

Data used were from the PRove-IT study, a prospective multicenter study of AIS patients undergoing baseline non-contrast CT (NCCT), single-phase CTA, mCTA, and CTP (12,15).

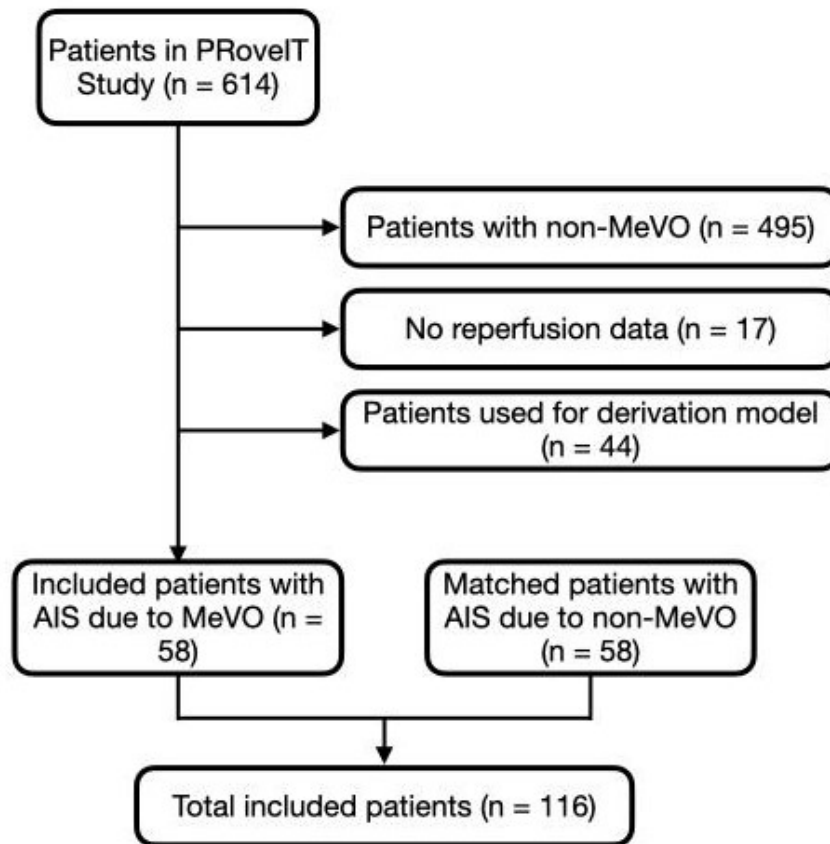
This study was approved by the local ethics committee. Data analysis was performed with Stata 15.1. Figures were created with Apple Keynote 11.0.1.

6.2.1 *Study participants*

Subjects who had 1) baseline NCCT and mCTA; 2) baseline CTP imaging with ≥ 8 cm z-axis coverage; 3) reperfusion assessed on conventional angiography after thrombolysis treatment (intravenous tissue plasminogen activator [tPA], EVT, or both) with mTICI scale; and 4) had 24/36-hour follow-up imaging on diffusion MRI or NCCT were included in this analysis.

Figure 6.1 describes the patient inclusion criteria. In this case-control study design, we included 116 patients, 58 with AIS due to MeVO and 58 with AIS due to non-MeVO (49 LVOs, 5 with no detectable occlusions, and 4 with occlusions of the vertebrobasilar circulation).

Figure 6.1. Patient inclusion flowchart. The patients with AIS due to non-MeVO were randomly selected as matched controls.



6.2.2 Imaging protocol

NCCT and mCTA: NCCT with 5 mm slice thickness was obtained, followed by mCTA with arch to vertex coverage in the first (arterial) and skull base to vertex coverage the second (peak venous) and third (late venous) phase. Detailed mCTA acquisition parameters have been published previously (12). Axial images with 1 mm overlap and multiplanar axial, coronal and sagittal reconstructions with 3 mm thickness, 1 mm intervals and 1 mm overlap for the first phase were obtained, along with axial maximum intensity projections (MIPs) for all three phases with 24 mm thickness and 4 mm intervals. CTP: 45 ml of iodinated contrast agent were injected at a rate of 4.5 ml/sec followed by a 40 ml saline bolus injected at a rate of 6 ml/sec. Image acquisition started 5 sec after contrast injection and 24 passes over 66 seconds were performed with 5 mm section thickness and a cranio-caudal coverage of 8 cm.

6.2.3 Image processing

First, skull stripping of the NCCT and mCTA images was performed (16). To account for patient movement, the three phases of the mCTA images were then aligned using rigid-body registration. The aligned 3-phase CTA images were registered onto NCCT images using affine registration.

We then used two machine learning models: 1) a core model; and 2) a penumbra model, as previously described (14), to generate mCTA derived tissue maps for the patients with reperfusion (mTICI 2b/2c/3, core prediction) and without reperfusion (mTICI 0/1/2a, penumbra prediction), respectively. mCTA predicted volume was obtained by thresholding the mCTA derived tissue maps (14).

Each CTP study was processed using commercially available delay-insensitive deconvolution software (CT Perfusion 4D, GE Healthcare, Waukesha, WI). Absolute maps of cerebral blood flow (CBF, $\text{mL} \cdot \text{min}^{-1} \cdot (100\text{g})^{-1}$), cerebral blood volume (CBV, $\text{mL} \cdot (100 \text{g})^{-1}$), and Tmax (seconds) were generated. Average maps were created by averaging the dynamic CTP source images. Time-dependent Tmax thresholds were used to generate baseline CTP thresholded maps, defined as CTP predicted infarct volume (17,18).

One radiologist (2-year experience) and one stroke neurologist (with 5 years of stroke image reading experience) assessed the source baseline mCTA images for the occlusion location, if any. Conflicts were resolved by consensus. These were considered the standard reference of expert reads for the qualitative portion of this study. Two radiologists (each with >5 years' experience) used ITK-SNAP (version 3.8.0, <http://www.itksnap.org>) to manually delineate the infarct region on follow-up diffusion weighted (DWI)/NCCT imaging, with conflicts resolved by consensus (19). The follow-up images, manual infarct segmentations, and CTP average maps were registered onto NCCT images, thus bringing all images into the same image space. When registration was sub-optimal, manual refinement of the registered infarct segmentations was attempted. The NiftyReg tool was used for all image registration tasks (20).

6.2.4 Qualitative image analysis for MeVO detection

Two radiologists (RM, PC) independently assessed the mCTA-derived tissue maps of 116 AIS cases (58 due to MeVO, 58 due to non-MeVO) for the presence of MeVO (binary yes/no), blinded to both clinical and imaging data. In a second step, the location of the occlusion was estimated based on the hypoperfusion pattern (if any) and scored according to a pre-determined classification: internal carotid artery (ICA), M1 segment of the middle cerebral artery (MCA),

anterior M2 segment of the MCA, posterior M2 segment of the MCA, M3 segment of the MCA or more distal, anterior cerebral artery (ACA), posterior cerebral artery (PCA), no occlusion, or “other” (e.g., occlusion of the vertebrobasilar circulation, **Figure 6.2 & 6.3**). Conflicts were resolved by consensus. Sensitivity, specificity, and area under the curve (AUC) for detection of MeVO were estimated in comparison to the reference standards of 1) expert readings of the baseline CTA and 2) CTP-based Tmax maps, as read by the readers of this study in a separate reading session one week later. Interrater agreement for MeVO detection on mCTA tissue maps was estimated using unweighted Cohen’s kappa.

Figure 6.2. Schematic examples of perfusion deficit patterns for various occlusion locations. A - anterior cerebral artery; B - posterior cerebral artery; C - internal carotid artery; D - M1 segment of the middle cerebral artery (MCA); E - anterior M2 segment of the MCA; F - posterior M2 segment of the MCA; G - M3 segment of the MCA

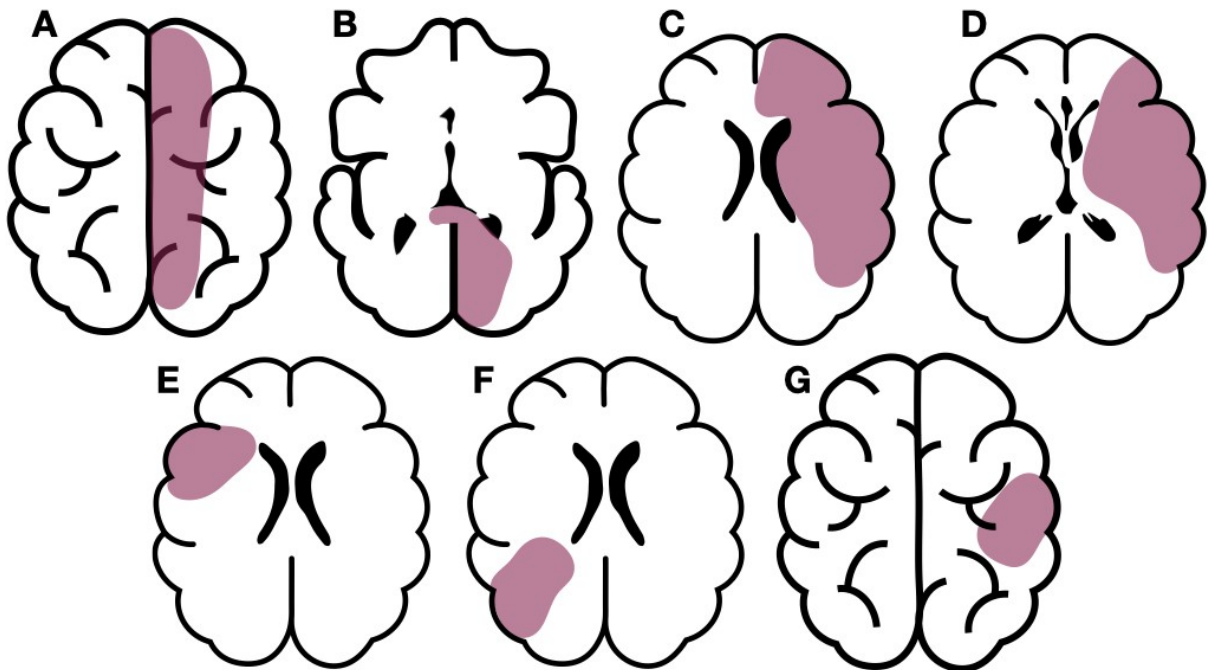
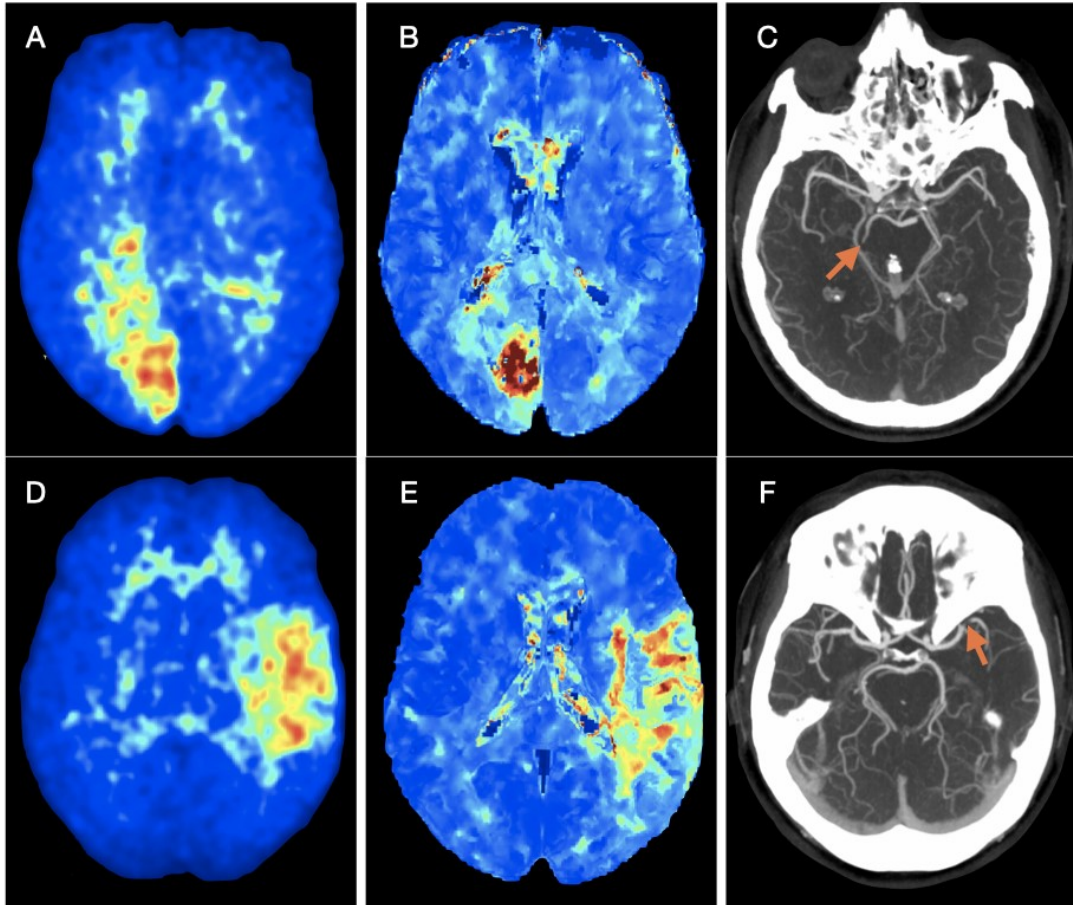


Figure 6.3. Exemplary cases. Right P2 PCA occlusion (C, red arrow) and left posterior M2 MCA occlusion (F, red arrow) with corresponding mCTA tissue maps (A, D) and CTP Tmax maps (B, E).



6.2.5 Volumetric and spatial analyses of mCTA-derived tissue maps

Volumetric agreement between mCTA tissue maps and CTP perfusion maps for core and penumbra volumes was assessed using concordance and intraclass correlation coefficients (CCC and ICC, respectively). The mean differences and limits of agreement (LoA) between the two types of generated volume were illustrated using Bland Altman plots, and spatial agreement between the two volumes was assessed using Dice Similarity Coefficient (DSC). When comparing mCTA tissue maps to CTP maps in their ability to predict follow-up infarction conditional on treatment, expert contoured follow up lesions (true follow up infarct) on 24h DWI/NCCT was used as the reference standard. Absolute volume agreement between mCTA predicted follow-up infarct/CTP predicted follow-up infarct and the reference standard (true follow up infarct) was reported using CCC and ICC. In addition, Bland-Altman plots were used to illustrate mean differences and LoA between predicted follow-up infarction volumes and CTP predicted volumes.

6.3 RESULTS

A total of 116 cases were included in this study, 58 with MeVO (23 occlusions of the M3/4 segment of the MCA, 22 of the posterior M2 segment of the MCA, 5 of the anterior M2 segment of the MCA, 2 of the A2/3 segment of the ACA, and 6 of the P2/3 segments of the PCA) and 58 with non-MeVO (7 occlusions of the ICA, 42 occlusions of the M1 segment of the MCA, 4 occlusions of the vertebrobasilar circulation, and 5 with no occlusion).

6.3.1 Feasibility of mCTA-based MeVO detection

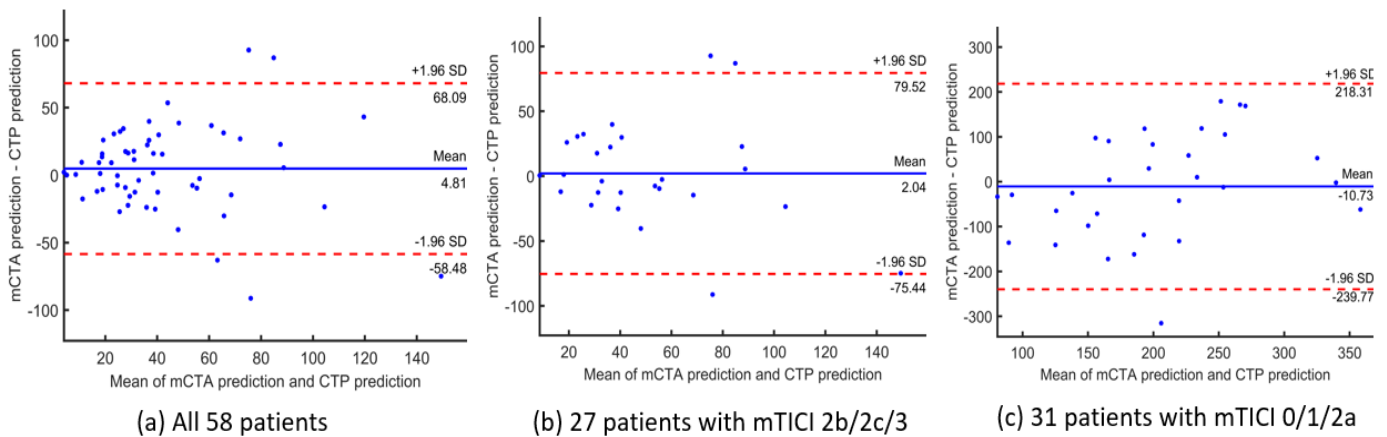
In this study, binary MeVO detection (yes/no) based on mCTA-derived tissue maps had a sensitivity of 90.7% (95%CI: 79.7-96.9%), specificity of 82.2% (95%CI: 70.5-90.8%), a positive predictive value of 81.7% (95%CI: 69.6-90.5), a negative predictive value of 91.1% (95%CI: 80.4-97.0), and an area under the curve (AUC) of 0.87 (95%CI: 0.80-0.93) compared to expert reads of baseline mCTA source images. Interrater agreement was good, with an unweighted Cohen's kappa of 0.72 (95%CI: 0.60-0.85) (21,22). When compared to the CTP map-based reference standard, mCTA tissue map-based MeVO detection had a sensitivity of 86.8% (95%CI: 74.7-94.5), a specificity of 78.3% (95%CI: 65.8-87.9), a positive predictive value of 78.0% (95%CI: 65.3-87.7), a negative predictive value of 87.0% (95%CI: 75.1-95.6), and an AUC of 0.82 (95%CI: 0.75-0.89). Interrater agreement was moderate, with an unweighted Cohen's kappa of 0.57 (95%CI: 0.42-0.72). The overall accuracy of mCTA tissue map based MeVO detection was 86% (100/116). Five cases were misclassified as being non-MeVOs (including 1 occlusion of the P2 segment of the PCA, 1 of the anterior M2, and 3 of the posterior M2), while the 11 cases that were incorrectly classified as MeVOs included occlusions of the vertebrobasilar circulation (n=3), the M1 segment of the MCA (n=7), and one case with no occlusion. Occlusion location based on mCTA tissue maps was correctly estimated in 70% (81/116) of cases.

6.3.2 Agreement of mCTA and CTP predicted infarct volumes

Figure 6.4 illustrates Bland-Altman plots showing agreement between the mCTA predicted infarct volume and pre-specified CTP predicted infarct volume for 58 patients with MeVO. The mean difference between the mCTA and CTP predicted infarct volumes was 4.8 mL (LoA, -58.5 to 68.1; P=0.56), CCC was 0.66 (95%CI: 0.56 to 0.76; P<0.01) and ICC was 0.68 (95%CI: 0.62 to 0.80; P<0.01). When stratifying the 58 patients into two subgroups with/without acute reperfusion, the mean difference between the mCTA and CTP predicted infarct volume for the 27 patients with complete reperfusion (mTICI 2b/2c/3) was 2.0 mL

(LoA, -75.4 to 79.5; P=0.54), CCC was 0.54 (95%CI: 0.47 to 0.68; P<0.01) and ICC was 0.57 (95% CI, 0.52 to 0.73; P<0.01); the mean difference between the mCTA and CTP predicted infarct volume for the 31 patients with incomplete reperfusion (mTICI 0/1/2a) was -10.7 mL (LoA, -239.8 to 218.3; P=0.45), CCC was 0.32 (95%CI: 0.25 to 0.48; P<0.01) and ICC was 0.33 (95%CI: 0.24 to 0.51; P<0.01)

Figure 6.4. Bland-Altman plots for predicted infarct volume. mCTA predicted infarct volume (ml) compared to CTP predicted infarct volume.



6.3.3. Agreement of mCTA predicted infarct volume and measured final infarct volume

Figure 6.5 illustrates Bland-Altman plots showing the agreement between mCTA predicted infarct volume and follow-up infarct volume in 58 patients with MeVO. The mean difference between the mCTA predicted infarct volume and follow-up infarct volume was -16.6 mL (LoA, -64.7 to 31.6; P=0.53), which was less than the CTP predicted infarct volume of -21.4 mL (LoA, -72.5 to 29.8; P=0.54). **Figure 6.6** shows exemplary mCTA tissue maps, CTP maps, and the associated follow-up images. The CCC between the mCTA predicted and follow-up infarct volume was 0.57 (95%CI: 0.43 to 0.70; P<0.01), and the ICC was 0.59 (95%CI: 0.48 to 0.72; P<0.01). The subgroup analyses by stratifying the 58 patients into those with reperfusion (mTICI 2b/2c/3) and those with non-reperfusion (mTICI 0/1/2a) groups show the comparable accuracy of mCTA in predicting follow up infarct compared to CTP imaging (**Figure 6.5b & 6.5c**).

Figure 6.5. Bland-Altman plots for predicted versus final infarct volume. mCTA and CTP predicted infarct volume (ml) compared to follow up infarct volume.

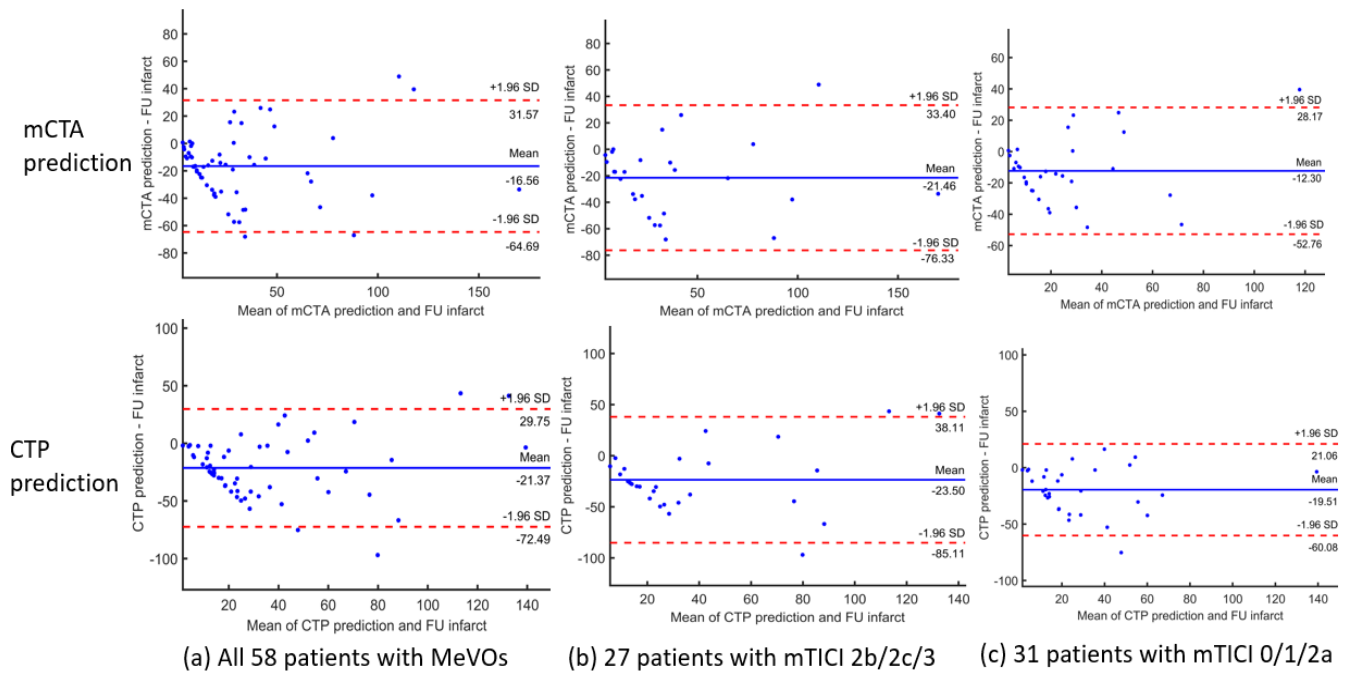
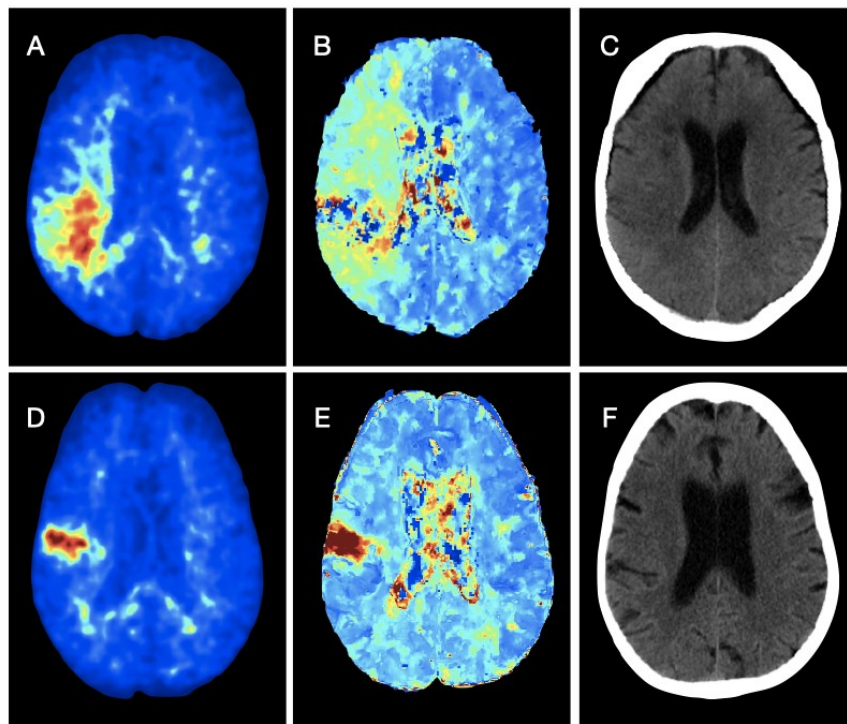


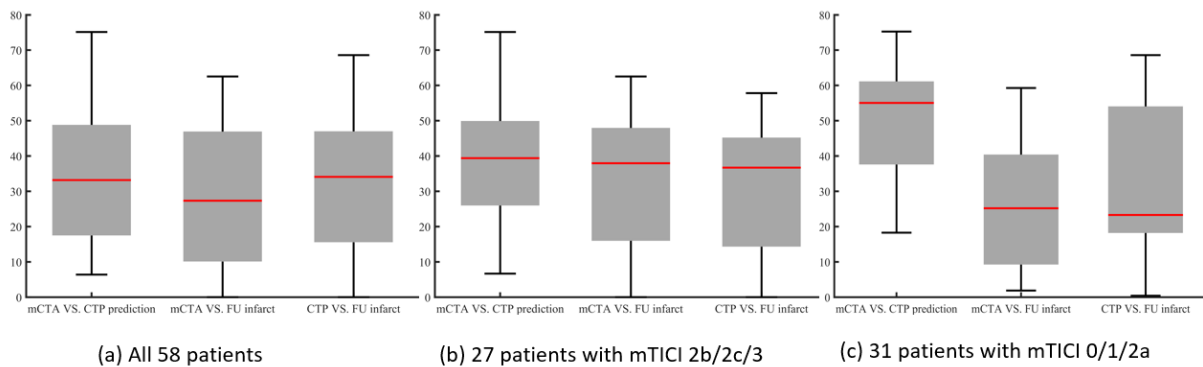
Figure 6.6. Exemplary cases. Right posterior M2 occlusion (A-C) and a right M3 occlusion (D-F) with associated mCTA tissue maps (A, D), CTP-generated Tmax maps (B, E), and follow-up images (C, F).



6.3.3 Spatial agreement between mCTA and CTP predicted infarct volume and measured final infarct volume

The median DSC between mCTA and CTP predicted infarct volume (**Figure 6.7**) was 33.5% (IQR: 18.7% to 48.8%) for 58 patients with MeVOs, 39.5% (IQR: 25.6% to 49.5%) for 27 patients with complete reperfusion, and 55.2% (IQR: 38.5% to 61.3%) for 31 patients with incomplete reperfusion. The median DSCs between mCTA predicted infarct volume and follow up infarct volume and between CTP predicted infarct volume and follow up infarct volume ranged from 23.5% to 37.8%.

Figure 6.7. Dice similarity coefficient (%) between mCTA predicted infarct, CTP predicted infarct, and follow up infarct.



6.4 DISCUSSION

EVT for AIS due to MeVOs is seen as the next frontier for the advancement of current stroke treatment paradigms (23,24). The advent of smaller, more flexible stent retrievers and catheters, as well as improvements in technique, have made EVT for MeVO stroke both possible and safe (23,25-27). Indeed, in a cross-sectional, multinational survey, the majority of physicians queried indicated that they would proceed directly to EVT for a variety of MeVO case scenarios (28). A randomized clinical trial is warranted to confirm these findings and to establish EVT for MeVO stroke as a standard of care, particularly due to the fact that the current standard, intravenous alteplase, results in approximately one-third of MeVO patients being dependent at the 90-day follow up (29). To this end, validated imaging tools for 1) detection of MeVOs and 2) appropriate selection of patients for EVT need to be developed. Parallel assessment of the three mCTA phases has previously been shown to improve MeVO detection when compared to single-phase CTA (30,31). This pilot study shows that mCTA-derived tissue

maps also allow for feasible detection of MeVOs in most cases. In the instances that a MeVO was misclassified, it was most often due to interpretation of the occlusion being an LVO; in no case was an occlusion completely missed, which has important implications for clinical practice.

Volumetric analyses showed a mean difference in predicted infarct volume of 4.8 ml when comparing mCTA and CTP maps, with a modest CCC of 0.65 and an ICC of 0.67. This difference decreased to less than 2 ml when stratifying the cohort according to successful versus non-successful reperfusion. Because CTP and mCTA employ similar imaging techniques, they can both be used to predict tissue fate on a voxel-by-voxel basis with good agreement, despite differences in temporal resolution. Furthermore, the differences between mCTA-based predicted final infarct volume and “true” (expert contoured) final infarct volumes on follow up was less than that which was predicted using CTP-derived maps, with a modest CCC and ICC of 0.55 and 0.58, respectively. Both CTP and mCTA predicted final infarct volumes were underestimated, regardless of reperfusion status. A previous study showed that Tmax-based prediction of final infarct volumes tended to be underestimated in patients without early recanalization, which could at least partially explain these results (32).

The overall spatial agreement between CTP and mCTA predicted infarct volumes was moderate, with a DSC 38.5%. The same was true between mCTA predicted follow-up infarct volume and measured infarct volume (DSC = 23.5%) and CTP predicted follow-up infarct volume and measured infarct volume (DSC = 32.5%). This is in line with a previous study (14) and likely at least partially due to continued infarct growth, which can occur even in cases of successful reperfusion. Indeed, spatial agreement was worse in the non-reperfused group, probably due to infarct growth, which biases the DSC. Furthermore, accurate quantification of irreversibly damaged versus salvageable tissue is difficult and likely influenced by multiple pathophysiological processes (e.g., cerebral autoregulation, collateral status, etc.). Another factor contributing to low spatial agreement could be the co-registration of different imaging modalities, e.g., overlaying DWI segmentations from follow-up MRI studies onto baseline CT (33).

This study has several limitations. First, the current models were derived using only imaging-based information; incorporating clinical parameters (e.g., time from onset, patient history, etc.) may increase the prediction accuracy (34). Second, accurate measurement of final infarct volume is challenging, with a multitude of factors such as modality, time from onset to imaging and reperfusion, collateral status, tissue tolerance to ischemia, and infarct location likely influencing the results (18,34,35). Third, although the mCTA models have now been

tested in patients with both LVOs and MeVOs, their applicability needs to be expanded to include more diverse cases (e.g., stroke mimics, small vessel occlusions) to further increase accuracy. Similarly, although the patient collective was from a multicenter study, testing of the models should be performed in external, larger, and more diverse datasets, a necessary step before implementing our results into clinical practice.

6.5 CONCLUSION

mCTA-derived tissue maps can be used to accurately detect MeVO stroke and automatically predict tissue fate with similar accuracy to CTP imaging. Thus, mCTA-derived tissue maps could be used as for patient selection in a randomized MeVO EVT trial as well as in daily clinical practice, particularly in centers in which CTP is not available.

REFERENCES

1. Berkhemer OA, Fransen PS, Beumer D, et al. A randomized trial of intraarterial treatment for acute ischemic stroke. *N Engl J Med* 2015;372:11-20.
2. Campbell BC, Mitchell PJ, Kleinig TJ, et al. Endovascular therapy for ischemic stroke with perfusion-imaging selection. *N Engl J Med* 2015;372:1009-18.
3. Goyal M, Demchuk AM, Menon BK, et al. Randomized assessment of rapid endovascular treatment of ischemic stroke. *N Engl J Med* 2015;372:1019-30.
4. Goyal M, Menon BK, van Zwam WH, et al. Endovascular thrombectomy after large-vessel ischaemic stroke: a meta-analysis of individual patient data from five randomised trials. *Lancet* 2016;387:1723-31.
5. Jovin TG, Chamorro A, Cobo E, et al. Thrombectomy within 8 Hours after Symptom Onset in Ischemic Stroke. *New England Journal of Medicine* 2015;372:2296-306.
6. Saver JL, Goyal M, Bonafe A, et al. Stent-retriever thrombectomy after intravenous t-PA vs. t-PA alone in stroke. *N Engl J Med* 2015;372:2285-95.
7. Duloquin G, Graber M, Garnier L, et al. Incidence of Acute Ischemic Stroke With Visible Arterial Occlusion: A Population-Based Study (Dijon Stroke Registry). *Stroke* 2020;51:2122-30.
8. Saver JL, Chapot R, Agid R, et al. Thrombectomy for Distal, Medium Vessel Occlusions: A Consensus Statement on Present Knowledge and Promising Directions. *Stroke* 2020;51:2872-84.
9. Fasen B, Heijboer RJJ, Hulsmans FH, Kwee RM. CT Angiography in Evaluating Large-Vessel Occlusion in Acute Anterior Circulation Ischemic Stroke: Factors Associated with Diagnostic Error in Clinical Practice. *AJNR Am J Neuroradiol* 2020;41:607-11.
10. Martins N, Aires A, Mendez B, et al. Ghost Infarct Core and Admission Computed Tomography Perfusion: Redefining the Role of Neuroimaging in Acute Ischemic Stroke. *Intervent Neurol* 2018;7:513-21.
11. Austein F, Riedel C, Kerby T, et al. Comparison of Perfusion CT Software to Predict the Final Infarct Volume After Thrombectomy. *Stroke* 2016;47:2311-7.
12. Menon BK, d'Este CD, Qazi EM, et al. Multiphase CT Angiography: A New Tool for the Imaging Triage of Patients with Acute Ischemic Stroke. *Radiology* 2015;275:510-20.
13. Hill MD, Goyal M, Menon BK, et al. Efficacy and safety of nerinetide for the treatment of acute ischaemic stroke (ESCAPE-NA1): a multicentre, double-blind, randomised controlled trial. *Lancet* 2020;395:878-87.

14. Qiu W, Kuang H, Ospel JM, et al. Automated Prediction of Ischemic Brain Tissue Fate from Multi-Phase CT-Angiography in Patients with Acute Ischemic Stroke Using Machine Learning. medRxiv 2020:2020.05.14.20101014.
15. d'Este CD, Trivedi A, Pordeli P, et al. Regional Comparison of Multiphase Computed Tomographic Angiography and Computed Tomographic Perfusion for Prediction of Tissue Fate in Ischemic Stroke. *Stroke* 2017;48:939-45.
16. Najm M, Kuang H, Federico A, et al. Automated brain extraction from head CT and CTA images using convex optimization with shape propagation. *Comput Methods Programs Biomed* 2019;176:1-8.
17. d'Este CD, Boesen ME, Ahn SH, et al. Time-Dependent Computed Tomographic Perfusion Thresholds for Patients With Acute Ischemic Stroke. *Stroke* 2015;46:3390-7.
18. Qiu W, Kuang H, Lee TY, et al. Confirmatory Study of Time-Dependent Computed Tomographic Perfusion Thresholds for Use in Acute Ischemic Stroke. *Stroke* 2019;50:3269-73.
19. Boers AMM, Jansen IGH, Beenen LFM, et al. Association of follow-up infarct volume with functional outcome in acute ischemic stroke: a pooled analysis of seven randomized trials. *J Neurointerv Surg* 2018;10:1137-42.
20. Modat M, Ridgway GR, Taylor ZA, et al. Fast free-form deformation using graphics processing units. *Comput Methods Programs Biomed* 2010;98:278-84.
21. Cicchetti DV, Sparrow SA. Developing criteria for establishing interrater reliability of specific items: applications to assessment of adaptive behavior. *Am J Ment Defic* 1981;86:127-37.
22. Regier DA, Narrow WE, Clarke DE, et al. DSM-5 field trials in the United States and Canada, Part II: test-retest reliability of selected categorical diagnoses. *Am J Psychiatry* 2013;170:59-70.
23. Ospel JM, Goyal M. A review of endovascular treatment for medium vessel occlusion stroke. *Journal of NeuroInterventional Surgery* 2021:neurintsurg-2021-017321.
24. Goyal M, Ospel JM, Menon BK, Hill MD. MeVO: the next frontier? *J Neurointerv Surg* 2020;12:545-7.
25. Barchetti G, Cagnazzo F, Raz E, Barbagallo G, Toccaceli G, Peschillo S. Mechanical Thrombectomy of Distal Occlusions Using a Direct Aspiration First Pass Technique Compared with New Generation of Mini-0.017 Microcatheter Compatible-Stent Retrievers: A Meta-Analysis. *World Neurosurg* 2020;134:111-9.

26. Hofmeister J, Kulcsar Z, Bernava G, et al. The Catch Mini stent retriever for mechanical thrombectomy in distal intracranial occlusions. *J Neuroradiol* 2018;45:305-9.
27. McTaggart RA, Ospel JM, Psychogios MN, et al. Optimization of Endovascular Therapy in the Neuroangiography Suite to Achieve Fast and Complete (Expanded Treatment in Cerebral Ischemia 2c-3) Reperfusion. *Stroke* 2020;51:1961-8.
28. Cimflova P, Kappelhof M, Singh N, et al. Factors influencing thrombectomy decision making for primary medium vessel occlusion stroke. *J Neurointerv Surg* 2021.
29. Ospel JM, Menon BK, Demchuk AM, et al. Clinical Course of Acute Ischemic Stroke Due to Medium Vessel Occlusion With and Without Intravenous Alteplase Treatment. *Stroke* 2020;51:3232-40.
30. Volny O, Cimflova P, Kadlecova P, et al. Single-Phase Versus Multiphase CT Angiography in Middle Cerebral Artery Clot Detection-Benefits for Less Experienced Radiologists and Neurologists. *J Stroke Cerebrovasc Dis* 2017;26:19-24.
31. Yu AY, Zerna C, Assis Z, et al. Multiphase CT angiography increases detection of anterior circulation intracranial occlusion. *Neurology* 2016;87:609-16.
32. Olivot JM, Mlynash M, Thijs VN, et al. Optimal Tmax threshold for predicting penumbral tissue in acute stroke. *Stroke* 2009;40:469-75.
33. Hoving JW, Marquering HA, Majoie C, et al. Volumetric and Spatial Accuracy of Computed Tomography Perfusion Estimated Ischemic Core Volume in Patients With Acute Ischemic Stroke. *Stroke* 2018;49:2368-75.
34. Qiu W, Kuang H, Menon BK. Response by Qiu et al to Letter Regarding Article, "Confirmatory Study of Time-Dependent Computed Tomographic Perfusion Thresholds for Use in Acute Ischemic Stroke". *Stroke* 2020;51:e8.
35. Goyal M, Ospel JM, Menon B, et al. Challenging the Ischemic Core Concept in Acute Ischemic Stroke Imaging. *Stroke* 2020;51:3147-55.

7. Chapter 7 – Results summary

The main aim of this thesis was to investigate and evaluate possible further utilizations of CT imaging modalities in acute stroke care. Several practical implications can be drawn from the finding reported in this thesis.

First, we showed in **Chapter 2** that collateral grading evaluated on the multiphase CTA correlates with increasing perfusion lesion volumes automatically derived from CTP. In the author's opinion these findings supports the paradigm that CTP is not necessary in patients presenting during the first 6 hours from the symptom onset while the median volume of the ischemic core remained relatively small even in the patients with poor collaterals. Moreover, the reported values of perfusion lesion volumes might be used as an estimate of the probable ischemic core volume and severely hypoperfused tissue based on the collateral grade on mCTA, which can be easily implemented without any additional technical requirements and thus can be an attractive tool in smaller hospitals and places where CTP is not available. The validation of these results should be performed on a large multicentre dataset.

It was demonstrated in **Chapter 3** that the early ischemic changes can be assessed with higher accuracy on CTP maps (specifically on $CBF < 30\%$ and $T_{max} > 10s$) compared to the expert reading on NCCT. Despite the automatic software analysis of early ischemic changes on NCTT showed the lowest accuracy and sensitivity, its accuracy of 0.76 was comparable with the expert consensus reading and can still be considered as good. In author's opinion, this finding encourages the use of automatic software analysis in clinical practice especially by less experienced readers (e.g. residents on-call) or clinicians in primary stroke care centres to fasten the AIS patients triage and prevent any delays in treatment initiation. The author of the thesis was involved in the implementation of use of the automatic software tools (RAPID-IA and e-ASPECTS Brainomix).

Results reported in **Chapter 4** demonstrating the high accuracy of the automatic anterior LVO detection using the machine learning based software tool supports the generalizability of the software's use in routine clinical practice. Although the tested version of the software tool was intended only for a detection of LVO in the anterior circulation, it provided a solid baseline for further software development to identify all intracranial occlusion (i.e. distally located

occlusions and occlusion in the posterior territory). Again, the findings of this study further encourages the use automatic software tools in acute stroke care to quickly and accurately detecting patients with LVO who may likely require immediate medical attention and benefit from timely treatment. The further software development shall be focused on detection of all intracranial occlusion including MeVOs and occlusions in the vertebrobasilar territory. Moreover, studies evaluating the software performance on the real world data in a prospective manner are warranted. The author of this thesis was involved in the development and evaluation of the Stroke*SENS* automatic software tools.

The novel time-variant (color-coded) mCTA display format was evaluated in **Chapter 5**. We showed that the collateral extent assessment on time-variant mCTA maps improved prediction of good outcome and had similar value in follow-up infarct volume prediction compared to conventional mCTA collateral grading. While the interpretation of collateral status on mCTA requires some degree of experience and suffers from some degree of inter-rater variability, the time-variant mCTA display format represents a suitable alternative to facilitate interpretation of the collateral status.

Another novel machine learning based application of mCTA was evaluated in **Chapter 6**. mCTA-derived tissue maps as an alternative to CTP maps predicting ischemic core and penumbra. In the presented study, we showed that mCTA-derived tissue maps can be used to accurately detect MeVO stroke which is believed to be the next frontier for EVT. We also demonstrated that tissue fate can be predicted with similar accuracy to CTP maps, with moderate spatial agreement between mCTA and CTP. The clinical implication of these findings lies in the possibility of using mCTA-derived tissue maps to detect MeVO EVT candidates and estimate the benefit of treatment (volume of potentially salvageable tissue) particularly in centers in which CTP is not available. Further research could be focused on validation of these results on a large prospectively collected dataset.

8. List of Figures

Figure 1.1. ASPECTS regions, p. 23

Figure 1.2. Collateral scoring on multi-phase CT angiography in the axial plane, p. 25

Figure 1.3. Perfusion time attenuation curve, p. 27

Figure 1.4. CT perfusion analysis using RAPID-AI, p. 31

Figure 2.1. mCTA collateral score versus CT perfusion lesion volumes, p.46

Figure 3.1. Comparison of CT imaging modalities and evaluation of early ischemic changes, p. 59

Figure 3.2. Accuracy, sensitivity, specificity, positive predictive value, negative predictive values of baseline ASPECTSs evaluated by e-ASPECTS, consensus (expert reading), CBF<30% and Tmax>10s), p. 62

Figure 3.3. Bland-Altman plots, p. 63

Figure 3.4. Subgroup analysis of patients with successful reperfusion, p. 66

Figure 3.5. Bland-Altman plots for the subgroup analysis of patients with successful recanalization/reperfusion (MT and IVT group pooled data), p. 67

Figure 3.6. Least square means estimates of fixed effect “region” computed from generalized mixed model, p. 68

Figure 4.1. Exemplary cases of Stroke*SENS*™ LVO software performance, p. 82

Figure 4.2. Diagram of scan selection, p. 85

Figure 4.3. Areas under the receiver operating characteristic curves (AUC) for the Stroke*SENS* LVO, p. 92

Figure 5.1. Conventional and color-based collateral scoring, p. 101

Figure 5.2. Flowchart of included and excluded patients, p. 105

Figure 6.1. Patient inclusion flowchart, p. 116

Figure 6.2. Schematic examples of perfusion deficit patterns for various occlusion locations, p. 118

Figure 6.3. Exemplary cases, p. 119

Figure 6.4. Bland-Altman plots for predicted infarct volume, p. 121

Figure 6.5. Bland-Altman plots for predicted versus final infarct volume, p. 122

Figure 6.6. Exemplary cases, p. 122

Figure 6.7. Dice similarity coefficient (%) between mCTA predicted infarct, CTP predicted infarct, and follow up infarct, p. 123

9. List of Tables

Table 1.1. Multiphase CTA collateral score, p. 26

Table 2.1. Hypoperfusion volumes in different collateral grades and their correlation, p. 45

Table 2.2. Correlation coefficients for hypoperfusion lesion volumes and collateral score, p. 46

Table 2.3. Optimal cut-off values defining poor collaterals, p. 47

Table 2.4. Baseline characteristics of the whole dataset and dataset used for the sensitivity analysis, p. 48

Table 2.5. Comparison of hypoperfusion volumes for different collateral grades in patient with M1-MCA and terminal ICA occlusion, p. 48

Table 2.6. Comparison of p-values derived from Wilcoxon rank sum test for perfusion lesion volumes and hypoperfusion intensity ratio, p. 49

Table 2.7. Correlation coefficients for hypoperfusion lesion volumes and collateral score in patient with M1-MCA and terminal ICA occlusion, p. 49

Table 3.1. Accuracy, sensitivity, specificity, PPV and NPV of baseline ASPECT(e-ASPECTS, consensus, CBF<30% and Tmax>10s) vs. follow-up imaging, p. 62

Table 3.2. Baseline characteristics, p. 65

Table 3.3. Subgroup analysis of patients with successful reperfusion/recanalization, p. 65

Table 3.4. Comparison of residuals for the follow-up ASPECTS and the baseline ASPECTS for the subgroups of patients with determined successful recanalization versus non-determined recanalization, p. 66

Table 4.1. Baseline clinical and imaging characteristics of subjects in the test set, p. 86

Table 4.2. Area under the curve, sensitivity and specificity for automated LVO detection using the machine learning-based algorithm, p. 87

Table 4.3. The summary of available automatic software tools for LVO detection, p. 93

Table 5.1. Patient baseline characteristics, p. 106

Table 5.2. Association of conventional and color-map based collateral grade and good clinical outcome, p. 107

Table 5.3. Association of conventional and color-map based collateral grade and final infarct volume, p. 107